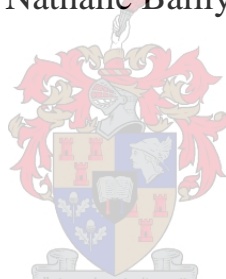


# ***N*-Vinylpyrrolidone - vinyl acetate block copolymers as drug delivery vehicles**

*Dissertation presented in partial fulfillment of the requirements for the degree of  
PhD (Polymer Science)*

by  
Nathalie Bailly



Promoter: Prof. Bert Klumperman

University of Stellenbosch- Faculty of Science  
Department of Chemistry and Polymer Science

March 2012

## **Declaration**

By submitting this dissertation electronically, I declare that the entirety of the work contained therein is my own, original work, that I am the owner of the copyright thereof (unless to the extent explicitly otherwise stated) and that I have not previously in its entirety or in part submitted it for obtaining any qualification

**Nathalie Bailly**

*Stellenbosch, March 2012*

*To my parents,  
Chantal and  
Claude*

### Abstract

The primary aim of this study was to investigate the feasibility of the amphiphilic block copolymer poly((vinylpyrrolidone)-*b*-poly(vinyl acetate)) (PVP-*b*-PVAc) as a vehicle for hydrophobic anti-cancer drugs.

PVP-*b*-PVAc block copolymers of constant hydrophilic PVP block length and varying hydrophobic PVAc block lengths were synthesized via xanthate-mediated controlled radical polymerization (CRP). The methodology consisted of growing the PVAc chain from a xanthate end-functional PVP. In an aqueous environment the amphiphilic block copolymers self-assembled into spherical vesicle-like structures consisting of a hydrophobic PVAc bilayer membrane, a hydrophilic PVP corona and an aqueous core. The self-assembly behaviour and the physicochemical properties of the self-assembled structures were investigated by <sup>1</sup>H NMR spectroscopy, fluorescence spectroscopy, transmission electron microscopy (TEM) and dynamic and static light scattering.

Drug loading studies were performed using a model hydrophobic drug, clofazimine, and a common anti-cancer drug paclitaxel (PTX) to evaluate the potential of the PVP-*b*-PVAc block copolymers for drug delivery. Clofazimine and PTX were physically entrapped into the hydrophobic domain of the self-assembled PVP-*b*-PVAc block copolymers via the dialysis method. The drug-loaded PVP-*b*-PVAc block copolymers were characterized regarding particle size, morphology, stability and drug loading capacity in order to assess their feasibility as a drug vehicle. The polymer vesicles had a relatively high drug loading capacity of 20 wt %. The effect of the hydrophobic PVAc block length on the drug loading capacity and encapsulation efficiency were also studied. Drug loading increased with increasing the hydrophobic PVAc block length. The effect of the drug feed ratio of clofazimine and PTX on the drug loading capacity and encapsulation efficiency were also investigated. The optimal formulation for the drug-loaded PVP-*b*-PVAc was determined and further investigated *in vitro*. The size stability of the drug-loaded PVP-*b*-PVAc block copolymers was also assessed under physiological conditions (PBS, pH 7.4, 37 °C) and were stable in the absence and presence of serum.

PVP-*b*-PVAc block copolymers were tested *in vitro* on MDA-MB-231 multi-drug-resistant human breast epithelial cancer cells and normal MCF12A breast epithelial cells to provide evidence of their antitumor efficacy. *In vitro* cell culture studies revealed that the PVP-*b*-PVAc drug carrier exhibited no cytotoxicity towards MDA-MB-231 and MCF12A cells, confirming the biocompatibility of the PVP-*b*-PVAc carrier. *In vitro* cytotoxicity assays using clofazimine-PVP-*b*-PVAc formulations showed that when MDA-MB-231 cells were exposed to the formulations, an enhanced therapeutic effect was observed compared to the free drug. Cellular internalization of the PVP-*b*-PVAc drug carrier was demonstrated by fluorescent labeling of the PVP-*b*-PVAc carrier. Fluorescence microscopy results showed that the carrier was internalized by the MDA-MB-231 cells after 3 hours and localized in the cytoplasm and the perinuclear region.

Overall, it was demonstrated that PVP-*b*-PVAc block copolymers appear to be promising candidates for the delivery of hydrophobic anti-cancer drugs.

### Opsomming

Die studie is gebaseer op die gebruik van amfifiliese blokkopolimere van poli(*N*-vinielpirolidoon)-*b*-poli(vinielasetaat) (PVP-*b*-PVAc) as potensiele geneesmiddeldraers.

PVP-*b*-PVAc blokkopolimere van konstante hidrofiliese bloklengte en verskillende hidrofobiese bloklengte is voorberei via die RAFT/MADIX-proses. Blokkopolimere met vinielasetaat is vanaf poli(*N*-vinielpirolidoon) met 'n xantaatendfunksie voorberei. In 'n wateromgewing vorm die PVP-*b*-PVAc blokkopolimere vesikel strukture met 'n hidrofobiese membraan en 'n hidrofiliese mantel.

Die fisies-chemiese eienskappe van die PVP-*b*-PVAc blokkopolimere is gekarakteriseer met gebruik van KMR spektroskopie, fluoresent spektroskopie, transmissie elektronmikroskopie (TEM) en dinamiese en statiese lig verstrooiing.

Die potensiaal van PVP-*b*-PVAc as 'n geneesmiddeldraer is ondersoek deur gebruik te maak van die hidrofobiese geneesmiddel, clofazimine, en 'n anti-kanker geneesmiddel, paclitaxel. Clofazimine en paclitaxel is ge-inkapsuleer in die hidrofobiese gedeelte van die blokkopolimere via die dialise-metode. Clofazimine-PVP-*b*-PVAc en paclitaxel-PVP-*b*-PVAc blokkopolimere is gekarakteriseer met betrekking tot die partikel grootte, morfologie, stabiliteit en laai kapasiteit om die PVP-*b*-PVAc blokkopolimere as geneesmiddeldraers te evalueer. Die PVP-*b*-PVAc geneesmiddeldraer het 'n relatiewe hoë laai kapasiteit van 20 gew % aangetoon. Die invloed van die bloklengte op die laai kapasiteit is ook ondersoek en beskryf. 'n Toename in die laai kapasiteit is gesien met 'n toename in die hidrofobiese bloklengte. Die invloed van die hoeveelheid geneesmiddel op die laai kapasiteit en die inkapsuleer doeltreffendheid is ook ondersoek. Die optimale formulering is gevind en verder gebruik vir *in vitro* studies. Die stabiliteit van die geneesmiddeldraer in fisiologiese omstandighede (pH 7.4, 37 °C) is ook beskryf. Resultate toon aan dat die sisteem stabiel is onder hierdie omstandighede in die afwesigheid en aanwesigheid van serum.

*In vitro* eksperimente is op MCF12A epiteel-borselle en MDA-MB-231 epiteel-borskankerselle getoets om die anti-tumoraktiwiteit te ondersoek. Resultate toon aan dat die PVP-*b*-PVAc geen sitotoxiese effek op die selle het nie, wat aandui dat die polimere bioverenigbaar is. Verder is dit bewys dat die PVP-*b*-PVAc geneesmiddel formuulsie 'n hoër sitotoxiteit besit as die vry-geneesmiddel. Fluoresent studies het aangetoon dat die geneesmiddeldraer na 3 uur opgeneen word deur MDA-MB231 selle en gelokaliseer is in die sitoplasma en in die omgewing van die kern van die selle.

In die algemeen is dit aangetoon dat PVP-*b*-PVAc blokkopolimere potensiële kandidate vir die lewering van hydrofobiese geneesmiddels is.

## Table of contents

List of acronyms .....	v
List of symbols.....	vi
List of schemes .....	vii
List of tables.....	viii
List of figures.....	ix

### Chapter 1: Introduction and objectives

1 Introduction.....	1
2. Amphiphilic block copolymers for drug delivery.....	2
3 Objective of dissertation .....	4
4. Outline of dissertation.....	4
5. References.....	6

### Chapter 2: Historical and theory

2.1 Introduction.....	8
2.2 Controlled radical polymerization .....	9
2.2.1 RAFT/MADIX-mediate polymerization .....	9
2.2.2 Xanthate-mediated synthesis of poly( <i>N</i> -vinylpyrrolidone) (PVP) and poly(vinyl acetate) (PVAc).....	10
2.3 Amphiphilic block copolymers in anti-cancer drug delivery .....	12
2.3.1 Amphiphilic block copolymers as drug delivery carriers .....	14
2.3.2 Amphiphilic block copolymer micelles and vesicles.....	14
2.3.3 Active and passive targeting .....	17
2.3.4 Inherent size of polymer drug carriers and biodistribution of the drug .....	19
2.3.5 Hydrophilic corona and hydrophobic core components of polymer micelles or vesicles .....	19
2.3.6 Stability of polymer drug carriers in aqueous and biological environment.....	21
2.4 Preparation and drug loading into polymer drug carriers .....	23
2.4.1 Drug loading methods for polymer micelles and vesicles .....	23



2.4.2 Factors affecting drug loading .....	25
2.5 Drug release and cellular internalization .....	27
2.5.1 Drug release .....	27
2.5.2 Cellular internalization.....	28
2.5.3 Polymer drug carriers and multiple drug resistance (MDR).....	30
2.6 Conclusion .....	30
2.7 References.....	31

**Chapter 3: Synthesis, characterization and self-assembly of PVP-*b*-PVAc**

3.1 Introduction.....	40
3.2 Materials and Methods.....	44
3.2.1 Materials .....	44
3.2.2 Synthesis of xanthate chain-transfer agent .....	44
3.2.3 Synthesis of PVP macro-RAFT agent .....	44
3.2.4 Synthesis of PVP- <i>b</i> -PVAc block copolymers .....	44
3.2.5 Polymer characterization .....	45
3.2.6 Self-assembly of PVP- <i>b</i> -PVAc block copolymers .....	46
3.2.7 Determination of the critical micelle concentration (CMC) of PVP- <i>b</i> -PVAc block copolymers .....	46
3.2.8 Size distribution and morphology of PVP- <i>b</i> -PVAc block copolymers .....	47
3.2.9 Multiangle static light scattering (MASLS).....	47
3.2.10 Stability of PVP- <i>b</i> -PVAc block copolymers in biological environment .....	49
3.3 Results and discussion .....	50
3.3.1 Synthesis and characterization of PVP macro-RAFT-agent and PVP- <i>b</i> -PVAc block copolymers .....	50
3.3.2 Gradient HPLC characterization of PVP- <i>b</i> -PVAc block copolymers .....	55
3.3.3 Self-assembly behavior of PVP- <i>b</i> -PVAc block copolymers .....	57
3.3.4 CMC of PVP- <i>b</i> -PVAc block copolymers .....	58
3.3.5 Size distribution and morphology of PVP- <i>b</i> -PVAc.....	61
3.3.6 Stability of PVP- <i>b</i> -PVAc vesicles under physiological conditions.....	66
3.4 Conclusion .....	67

3.5 References.....	68
---------------------	----

#### **Chapter 4: PVP-*b*-PVAc: A potential drug carrier**

4.1 Introduction.....	72
4.2 Materials and methods .....	75
4.2.1 Chemicals.....	75
4.2.2 Loading of clofazimine into PVP- <i>b</i> -PVAc block copolymers .....	75
4.2.3 <sup>1</sup> H NMR measurements of block copolymers .....	75
4.2.4. Size distribution and morphology of clofazimine-loaded PVP- <i>b</i> -PVAc.....	75
4.2.5 Evaluation of the drug loading capacity and encapsulation efficiency of clofazimine-loaded PVP- <i>b</i> -PVAc .....	76
4.2.6 Stability studies of clofazimine-loaded PVP- <i>b</i> -PVAc .....	77
4.3. Results and discussion .....	77
4.3.1 Preparation and characterization of clofazimine-loaded PVP- <i>b</i> -PVAc block copolymer.....	77
4.3.2 Size distribution and morphology of clofazimine-loaded PVP- <i>b</i> -PVAc.....	79
4.3.3 Drug loading capacity and encapsulation efficiency .....	82
4.3.4 Stability studies of clofazimine-loaded PVP- <i>b</i> -PVAc .....	86
4.4 Conclusion .....	88
4.5 References.....	89

#### **Chapter 5: *In vitro* cytotoxicity and cellular uptake of PVP-*b*-PVAc**

5.1 Introduction.....	91
5.2 Materials and methods .....	95
5.2.1 Materials .....	95
5.2.2 Cell culture and culture conditions .....	95
5.2.3 <i>In vitro</i> cytotoxicity assay.....	95
5.2.4 Synthesis of fluorescently labeled PVP- <i>b</i> -PVAc.....	96
5.2.5 Preparation of perylene red-loaded PVP- <i>b</i> -PVAc .....	97
5.2.6 Cellular uptake .....	97
5.3 Results and discussion .....	98

5.3.1 <i>In vitro</i> cytotoxicity studies .....	98
5.3.2 Cellular uptake studies of fluorescently labeled PVP- <i>b</i> -PVAc .....	103
5.4 Conclusion .....	109
5.5 References.....	110

**Chapter 6: Summary and Perspectives**

6.1 Summary .....	113
6.2 Perspectives.....	116
6.3 References.....	119

## List of acronyms

AIBN	Azobisisobutyronitrile
ATRP	Atom transfer radical polymerization
CI	Combination Index Analysis
CMC	Critical micelle concentration
CRP	Controlled radical polymerization
DDI	Distilled deionized water
DLS	Dynamic light scattering
DMEM	Dulbecco's modification of Eagle's Medium
ELSD	Evaporative light scattering detector
EPR	Enhanced permeation and retention
FRDC	Fixed ratio drug combination
FRET	Forster resonance emission transfer
FCS	Fetal calf serum
GPEC	Gradient polymer elution chromatography
MDR	Multi-drug-resistance
MPS	Mononuclear phagocytic system
MTT	(4,5-dimethylthiazol-2-yl)-2,5-diphenyltetrazolium bromide
MADIX	Macromolecular design via the interchange of xanthate
MWCO	Molecular weight cut-off
NMP	Nitroxide mediated polymerization
NVP	<i>N</i> -vinyl pyrrolidone
NMR	Nuclear magnetic resonance
PBS	Phosphate buffered saline
PTX	Paclitaxel
PVP	poly( <i>N</i> -vinylpyrrolidone)
PVAc	poly(vinyl acetate)
RAFT	Reversible addition-fragmentation transfer
RES	Reticulo-endothelial system
RI	Refractive index
SFRP	Stable free radical polymerization

SLS	Static light scattering
SEC	Size exclusion chromatography
TCEP	tris(2-carboxyethyl)phosphine
TEM	Transmission electron microscopy
UV	Ultraviolet
VAc	Vinyl acetate

### List of Symbols

$A_2$	virial coefficient
$D$	dispersity
$I$	scattering intensity
$M_n$	number average molar mass
$M_{w (particle)}$	weight average molecular weight of particle
$N_A$	Avagadro's number
$R_h$	Hydrodynamic radius
$R_g$	Radius of gyration
$R$	Rayleigh ratio
$t$	time
$T$	absolute temperature
$Z_{Ave}$	Z-average particle size
$\alpha$	conversion
$\rho$	density
$\theta$	angle of measurement
$\eta$	viscosity of solution
$\chi$	Flory Huggins interaction parameter
$\lambda$	wavelength of the light in vacuum
$q$	scattering vector

## List of Schemes

**Scheme 1:** Amphiphilic block copolymers self-assemble into core-shell or vesicular structures in aqueous environment. For spherical micelles the hydrophilic shell stabilizes the micelle and protects the hydrophobic core which acts as a depot for hydrophobic guest molecules (top). Vesicle structures have a bilayer membrane and hydrophilic core. The hydrophilic core acts as a depot for hydrophilic drugs and the hydrophobic bilayer membrane, for hydrophobic drugs (enlarged region)

**Scheme 2.1:** Main equilibrium of the RAFT process

**Scheme 3.1:** Two-step reaction procedure for the synthesis of PVP-*b*-PVAc block copolymers

## List of Tables

**Table 2.1:** Various drug delivery carriers for the solubilisation and delivery of therapeutic agents

**Table 2.2:** Selection of hydrophilic and hydrophobic polymers often used for the preparation of micelles or vesicles as drug carriers

**Table 3.1:** Polymerization conditions, conversion and molecular weight of PVP macro-RAFT-agent

**Table 3.2:** Synthesis of PVP and PVP-*b*-PVAc block copolymers with different PVAc block length

**Table 3.3:** Particle size of PVP-*b*-PVAc block copolymers of varying PVAc block length determined by DLS and TEM

**Table 3.4:** Physicochemical parameters of PVP-*b*-PVAc block copolymers obtained by SLS and DLS

**Table 4.1:** Particle sizes of unloaded and drug-loaded PVP-*b*-PVAc (20 % (w/w) clofazimine/PVP-*b*-PVAc) measured by DLS analysis

## List of Figures

**Figure 1:** Four main divisions of “nanomedicine”

**Figure 2.1:** Particle sizes of various colloidal drug carrier systems

**Figure 2.2:** TEM images illustrating the effect of block length on the morphology of micelles: a) vesicles from an aqueous solution of the diblock copolymer PS<sub>240</sub>-*b*-PEO<sub>15</sub> b) rodlike and spherical structures from an aqueous solution of the diblock copolymer PS<sub>240</sub>-*b*-PEO<sub>80</sub>

**Figure 2.3:** Schematic representation of polymer micelles

**Figure 2.4:** TEM image (left) and schematic representation (right) of a polymer vesicle

**Figure 2.5:** Schematic representation of the EPR effect- the nonfunctionalised micelles or vesicles extravastate in the leaky tumor vasculatures

**Figure 2.6:** Illustration of the dialysis method for drug encapsulation into resulting in drug-loaded micelles or vesicles

**Figure 2.7:** Schematic representation of cellular uptake and release of the hydrophobic drug from the polymer carrier

**Figure 3.1:** <sup>1</sup>H NMR spectrum of PVP macro-RAFT agent in CDCl<sub>3</sub>

**Figure 3.2:** <sup>1</sup>H NMR spectrum of PVP<sub>90</sub>-*b*-PVAc<sub>290</sub> in CDCl<sub>3</sub>



**Figure 3.3:** Normalized SEC chromatograms for the chain extension of starting homopolymer chain-transfer agent (PVP macro-RAFT) with vinyl acetate

**Figure 3.4:**  $^1\text{H}$  NMR spectra of a) PVP-*b*-PVAc in  $\text{CDCl}_3$  not dialyzed (unpurified) b) PVP-*b*-PVAc in  $\text{CDCl}_3$  dialyzed (purified)

**Figure 3.5:** Gradient polymer elution chromatogram of a) PVP<sub>90</sub> prepared in bulk in the presence of S-2-(cyano-2-propyl)-(O-ethyl xanthate) b) PVAc<sub>200</sub> prepared in bulk in the presence of S-(2-ethylpropionate)-(O-ethyl xanthate) c) PVP<sub>90</sub>-*b*-PVAc<sub>290</sub> (-), PVP<sub>90</sub>-*b*-PVAc<sub>210</sub> (- -) block copolymers

**Figure 3.6:** Gradient polymer elution chromatogram of a) mixture of PVP<sub>90</sub>, PVAc<sub>200</sub> and PVP-*b*-PVAc<sub>290</sub> b) PVP-*b*-PVAc<sub>290</sub> (-) and PVP-*b*-PVAc<sub>210</sub> (- -) of varying PVAc block length

**Figure 3.7:**  $^1\text{H}$  NMR spectra of a) PVP-*b*-PVAc in  $\text{CDCl}_3$  b) PVP-*b*-PVAc in  $\text{D}_2\text{O}$

**Figure 3.8:** Fluorescence excitation spectra of pyrene ( $6.0 \times 10^{-7}$  M) containing PVP<sub>90</sub>-*b*-PVAc<sub>290</sub> at different concentrations (0.0001 – 1 mg/mL)

**Figure 3.9:** Fluorescence intensity ratio  $I_{338}/I_{336}$  for pyrene as a function of logarithm of concentration for PVP<sub>90</sub>-*b*-PVAc<sub>290</sub>. The CMC was calculated from the intersection of the horizontal line at low polymer concentration and the tangent of the curve at high polymer concentration

**Figure 3.10:** DLS size distributions of PVP-*b*-PVAc of varying PVAc block length

**Figure 3.11:** TEM image of PVP<sub>90</sub>-*b*-PVAc<sub>290</sub> block copolymer. Black corresponds to hydrophobic region (bilayer) and grey to hydrophilic regions. The insert is a schematic representation of the self-assembled, vesicular-like structure of the PVP-*b*-PVAc

**Figure 3.12:** Zimm plot for PVP<sub>90</sub>-*b*-PVAc<sub>210</sub> extrapolated to zero angle and zero concentration in water at 25 °C. Squares represent experimental data, measurements at four different concentrations, from 50 ° – 120 °. Circles represent simulated data

**Figure 3.13:** Stability of PVP<sub>90</sub>-*b*-PVAc<sub>290</sub> (left) and PVP-*b*-PVAc<sub>210</sub> micelles (right) at 37 °C in PBS (pH 7.5) and PBS/FCS as determined by DLS

**Figure 4.1:** Chemical structure of parent compound clofazimine and its derivatives (riminophenazines) R1 and R2 are chlorine substituted rings

**Figure 4.2:** Schematic representation of the encapsulation of clofazimine into PVP-*b*-PVAc polymer vesicles

**Figure 4.3:** A) Clofazimine insoluble in aqueous media B) Clofazimine physically encapsulated in PVP-*b*-PVAc in aqueous media

**Figure 4.4:** <sup>1</sup>H NMR spectra of a) clofazimine-loaded PVP<sub>90</sub>-*b*-PVAc<sub>210</sub> in DMSO-*d*<sub>6</sub> b) clofazimine-loaded PVP<sub>90</sub>-*b*-PVAc<sub>210</sub> in D<sub>2</sub>O

**Figure 4.5:** Size distribution of clofazimine-loaded PVP-*b*-PVAc of varying PVAc block length

**Figure 4.6:** The effect of different drug feed ratios (% (w/w) clofazimine/polymer) on the particle size of clofazimine-loaded PVP-*b*-PVAc of varying PVAc block length. Error bars represent the standard deviation (n = 3)

**Figure 4.7:** TEM image of clofazimine-loaded PVP<sub>90</sub>-*b*-PVAc<sub>290</sub> showing vesicular structure

**Figure 4.8:** Drug loading capacity and encapsulation efficiency of clofazimine-loaded PVP-*b*-PVAc of different hydrophobic PVAc block length. Feed ratios were 5, 10, 20, or 30 weight percentage (% w/w) of clofazimine relative to PVP-*b*-PVAc. Error bars represent the standard deviation (n = 3)

**Figure 4.9:** Drug loading capacity and encapsulation efficiency of paclitaxel-loaded PVP-*b*-PVAc of different hydrophobic PVAc block length. Feed ratios were 5, 10, or 20, weight percentage (% w/w) of PTX relative to PVP-*b*-PVAc. Error bars present the standard deviation (n = 3)

**Figure 4.10:** Particle size ( $Z_{ave}$ ) of clofazimine-loaded (a) PVP<sub>90</sub>-*b*-PVAc<sub>290</sub> (b) PVP<sub>90</sub>-*b*-PVAc<sub>210</sub> in (▲) PBS pH 7.4 and (●) PBS/FCS pH 7.4, as a function of time at 37 °C

**Figure 5.1:** Cell viability (MTT) assays of (a) PVP-*b*-PVAc (b) clofazimine-loaded PVP-*b*-PVAc against MCF12A breast cell line (Mean ±SD n=3) after 24 hours

**Figure 5.2:** Cell viability (MTT) assay of PVP-*b*-PVAc against MDR MDA-MB-231 breast cancer cell line (Mean ±SD n=3) after 24 hours

**Figure 5.3:** Cell viability (MTT) assays of free drug and clofazimine-loaded PVP-*b*-PVAc against MDR MDA-MB-231 breast cancer cell line (Mean ±SD n=3 ) after 24 hours

**Figure 5.4:** Cell viability (MTT) assays of free drug and PTX-loaded PVP-*b*-PVAc against MDR MDA-MB-231 breast cancer cell line (Mean ±SD n=3 ) after 24 hours

**Figure 5.5:** Reaction scheme for the attachment of fluorescein maleimide, a thiol-reactive fluorescein dye, to PVP-*b*-PVAc

**Figure 5.6:** Fluorescence micrographs of MDA-MB-231 breast cancer cells incubated with perylene red (control) for A)  $t = 0$  hr B)  $t = 6$  hr C) Fluorescein maleimide (control)

**Figure 5.7:** Fluorescence micrographs of MDA-MB-231 breast cancer cells incubated with: (A) fluorescently labeled perylene red-loaded PVP-*b*-PVAc at 0 hr. (B) after 3h (C) after 6h. For each panel, images from left to right show the cells with nuclear staining by Hoechst 33342 and fluorescein-maleimide labeled PVP-*b*-PVAc, fluorescein-maleimide labeled PVP-*b*-PVAc encapsulated with perylene red, and the overlays of both images. Scale bars correspond to 20  $\mu\text{m}$

**Figure 5.8:** Slice viewer plots of fluorescently labeled PVP-*b*-PVAc loaded with perylene red in MDA-MB-231 breast cancer cells (A)  $t = 0$  (B)  $t = 6$  hr

**Figure 5.9:** Iso-surface projection plots of fluorescently labeled PVP-*b*-PVAc loaded with perylene red in MDA-MB-231 breast cancer cells (A)  $t = 0$  (B)  $t = 3$ hr (C)  $t = 6$  hr.

## Chapter 1 Introduction and objectives

### 1. Introduction

Over the past years, a large variety of synthetic polymeric materials have been used for biomedical applications. With the advent and development of controlled radical polymerization, polymers of controlled architecture such as diblock, triblock, star-shaped and branched structures have been prepared to accommodate the needs for applications in very specialized fields of medicine.<sup>1</sup> These polymer materials have been used in the various sectors of “nanomedicine<sup>2-4</sup>” as illustrated in Figure 1

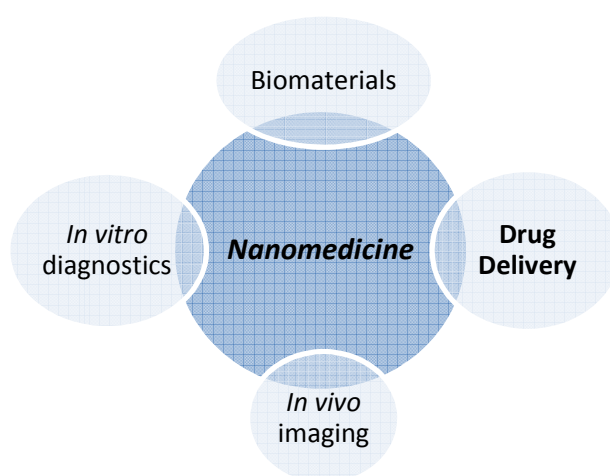


**Figure 1:** Four main divisions of “nanomedicine”

In the study presented, the application of polymers in the field of drug delivery is of particular interest. Currently, more than 40 % of novel drugs for life-threatening and genetic diseases are found to be hydrophobic in nature.<sup>5,6</sup> This is a major problem faced by the pharmaceutical drug formulation industry. Intravenous administration of these hydrophobic drugs often results in precipitation and degradation in the bloodstream without reaching the target site, resulting in undesirable side effects. The poor solubility of these hydrophobic molecules therefore poses problems and limits their possible application as drugs. In addition, most of the poorly soluble drugs including the current formulations used to solubilize the drugs have unacceptable levels of toxicity. This further limits them to their potential use. As a result, a large number of potentially beneficial drugs do not reach clinical trials due to their poor bioavailability.

To overcome this hurdle, various polymers such as polymer-drug conjugates,<sup>7,8</sup> liposomes,<sup>9</sup> polymer micelles<sup>10,11</sup> and polymer vesicles,<sup>12,13</sup> have been developed as carriers to administer hydrophobic drugs. The above mentioned polymer systems are not solely used as solubilizing agents for these hydrophobic pharmaceutical agents. Other existing challenges include the stabilization and ability for controlled and sustained delivery of these pharmaceutical agents to the desired biological sites, which will further improve the therapeutic efficacy of these active pharmaceutical agents.<sup>14</sup> A drug delivery system can therefore be defined as “*one in which a drug (one component of the system) is integrated with another chemical, or a drug administration device, or a drug administration process to control the rate of drug release, the tissue site of drug release, or both.*”<sup>15</sup>”

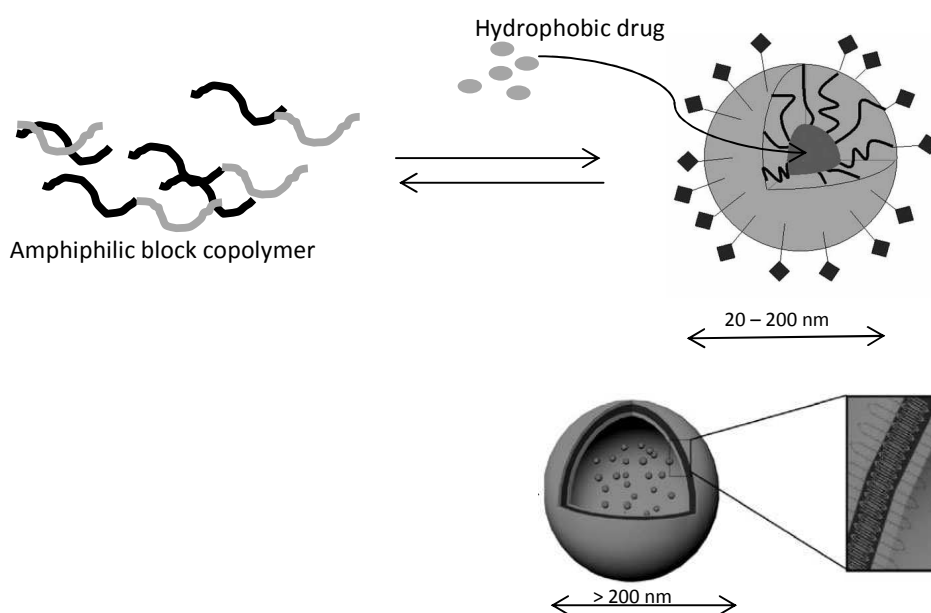
## **2. Amphiphilic block copolymers for drug delivery**

Amphiphilic block copolymers are composed of a hydrophilic segment and a hydrophobic segment. When the polymer is dissolved in selective solvents above their so-called critical micelle concentration (CMC), they self-assemble into well-defined structures as illustrated in Scheme 1. Depending on the molecular characteristics and molecular weight of the constituting blocks, amphiphilic block copolymers can self-assemble into various ordered structures such as spherical, worm-like or rod-like micelles, lamellar structures or vesicles.<sup>16</sup> The hydrophobic or electrostatic interaction is the driving force behind the segregation of the core from the surrounding media resulting in core-shell structures.

Polymer micelles are composed of an outer hydrophilic shell and an inner hydrophobic core. The hydrophilic shell shields the hydrophobic core and protects it from interactions with blood components. This further allows for prolonged circulation times after intravenous administration, which is a prerequisite for a drug delivery system. The hydrophobic core acts as a reservoir to accommodate bioactive guest molecules such as hydrophobic drugs, which can either be physically encapsulated or covalently bound to the core.<sup>17,18</sup> On the other hand, polymer vesicles (or polymersomes), are usually hollow spheres with a hydrophobic bilayer membrane and hydrophilic internal and external coronas (Scheme 1). The hydrated hydrophilic coronas are expressed on both the inside and outside of the hydrophobic membrane.

Therefore, vesicles have a hydrophilic core, which can accommodate hydrophilic guest molecules and a hydrophobic bilayer membrane which can be used to solubilize and retain hydrophobic guest molecules. Both the properties of the hydrophilic segment and the hydrophobic segment influence the size, stability and the performance of a vesicle as drug carrier.

The attractive properties of amphiphilic block polymers have found great interest and promise in the delivery of anticancer agents, anti-inflammatory, antiviral, antibacterial and imaging agents.<sup>19</sup>



**Scheme 1:** Amphiphilic block copolymers self-assemble into core-shell or vesicular structures in aqueous environment. For spherical micelles the hydrophilic shell stabilizes the micelle and protects the hydrophobic core which acts as a depot for hydrophobic guest molecules (top). Vesicle structures have a bilayer membrane and hydrophilic core. The hydrophilic core acts as a depot for hydrophilic drugs and the hydrophobic bilayer membrane, for hydrophobic drugs (enlarged region)<sup>4</sup>

The dissertation focuses on the development of an amphiphilic block copolymer comprised of a hydrophilic poly(*N*-vinylpyrrolidone) (PVP) segment and a hydrophobic poly(vinyl acetate) (PVAc) segment. PVP is highly hydrophilic, flexible, non-toxic and biocompatible making it an attractive candidate for application in drug delivery. PVP has previously found application in polymer-drug conjugates and polymeric micelles for the solubilization of hydrophobic drugs,<sup>20</sup>

hydrogels,<sup>21</sup> tissue engineering<sup>22,23</sup> and in pharmaceutical formulations.<sup>24</sup> Interestingly, its application as a shell-forming block in polymeric micelles has shown superior properties to poly(ethylene glycol) (PEG), the most commonly used hydrophilic polymer in drug delivery systems.<sup>25</sup> PVAc is a hydrophobic polymer used in applications ranging from adhesives, paints, additives to pharmaceuticals. PVAc has found use within pharmaceuticals as a precursor to poly(vinyl alcohol) (PVA), a water-soluble, non-toxic polymer with bio-adhesive properties. Block copolymers of PVP-*b*-PVAc have been previously reported in the literature.<sup>26,27,28</sup> To our knowledge no publications have been documented on the application and ability of PVP-*b*-PVAc block copolymers as carriers for hydrophobic anti-cancer drugs.

### **3. Objective of dissertation**

The purpose of the study was to investigate the potential of PVP-*b*-PVAc block copolymers as a drug delivery vehicle for hydrophobic anti-cancer drugs.

The objectives of the study can be summarized as follows:

1. To synthesize amphiphilic block copolymers of PVP-*b*-PVAc via controlled radical polymerization (CRP).
2. To study the self-assembly behaviour of the PVP-*b*-PVAc block copolymers in aqueous media.
3. To establish the system as a suitable drug carrier by investigating the physiochemical and biological properties of the amphiphilic block copolymers.
4. To demonstrate the potential of PVP-*b*-PVAc block copolymers as carriers for hydrophobic drugs by the physical encapsulation of clofazimine (model drug) and a widely used anti-cancer drug, paclitaxel, into the PVP-*b*-PVAc aggregates.
5. To conduct *in vitro* cytotoxicity and cellular uptake studies of the drug-loaded polymer carrier in breast cancer cells to provide evidence of their antitumor efficacy.



#### **4. Outline of dissertation**

The dissertation comprises six chapters.

##### **Chapter 1 Introduction and objectives**

A brief introduction to the application of amphiphilic block copolymers in drug delivery is described. The objectives of the research project are presented.

##### **Chapter 2 Historical and theory**

A literature review that provides a comprehensive overview of the critical features of polymer drug carriers, including stability, drug loading, drug internalization and drug release of the incorporated hydrophobic drugs is presented.

##### **Chapter 3 Synthesis, characterization and self-assembly of poly(vinylpyrrolidone)-*b*-poly(vinyl acetate)**

The chapter addresses the synthesis and characterization of PVP-*b*-PVAc block copolymers. The physicochemical properties relating to their potential as drug carriers for hydrophobic anti-cancer drugs are described.

##### **Chapter 4 Poly(vinylpyrrolidone)-*b*-poly(vinyl acetate): A potential drug carrier**

The encapsulation of a model drug (clofazimine) and a common anti-cancer drug (paclitaxel) into PVP-*b*-PVAc aggregates is reported. The drug-loaded PVP-*b*-PVAc are characterized regarding particle size, morphology, stability and drug loading capacity in order to assess their feasibility as a drug carrier.

##### **Chapter 5 *In vitro* cytotoxicity and cellular uptake of PVP-*b*-PVAc**

*In vitro* cytotoxicity and cellular uptake of the PVP-*b*-PVAc carrier are presented and discussed.

##### **Chapter 6 Summary and Perspectives**

The chapter provides a summary of the work described in this dissertation. Suggestions for future research for the development of PVP-*b*-PVAc block copolymers for anti-cancer drug delivery are also presented.

## 5. References

- (1) Grodzinski, J. J. *Polym. Adv. Technol.* **2006**, *17*, 395 - 418.
- (2) Duncan, R. *Curr. Opin. Biotechnol.* **2011**, *22*, 492 - 501.
- (3) Farokhzad, O. C.; Langer, R. *Adv. Drug Deliv. Rev.* **2006**, *58*, 1456 - 1459.
- (4) Tong, R.; Cheng, J. *Polym. Rev.* **2007**, *47*, 345 - 381.
- (5) Lipinski, C. *Amer. Pharm. Rev.* **2002**, *5*, 82 - 85.
- (6) Merisko-Liversidge, E. M.; Liversidge, G. G. *Toxicol. Pathol.* **2008**, *36*, 43 - 48.
- (7) Duncan, R. *Nat. Rev. Cancer* **2006**, *6*, 688 - 701.
- (8) Haag, R.; Kratz, F. *Angew. Makromol. Chem.* **2006**, *45*, 1198 - 1215.
- (9) Barenholz, Y. *Curr. Opin. Colloid Interface Sci.* **2001**, *6*, 66 - 77.
- (10) Mikhail, A. S.; Allen, C. J. *Control. Rel.* **2009**, *138*, 214 - 223.
- (11) Nishiyama, N.; Kataoka, K. *Pharmacol. Ther.* **2006**, *112*, 630 - 648.
- (12) Choucair, A.; Soo, P. L.; Eisenberg, A. *Langmuir* **2005**, *21*, 9308-9313.
- (13) Sanson, C.; Schatz, C.; Meins, J. L.; Soum, A.; Thévenot, J.; Garanger, E.; Lecommandoux, S. *J. Control. Rel.* **2010**, *147*, 428 - 435.
- (14) Croy, S. R.; Kwon, G. S. *Curr. Pharm. Des.* **2006**, *12*, 4669 - 4684.
- (15) Panchagnula, R. *Int. J. Pharm.* **1998**, *172*, 1 - 15.
- (16) Kwon, G. S.; Kataoka, K. *Adv. Drug Deliv. Rev.* **1995**, 295 - 309.
- (17) Allen, C.; Maysinger, D.; Eisenberg, A. *Colloids Surf., B* **1999**, *16*, 3 - 27.
- (18) Kataoka, K.; Harada, A.; Nagasaki, Y. *Adv. Drug Deliv. Rev.* **2001**, *47*, 113 - 131.
- (19) Adams, M. L.; Lavasanifar, A.; Kwon, G. S. *J Pharm. Sci.* **2003**, *92*, 1343 - 1355.
- (20) Garrec, D. L.; Gori, S.; Luo, L.; Lessard, D.; Smith, D. C.; Yessine, M.-A.; Ranger, M.; Leroux, J.-C.; Ranger, M. *J. Control. Rel.* **2004**, *99* 83 - 101.
- (21) Yu, H.; X. Xu; Chen, X.; Lu, T.; Zhang, P.; Jing, X. *J. Appl. Poly. Sci.* **2007**, *103*, 125 - 133.
- (22) Krasovskaya, S. M.; Uzhinova, L. D.; Andrianova, M. Y.; Prischenko, M. Y.; Livantsov, M. V. *Biomaterials* **1991**, *12*, 817 - 820.
- (23) Tunney, M. M.; Gorman, S. P. *Biomaterials* **2002**, *23*, 4601 - 4608.
- (24) Gaucher, G.; Asahina, K.; Wang, J.; Leroux, J. *Biomacromolecules* **2009**, *10*, 408 - 416.

- (25) Kaneda, Y.; Tsutsumi, Y.; Yoshioka, Y.; Kamada, H.; Yamamoto, Y.; Kodaira, H.; Tsunoda, S.; Okamoto, T.; Mukai, Y.; Shibata, H.; Nakagawa, S.; Mayumi, T. *Biomaterials* **2004**, *25*, 3259 - 3266.
- (26) Nguyen, T. L. U.; Eagles, K.; Davies, T. P.; Barner-Kowollik, C.; Stenzel, M. H. *J. Polym. Sci., Part A: Polym. Chem.* **2006**, *44*, 4372-4383
- (27) Pound, G.; Aguesse, F.; McLeary, J. B.; Lange, R. F. M.; Klumperman, B. *Macromolecules* **2007**, *40*, 8861 - 8871.
- (28) Fandrich, N.; Falkenhagen, J.; Weidner, S. M.; Pfeifer, D.; Staal, B.; Thunemann, A. F.; Laschewsky, A. *Macromol. Chem. Phys.* **2010**, *211*, 1678 - 1688.

## Chapter 2 Historical and theory

### 2.1 Introduction

The application of natural and synthetic polymers for medical purposes has been an area of great interest over the last decade in biomedical research.<sup>1</sup> Synthetic polymers are ideal tools for biomedical applications because they can be highly tailored in terms of composition and architecture.

In the 1990s, the use of polymer-based drugs and drug delivery systems emerged as a potential strategy in the treatment of various life-threatening diseases.<sup>2</sup> As a result of the rapid development in nanotechnology, the use of polymeric nanoparticle systems has shown potential use in drug delivery systems, more specifically in drug solubilization, controlled drug release and drug targeting. These “nanopharmaceuticals” are considered as first generation medicines and contribute to the improvement in the treatment of genetic and life-threatening diseases.<sup>3,4</sup>

Polymers applied in drug delivery systems are divided into two main classes namely the covalently linked polymer-drug conjugates and non-covalently, self-assembled conjugates. Covalently linked conjugates are polymer-drug conjugates where the polymer is covalently linked to the drug by a cleavable bond. Self-assembled, colloidal drug carrier systems include polymeric nanoparticles, micelles, vesicles, liposomes, viruses (viral nanoparticles), and organometallic compounds (nanotubes) in which the drug is physically entrapped (non-covalently bound) to the polymer. These self-assembled structures differ in terms of their particle size (10 nm – 1  $\mu$ m) and morphology (Figure 2.1). The various drug delivery systems - polymer-drug conjugates, polymer-protein conjugates, and colloidal drug delivery systems are collectively termed as “polymer therapeutics”.<sup>2</sup>

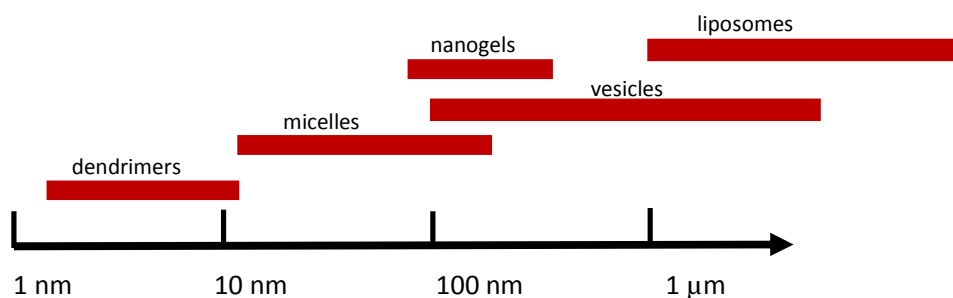


Figure 2.1: Particle sizes of various colloidal drug carrier systems

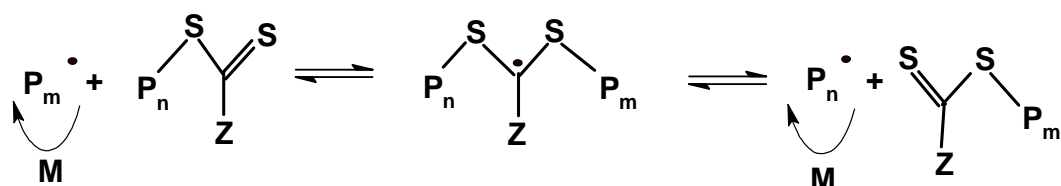
## 2.2 Controlled radical polymerization

In the mid 1970s, Ringsdorf and coworkers proposed a model for drug delivery. However, during those times the control of polymer architecture, molecular weight and molecular weight distribution was an obstacle, which limited their ability to develop well-tuned drug delivery vehicles.<sup>5,6</sup> Controlled radical polymerization (CRP) was developed in the recent past as an answer to the increasing demand for new materials with controlled properties. This concept is a valuable approach to provide a large range of polymers with well-defined molecular characteristics (length, composition and architecture) under not very demanding conditions. The development of CRP therefore, now allows for control over several necessary design criteria for well-tuned drug delivery systems. CRP techniques include Nitroxide-mediated Polymerization (NMP), Atom Transfer Radical Polymerization (ATRP), Reversible Addition/Fragmentation chain Transfer (RAFT), Macromolecular Design via the Interchange of Xanthate (MADIX), Organotellurium-mediated radical polymerization (TERP) and Cobalt-mediated radical polymerization (CMRP). These techniques are CRP techniques that are currently most popular and are being used to control polymer molecular weight, polymer compositions, polymer topologies, and functionalities.

### 2.2.1 RAFT/MADIX-mediated polymerization

In the late 1990s, the concept of RAFT/MADIX-mediated polymerization was first reported. The CSIRO group reported on the use of thiocarbonyl thio compounds such as dithioesters, trithiocarbonates and dithiocarbamates as chain transfer agents<sup>7,8</sup> (CTAs) while Zard's group claimed the term MADIX, for the use of xanthates as CTAs.<sup>7,9,10</sup>

MADIX proceeds via an identical mechanism as the CSIRO-reported RAFT process. The elementary steps of initiation, propagation and termination are present in the mechanism. The important equilibrium step is illustrated in Scheme 2.1. Rapid equilibrium between the active propagating radicals ( $P_m^\bullet$  and  $P_n^\bullet$ ) and the dormant species end-capped with the CTA ensures equal probability for chains to grow. The mechanism is well documented in the literature and will therefore not be discussed in detail.<sup>10,11</sup>



**Scheme 2.1:** Main equilibrium of the RAFT process

### 2.2.2 Xanthate-mediated synthesis of poly(*N*-vinylpyrrolidone) (PVP) and poly(vinyl acetate) (PVAc)

PVP is an attractive water-soluble and biocompatible polymer and has been extensively used in pharmaceuticals, cosmetics, foods, printing inks, textiles, and many more diverse applications. PVAc is a water-insoluble polymer and it is used in applications ranging from adhesives, paints, concrete additives to pharmaceuticals. CRP of most conjugated monomers has shown to be very effective, however for non-conjugated monomers, such as VAc<sup>12,13</sup> and NVP, CRP is more challenging. The limited success to control these monomers is speculated to be due to the high reactivity of the chain-end radicals which are prone to side-reactions resulting in dead polymer chains.<sup>14</sup>

NVP can be polymerized by conventional radical polymerization to high molecular weight. CRP techniques such as ATRP,<sup>15</sup> NMP<sup>16</sup> and organostibine-mediated polymerization<sup>17</sup> have been reported for the CRP of NVP. Xanthates have also been identified as being suitable for polymerization of NVP resulting in narrow molar mass distributions. The group of Kamigaito and Okamoto published the first paper on xanthate-mediated polymerization of NVP.<sup>18</sup> Since then, other xanthates have been reported. Pound *et al.*<sup>19</sup> conducted a detailed study on NVP polymerization using various *O*-ethyl xanthates with different R groups including PEG-based chains. The results showed good control of the molecular weight with narrow molar mass distributions.

The synthesis of PVAc with controlled molecular weight and functionality has become an attractive goal. Although there has been limited success for the control of PVAc, several studies in the literature have reported on the use of CRP of VAc. CRP techniques for VAc include

MADIX/RAFT,<sup>20-22</sup> iron-catalysed,<sup>23</sup> cobalt-mediated,<sup>24,25</sup> organotellurium and organostibine-mediated polymerization.<sup>26</sup> Successful control of VAc polymerization has only been reported using xanthates as mediating agent under a RAFT mechanism.<sup>20</sup>

Many researchers have reported the use of CRP for the synthesis of well-defined block copolymers and (end) functional polymers producing synthetic biomaterials and therapeutics.<sup>6</sup> Amphiphilic block copolymers consisting of a hydrophilic monomer, (*e.g.* NVP) and a hydrophobic monomer (*e.g.* VAc) have been reported previously. The first examples of block copolymers containing a PVP block prepared via CRP were reported recently, with the syntheses of poly(styrene)-*b*-poly(*N*-vinylpyrrolidone) and poly-(methyl methacrylate)-*b*-poly(*N*-vinylpyrrolidone) via organostibine-mediated polymerization.<sup>27</sup> Matyjaszewski *et al.*<sup>28</sup> studied CMRP for NVP and VAc. The results showed poor control for NVP compared to VAc, however, statistical PVAc-*co*-PVP copolymers were synthesized in a controlled manner. Debuigne and coworkers showed the polymerization of NVP using VAc macroinitiators of different chain lengths.<sup>29</sup> NVP was effectively initiated by various PVAc macroinitiators and well-defined amphiphilic block copolymers (molecular weights 40 000 – 60 000 g/mol,  $\bar{D} = 1.4 - 1.5$ ) were synthesized by CMRP. Recently Fandrich *et al.*<sup>30</sup> synthesized amphiphilic block copolymers consisting of PVP and PVAc via a xanthate-mediated polymerization system. PVP macroinitiator was synthesized using *S*-2-propionic acid *O*-ethyl xanthate and further used for chain extension with VAc. Random copolymers of P(VP-*co*-VAc) instead of well-defined PVP-*b*-PVAc block copolymers were obtained. Their results indicated that side reactions during RAFT polymerization have a strong influence over the control of the molar masses of the block copolymers.

The study presented in this dissertation focuses on the use of PVP-*b*-PVAc block copolymers as potential drug carriers. CRP is therefore favorable and advantageous as it allows one to tailor-make polymers to fulfil the requirements for a suitable drug carrier system. However, in order to design a drug carrier, it is necessary to understand the requirements for the polymers to be used. In the section to follow, an overview of drug carriers mainly polymer micelles and vesicles will be given.

### **2.3 Amphiphilic block copolymers in anti-cancer drug delivery**

Chemotherapy has been a prominent and common way for treating cancer. However, there are several obstacles that make chemotherapy challenging. Many therapeutic compounds are available as drug candidates but one third of them are poorly water-soluble making delivery of these agents to targeted sites challenging.<sup>31,32</sup> Furthermore the inability to deliver adequate doses of anti-cancer drugs to tumors in the body is a major obstacle in chemotherapy. The high toxicity of these drugs limits their dose which is required in order for the treatment to be effective.<sup>33</sup> Various drug delivery systems based on polymeric nanomaterials are currently under development in biomedical research in order to reduce toxicity, to minimize drug degradation and loss upon intravenous administration, to prevent harmful side effects and to increase the drug bioavailability. Several methods are available to improve the solubility of these hydrophobic agents and simultaneously act as drug carrier for drug delivery.<sup>34</sup> One of the most widely used drug delivery systems are amphiphilic block copolymers that have the ability to self-assemble in aqueous environment to form polymer micelles or vesicles.<sup>35</sup> A few examples have been briefly described in Table 2.1 with each method having its own advantages and disadvantages.



**Table 2.1:** Various drug delivery carriers for the solubilisation and delivery of therapeutic agents

<b>Drug carrier</b>	<b>Structure</b>	<b>Advantages</b>	<b>Disadvantages</b>
<b>Polymer-drug conjugates</b>	Drugs are conjugated to the side chain of a linear polymer via a labile bond	Administered by injection or infusion  Multifunctionality  Polymer backbone can be modified by adding targeting ligands or imaging agents	Chemical modification of drug could result in loss of bioactivity of the drug  Only drugs with reactive side groups are potential candidates
<b>Polymer micelles / Polymersomes (vesicles)</b>	Amphiphilic block copolymers assemble and form micelles/vesicles in aqueous environment	Administered by injection or infusion  Well defined structures. Chemical composition, molecular weight and block length ratios can be tailored, allowing control of the size and morphology  Targeting potential -Active and passive targeting (EPR effect)  Suitable carrier for water-soluble/insoluble drug (or multiple drugs in the same carrier)  Variety of techniques can be used to encapsulate drug  Ease of functional modification => control and stimuli-response drug release	Often limited loading capacity and efficiency  Difficulty in transporting through cell membrane  Instability in aqueous environment and in the presence of blood components
<b>Liposomes</b>	Self-assembled colloidal structures made of lipid bilayers	Administered by injection or infusion  Targeting potential  Ease of modification	Often limited loading capacity  Instability in the presence of blood components

### 2.3.1 Amphiphilic block copolymers as drug delivery carriers

In the 1970s Ringsdorf was the first to report on the idea of the application of block copolymer micelles for sustained release of drugs in drug delivery.<sup>36,37</sup> In their approach, the drug was covalently linked to one of the blocks of the copolymer via a cleavable linkage. In the late 1980s the concept termed “micellar microcontainers” was introduced by the group of Kabanov.<sup>38</sup> In their approach, the drug was non-covalently fixed in the hydrophobic core of block copolymers micelles. Thereafter, much research has been reported by the groups of Kataoka and Kabanov on ‘micellar microcontainers’. To date, it has become the preferred strategy in drug delivery.<sup>39</sup>

### 2.3.2 Amphiphilic block copolymer micelles and vesicles

In aqueous solution, AB block copolymers consisting of both a hydrophilic and a hydrophobic block self-assemble into distinct nano-sized structures which range between 10 – 200 nm. The micellar aggregates can adopt different morphologies, such as spherical, rod-like, core-corona, vesicle, and worm-like micelles depending on the length of the hydrophilic and the hydrophobic segments, the solvent system and the preparation method (Figure 2.2).<sup>40,41</sup>

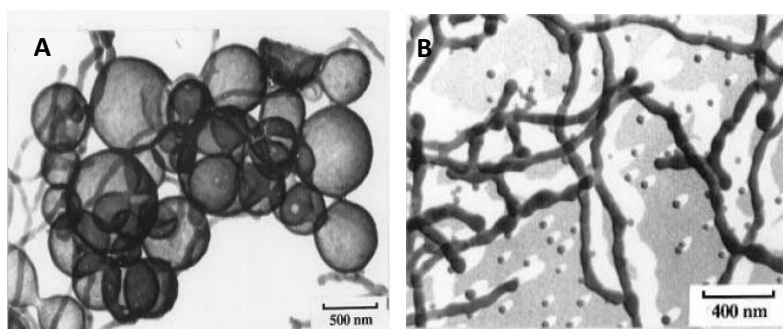


**Figure 2.2** TEM images illustrating the effect of block length on the morphology of micelles: a) vesicles from an aqueous solution of the diblock copolymer  $PS_{240}\text{-}b\text{-}PEO_{15}$  b) rodlike and spherical structures from an aqueous solution of the diblock copolymer  $PS_{240}\text{-}b\text{-}PEO_{80}$ <sup>42</sup>

Spherical micelles are made up of a hydrophilic outer corona and an inner hydrophobic core as illustrated in Figure 2.3. The micelles are structured in a way that the outer corona of the micelle is made up of components that are unreactive towards the blood or tissue components. The corona of the micelles acts as a protective shell that prevents hydrolysis and enzymatic degradation of the drug during transport. It also prevents the drug from being

recognized by the reticuloendothelial system (RES) (a class of cells responsible for clearing foreign substances and pathogens from the bloodstream) thereby prolonging the circulation time of the drug in the bloodstream. The hydrophobic core acts as a reservoir in which the hydrophobic drug or multiple drugs<sup>43</sup> can be loaded and carried to the target site. For example, paclitaxel (PTX) is a poorly water-soluble anti-cancer drug. To improve the drug solubility, surfactant or solvent (such as an ethanol/cremophor mixture for PTX) is normally used in combination with these drugs.<sup>44</sup> However, most surfactants and solvents are not fully biocompatible. They are toxic to the human body and result in undesirable side-effects. Therefore, the use of polymer micelles to improve the solubility of the drug (replacing the toxic solubilising agent and thus allowing administration of higher doses), is an alternative approach. Soga *et al.*<sup>45</sup> showed that the water solubility of the anti-cancer drug PTX, increased from 0.0015 mg/mL to 2 mg/mL by the encapsulation into a polymer micelle. This is an important improvement in drug delivery as it increases the availability of the drug for action within the tumor. Furthermore it allows the drug to be administered, transported and delivered more effectively to the desired area through the bloodstream which is mostly comprised of water. Several anti-cancer drugs and polynucleotides have been effectively solubilised by polymeric micelles and have demonstrated superior properties and lower toxicity compared to free drugs.

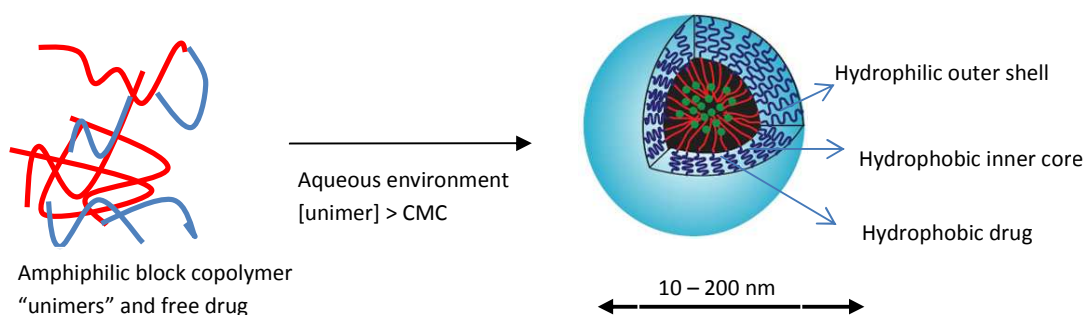


**Figure 2.3:** Schematic representation of polymer micelles<sup>43</sup>

Polymer micelles can also be functionalized to improve the physicochemical and biological properties of the self-assembled drug carriers. Substituents can be attached to both hydrophobic and hydrophilic segments in order to start crosslinking in the core or corona region respectively. The second use of substituents might be to enhance the functionality of the micelle surface. Furthermore, the micelles can be chemically modified without changing the physicochemical

properties of the micelles, which makes them unique and “superior” over other drug carrier systems.<sup>46</sup>

Polymer vesicles have attracted increased attention in recent years due to their similarity to liposomes. Compared to liposomes that are composed of low molecular weight phospholipids or surfactants, vesicles are based on high molecular weight amphiphilic block copolymers.<sup>34</sup> Polymer vesicles are hollow, lamellar spherical structures with a hydrophilic surface a hydrophobic membrane and an aqueous interior as illustrated in Figure 2.4. Like micelles, vesicles also have a wide range of morphological variations (*e.g.* onion-like vesicles, elongated tubular vesicles and large compound vesicles, flower-like vesicles).<sup>47</sup> They range in diameter from 0.1 – 1  $\mu\text{m}$  and consist of a bilayer membrane having physical and chemical stability which is advantageous for many applications such as drug delivery.<sup>48</sup>

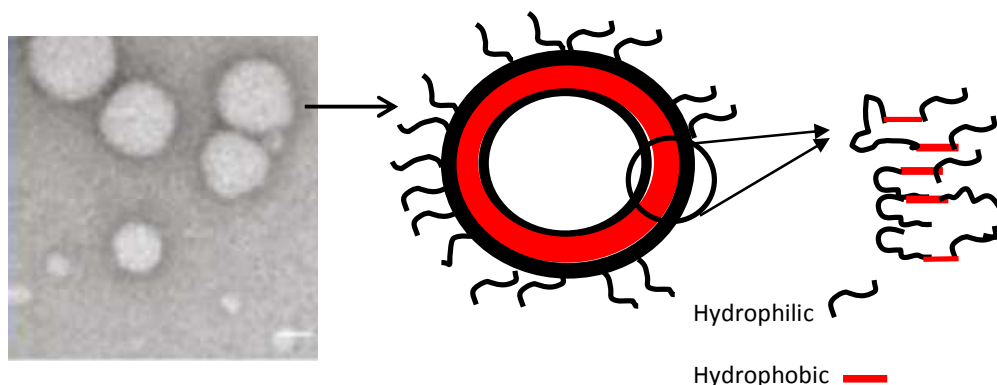


**Figure 2.4:** TEM image (left) and schematic representation (right) of a polymer vesicle<sup>49</sup>

Unlike polymer micelles, which are mostly used for loading hydrophobic drugs (having only a hydrophobic core), vesicles are capable of being loaded with both hydrophilic drugs (within the aqueous interior) and hydrophobic drugs (in the bilayer membrane). The bilayer membrane provides a physical barrier that isolates the encapsulated molecules from the external environment. In recent years, combination therapy whereby a combination of multiple drugs as opposed to a single drug are used for cancer treatment has gained significant interest. The synergistic effects of cancer drugs has been extensively investigated and has found great success.<sup>50</sup> Ahmed *et al.*<sup>51</sup> used PEG-*b*-PLA and PEG-*b*-polybutadiene (PEG-*b*-PBD) for the delivery of two anticancer drugs. The relatively hydrophilic drug doxorubicin (DOX) was located in the lumen, whereas the hydrophobic drug paclitaxel (PTX) was entrapped in the bilayer. *In vitro* experiments showed that after one day, 80 % of DOX and 60 % of PTX were

released from the vesicles. *In vivo* studies on human breast tumors in nude mice showed that higher concentrations of drug could be administered for the DOX and PTX-loaded vesicles compared to the free drug cocktail. Eisenberg and co-workers synthesized DOX-loaded vesicles that were able to release the drug at a slower rate (30 % in 5 minutes) and in a controlled manner compared to free DOX (80 % in 5 minutes).<sup>52</sup>

### 2.3.3 Active and passive drug targeting

The application of amphiphilic block copolymers as drug carriers is advantageous in that they are able to solubilise hydrophobic drugs and be used in *passive* and *active* targeting. Polymer drug carriers such as micelles and vesicles have shown to target tumors through passive accumulation through the enhanced permeation and retention (EPR) effect. This concept was coined by Maeda *et al.* in 1989.<sup>53</sup> The EPR effect (Figure 2.5) explains the mechanism through which the drug carrier accumulates in the tumor tissue for prolonged times by taking advantage of the leaky vasculature.<sup>54</sup> Tumor cells have large leaky vasculature with poorly aligned epithelial cells with wide openings. This enables the micellar drugs to become trapped and accumulate within the tumor due to impaired lymphatic drainage at these areas. Simultaneously, extravasation of the drug-loaded micelle or vesicles in normal healthy tissue is decreased, compared to low molecular weight drugs, which extravasate in various tissues and are easily removed from the body via renal clearance, resulting in toxicity to the kidneys. The size of the tumor vasculature is dependent on the age and the type of tumor, having a pore size from 0.1 – 2 $\mu$ m.<sup>55</sup> On the other hand, active targeting is achieved by the attachment of targeting ligands to the micelles or vesicles so as to be recognized by cell receptors for binding. In these cases, the likelihood that the drug-loaded micelle or vesicle will reach the tumor and be internalized by the cancer cells is greater. Folate receptors are often used for active targeting of cancerous tumor sites.<sup>56-58</sup>

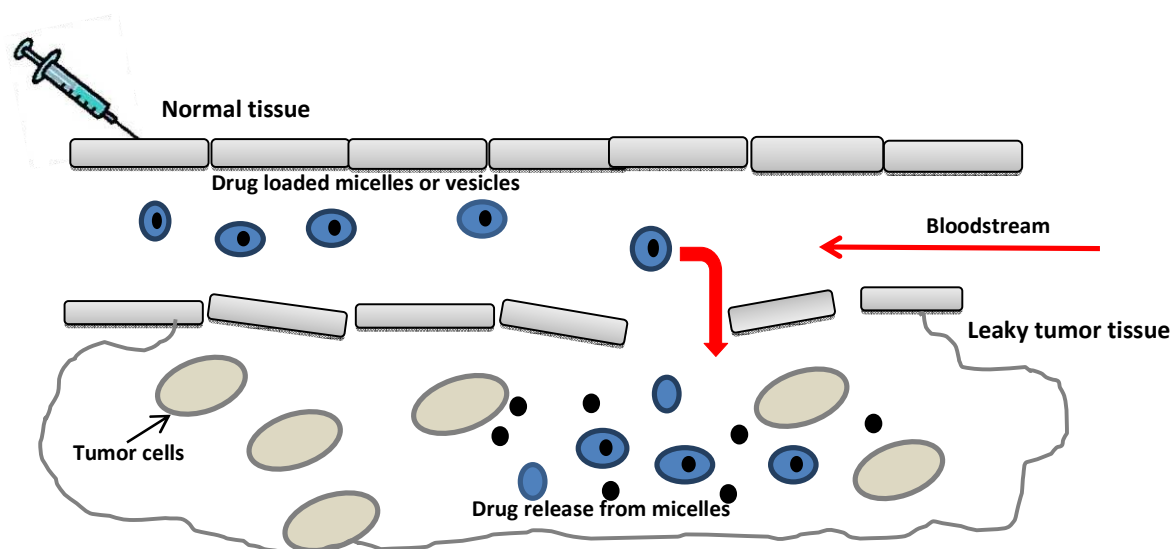


**Figure 2.5:** Schematic representation of the EPR effect- the nonfunctionalized micelles or vesicles extravasate in the leaky tumor vasculatures

#### 2.3.4 Inherent size of polymer drug carriers and the biodistribution of the drug

The polymer drug carrier size and biodistribution of the drug is one of the determining factors of the drug carrier efficacy. The size of the carrier is dependent on a number of variables including the molecular weight of the copolymer and the length of the hydrophilic and hydrophobic blocks.<sup>59</sup> For passive drug targeting, the polymer carrier size should range from 10 – 200 nm. These sizes are desirable in order to avoid renal excretion (< 10 nm), to prolong the circulation in the bloodstream. This avoids RES elimination (> 200 nm)<sup>60</sup> and allows for selective tumor accumulation based on the EPR effect.<sup>33,61</sup> The EPR effect is observed for macromolecules with molecular weights greater than 20 kDa. In recent years, most research groups selected polymer drug carriers with molecular weights in the range of 20 to 200 kDa. The renal excretion limit is less than approximately 20 – 40 kDa.<sup>62</sup> The molecular weight of the polymer micelles is usually higher than this limit, making them difficult to be removed via renal clearance. It is, therefore, assumed that only when the micelles fall apart through degradation or dilution, the copolymer unimers could be eliminated via renal excretion. Opsonization is a process whereby proteins adhere to the drug carrier when intravenously administered.<sup>63</sup> This results in the drug being released from the carrier and also in elimination of the carrier by the mononuclear phagocytic system (MPS). These are phagocytic cells that recognize certain proteins on the surface of the carrier and remove them from the bloodstream. The size and the surface properties of the

polymer drug carrier, therefore, influence the extent of opsonisation and further influence the biodistribution and pharmacokinetics of the polymer drug carrier.

### *2.3.5 Hydrophilic corona and hydrophobic core components of polymer drug carriers*

PEG is a water soluble, biocompatible polymer with low toxicity and immunogenicity. It is undoubtedly the most frequently used hydrophilic polymer in amphiphilic block copolymers for drug delivery application. Recently, it was shown that PVP is a viable alternative for PEG.<sup>64</sup> PVP is a well known water-soluble, biocompatible and relatively amphiphilic polymer. In selected applications, PVP has been shown to have superior properties compared to PEG. Research has shown that a tumor necrosis factor (TNF) conjugated to PVP shows a higher anti-cancer activity compared to that of the corresponding PEG conjugate.<sup>65</sup> Mayumi *et al.* also found a PVP-TNF- $\alpha$ -conjugation was a more potent antitumor therapeutic agent than PEGylated TNF- $\alpha$ .<sup>65</sup> PVP-based drug carriers have also shown to improve the plasma half-life of drugs.<sup>66</sup> Recently it has been reported that PVP is able to prevent protein absorption.<sup>67</sup> Several amphiphilic PVP-based block copolymers have been reported, for example block copolymers with poly ( $\epsilon$ -caprolactone) (PCL),<sup>68</sup> poly(*N*-isopropyl acrylamide) (PNIPAM),<sup>69</sup> poly (*D,L* lactide) (PDLLA)<sup>67</sup> and poly(styrene) (PSty).<sup>70</sup>

Due to the large number of hydrophobic drugs available, several hydrophobic polymers as core forming segments have been investigated. The hydrophobic core of micelles or bilayer membrane of vesicles acts as a reservoir in which the hydrophobic drug is solubilized and the affinity for the drug and the hydrophobic polymer determines the degree of solubilization. In order for selective drug accumulation to take place, leakage of the drug from the micelles or vesicles and early release of the drug need to be prevented. Therefore, the overall stability, the drug loading capacity and the drug release profile are dependent on the hydrophobic block. Examples of frequently used hydrophilic and hydrophobic polymers used are presented in Table 2.2. The encapsulation of commonly used anticancer drugs such as PTX,<sup>68,71</sup> DOX,<sup>72-74</sup> and indomethacin<sup>75</sup> into these hydrophobic core forming blocks has been well documented in the literature.

**Table 2.2:** Selection of hydrophilic and hydrophobic polymers often used for the preparation of micelles or vesicles as drug carriers

Hydrophilic polymer	Abbreviation	Chemical structure
Poly(ethylene glycol)	PEG <sup>75,76</sup>	
Poly(N-vinyl pyrrolidone)	PVP <sup>77-79</sup>	
Poly(acrylamide)	PAM <sup>49</sup>	
Hydrophobic polymer	Abbreviation	Chemical structure
Poly (lactic) acid	PLA <sup>80,81</sup>	
Poly(ε- caprolactone)	PCL <sup>76,79,82</sup>	
Poly(N-isopropyl acrylamide)	PNIPAM <sup>83,84</sup>	
Poly(β-L-benzyl aspartate) Poly(benzyl-L- glutamate)	PBLA <sup>85,86</sup> PBLG <sup>87</sup>	



### 2.3.6 Stability of polymer drug carriers in aqueous and biological environment

In a selective solvent, block copolymers self-assemble into ordered structures (*e.g.* micelles or vesicles) via a so-called closed association process, above the critical micelle concentration (CMC). Below the CMC (*i.e.* at very low concentrations), the polymers only exist as single chains (unimers).<sup>39</sup> Above the CMC, micelles are in equilibrium with the unimers. The CMC of polymer micelles are generally  $10^{-6} - 10^{-7}$  M.<sup>39</sup> Therefore, dissociation of the drug carrier occurs at very low concentrations. This is essential for drug delivery, because the micelles are subject to dilution upon intravenous administration and have to maintain the micellar form for prolonged circulation in the bloodstream.<sup>88</sup>

Polymer micelles can be considered as thermodynamically stable (the *potential* of disassembly) or kinetically stable (the *rate* of disassembly). The thermodynamic stability is dependent on the length of the hydrophobic block, and inversely related to the CMC (for instance an increase in the hydrophobic block length, decreases the CMC and increases the thermodynamic stability).<sup>49,89</sup> The kinetic stability refers to the *rate* at which dissociation of the micelles into unimers occurs. The kinetic stability is dependent on both the hydrophilic and the hydrophobic block, but the nature of the hydrophobic block has a more profound impact.<sup>38,90,91</sup> Based on the theory of micellization, other factors such as the nature of the hydrophobic block (being more or less hydrophobic) and the hydrophilic block (neutral *vs.* charged), block length, polymer concentration, and molecular weight may also affect the size, morphology and the stability of the resulting carrier. It has been reported that the encapsulation of drugs can enhance the stability of the micelles.<sup>92</sup>

Although the potential of block copolymer micelles or vesicles as carriers in drug delivery are foreseen, the clinical application is limited until now. This is due to the large dilution effect, which causes micelle or vesicle destabilization in the bloodstream. Polymer concentrations drop below the CMC, which results in the collapse of the micelle or vesicle structures.<sup>93,94</sup> In addition, serum albumin, enzymes and other proteins present in the bloodstream have also shown to interact with the carriers, affecting the stability.<sup>93,95-97</sup> Garreau *et al.* reported evidence that proteins possibly penetrate into the hydrophilic shell of PEG-*b*-PCL block micelles resulting in their degradation.<sup>98</sup>

Förster resonance emission transfer (FRET) microscopy is often used to monitor the stability of micelles in real time after intravenous injection. Chen *et al.*<sup>99</sup> used this technique to show that PEG-*b*-PDLLA micelles were unstable in the blood. Recently Lu *et al.*<sup>100</sup> reported on the stability of (D,L-lactide-*co*-2-methyl-2-carboxytrimethylene carbonate)-*g*-poly(ethylene glycol), P(LA-*co*-TMCC)-*g*-PEG, in the presence of all the major proteins present in serum using FRET.

One way to increase the biological stability of the drug carrier (and subsequently prolong the circulation time in the blood) is by the presence of a high surface coverage of hydrophilic chains on the surface of the carrier. As mentioned previously, the hydrophilic corona is responsible for the stability of the carrier. The extent to which the corona can stabilise the carrier depends on the surface density and the thickness of the hydrophilic shell. Several publications have shown that a high coverage of PEG on surfaces enhances the circulation longevity of carriers by reducing interactions with plasma proteins and cell-surface proteins.<sup>101</sup> Recently, PVP has come to be recognized as effective in resisting non-specific protein adsorption.<sup>102,103</sup> Numerous other approaches are starting to emerge in aiming to improve the stabilization of drug-loaded polymer carriers under physiological conditions. For example, in the case of micelles, strategies such as the introduction of strong hydrophobic interactions or hydrogen bonds in the micelle cores, core-crosslinking, shell-crosslinking and waist-crosslinking micelles have been undertaken to improve the stability of micelles.<sup>104-108</sup> However, cross-linked micelles do suffer from several drawbacks, one being non-biodegradability and difficulty of the cross-linked micelles to be eliminated from the body.<sup>109</sup> Similar approaches have also been applied to vesicles in which crosslinking the bilayer structure of the vesicle membrane further improves the stability.<sup>110</sup> The subject of cross-linked micelles and vesicles shall not be addressed in this chapter and the reader is referred to the above references for more information.

## 2.4 Preparation and drug loading into polymer drug carriers

### 2.4.1 Drug loading methods for polymer micelles and vesicles

Hydrophobic drugs can be incorporated into micelles or vesicles by chemical conjugation, physical entrapment or polyionic complexation. Chemical conjugation implies the formation of a covalent bond between a chemical group on the drug and one on the hydrophobic block of the block copolymer via a biodegradable, pH- or enzyme-sensitive linker. Upon exposure to the right trigger, release of the drug into the cells takes place. Despite the advantage that the drug is stably retained in the hydrophobic domain, this technique suffers from several drawbacks. Drug molecules and polymer do not always contain reactive functional groups. Specific block copolymers, therefore, need to be synthesized for a specific drug in order to allow chemical conjugation. In addition, chemical modification of a drug could result in alteration or loss of its bioactivity. Polyionic complexation involves the use of charged therapeutic agents (*e.g.* polynucleic acids) which are incorporated through electrostatic interaction with the oppositely charged ionic segment of the block copolymer.<sup>111</sup>

In most cases, the preferred method for the incorporation of a drug into polymer is by physical entrapment. A variety of drugs can be encapsulated in the hydrophobic core of micelles or the hydrophobic bilayer membrane of vesicles, irrespective of the chemical structure of the drug and the chemical structure of the block copolymer. The encapsulation of multiple drugs is advantageous in that synergistic effects of cancer drugs have shown promising results from multiple clinical trials.<sup>50</sup> Commonly used preparation and drug loading methods via physical entrapment are dialysis, oil-in-water (o/w) emulsion, solvent evaporation, solution casting and freeze drying. These methods are briefly described below. It must be mentioned that depending on the polymer system, each method can yield varying self-assembled structures (spherical micelles, rod-like micelles, flower-like micelles, vesicles etc.). Factors such as the length of the individual blocks, the nature of the solvent, the water content and the preparation method, all provide control over the types of self-assemblies formed.<sup>112</sup>

- Dialysis method

In this study, the dialysis method was implemented. In the dialysis method, the polymer and the hydrophobic drug are dissolved in a water-miscible organic solvent such as dimethylsulfoxide

(DMSO), dimethylformamide (DMF) or tetrahydrofuran (THF).<sup>61</sup> The homogeneous solution is then dialysed against distilled deionised water. The gradual replacement of the organic solvent with water (non-solvent for the hydrophobic block) allows for the self-association of block copolymers and the entrapment of the drug in the

hydrophobic core. Provided that the molecular weight of the polymer is high enough (*i.e.* the molecular weight cut off (MWCO) of the dialysis tube is not too high), the dialysis membrane keeps the micelles or vesicles inside the dialysis tube, but allows the removal of solvent and unloaded free drug. Figure 2.6 illustrates this procedure

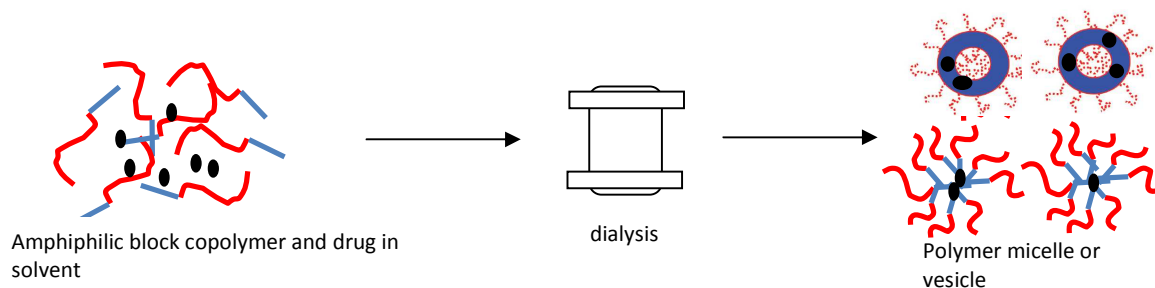


**Figure 2.6:** Illustration of the dialysis method for drug encapsulation into resulting in drug-loaded micelles or vesicles

Literature studies have shown that the size of the self-assembled block copolymers is dependent on the organic solvent chosen in this method.<sup>61,113</sup> For example, La *et al.*<sup>85</sup> used the dialysis method in their micelle system of PEO-*b*-PBLA and studied the effect of the organic solvents DMSO and *N,N*-dimethylacetamide (DMAc) on the particle size of the micelles. The results obtained showed a difference in the particle size depending on the solvent used. Consequently, the dialysis method is advantageous as it can be used to modify the properties of the micelles for their specific application.

- Oil/water emulsion method

The polymer and the drug are dissolved in a water-immiscible organic solvent followed by the addition of water. The mixture is then sonicated or stirred vigorously leading to the formation of nano-sized droplets within the aqueous phase. The organic solvent is then removed by evaporation resulting in drug-loaded micelles or vesicles.<sup>61,85,114</sup>

- Solvent evaporation method

This method is based on dissolving the drug and the polymer in an organic solvent followed by the removal of the solvent leading to the formation of a film. The film is then reconstituted in the aqueous phase. This method is however limited to block copolymers having high hydrophilic lipophilic balance (HLB) values such that the polymer film can easily dissolve in aqueous media.<sup>61,82</sup>

- Freeze drying method

The freeze-drying method has been reported and appears to be effective for PVP-based block copolymers. The polymer and the drug are dissolved in water and a solvent (*e.g.* *tert*-butyl alcohol). The mixture is frozen and the aqueous phase removed via freeze-drying. The solid polymer cake is then dissolved in a medium such as an aqueous sodium chloride or dextrose solution, forming drug-loaded micelles.<sup>61,115</sup> The freeze-drying method has been used for the encapsulation of PTX and its derivatives in PVP-*b*-PDLLA block copolymers.<sup>91,116</sup>

#### 2.4.2 Factors affecting the drug loading

In order to limit the toxicity and the undesirable side-effects that can arise from the drug carrier, the loading efficiency is crucial. Furthermore, minimising the overall costs of the formulation is also important. There are several factors that affect the drug encapsulation which will be discussed briefly.

Drug loading is a process of solubilising drug in a polymer matrix. The mechanism of drug loading can therefore be explained in terms of solubility parameters. An important factor that controls the drug loading content is the drug-core compatibility. The Flory-Huggins interaction parameter can be used to predict and to quantify the compatibility between the polymer and drug.

The Flory-Huggins interaction parameter,  $\chi_{dp}$ , between the drug and the polymer is expressed as:<sup>117</sup>

$$\chi_{dp} = (\delta_d - \delta_p)^2 \frac{V_d}{RT}$$

where  $\delta_d$  and  $\delta_p$  are the Scatchard-Hildebrand solubility parameters of the drug (d) and the core forming polymer (p) respectively,  $V_d$  is the molecular volume of the drug,  $R$  is the ideal gas constant and  $T$  the absolute temperature. It is expected that the lower the interaction parameter, the greater the compatibility between the drug and the core forming polymer. The higher the compatibility, the higher the loading capacity.

Interactions between the drug and hydrophilic block can also influence the loading capacity. Benahmed *et al.*<sup>78</sup> showed that block copolymers of PVP-*b*-PDLLA showed higher drug loading efficiency than PEG-*b*-PDLLA micelles. This might be due to the binding of the drug (*i.e.* indomethacin) to PVP probably *via* intermolecular hydrogen bonding between the drug hydroxyl and PVP carbonyl groups. The length of both the hydrophobic and hydrophilic blocks also are an important factor.<sup>118</sup> In the first case, the longer the hydrophobic block, the larger the hydrophobic domain and domain-space available, therefore, higher amounts of hydrophobic drug can be entrapped resulting in higher drug loading. In the second case, increasing the length of the corona hydrophilic block increased the CMC. Therefore, a smaller fraction of the polymer will be present in micellar/vesicular form in aqueous solution. This results in a decrease in the hydrophobic regions thus, the total amount of drug encapsulated. Letchford *et al.*<sup>119</sup> studied the effect of the hydrophobic block length of PEG-*b*-PCL micelles on the drug loading capacity. Longer PCL blocks resulted in higher drug loading. An increase in the hydrophobic core segment resulted in an increase in the partition coefficient resulting in an increase in loading capacity. The entrapment efficiency can also depend on the initial amount of drug to be solubilised. Incorporation of large amounts of drug into the micelles or vesicles can result in precipitation of the drug and reduce the loading yield.<sup>120</sup> The localization of the drug molecules in the micelles also plays an important role. For example, in drug-loaded micelles it is often assumed that the drug is only incorporated in the hydrophobic core. However, the drug can be incorporated in either the corona, the hydrophobic core or at the interface of the corona-core, which would influence the loading capacity.<sup>61</sup>

## **2.5 Drug release and cellular internalization of polymer drug carriers**

### *2.5.1 Drug release*

Drug release from the polymer drug carriers for drugs that have been encapsulated via physical entrapment occurs by diffusion. One of the challenges in polymer-based drug delivery is the ability to control the drug release kinetics. Polymeric self-assembled structures, for example, can release more than 50 % of the encapsulated drugs within the first several hours due to the so-called “burst effect.”<sup>121</sup> This could be problematic as the carrier needs sufficient time to reach the targeted tumor and deliver the drug (without any premature leakage of the drug from the carrier) to the desired site. The release is controlled by the rate of diffusion of the drug from the drug carrier, the stability of the drug carrier, and the rate of degradation of the block copolymer.

In order to achieve effective drug targeting, the drug must reach the target site intact and selectively be released from polymer micelles or vesicles at the targeted site. Drug-loaded polymer carriers should, therefore, have sufficient stability in the blood stream. Fast release of drugs from polymer micelles or vesicles can result in precipitation of the hydrophobic drug in the body and allow insufficient time for polymer micelles or vesicles to accumulate at the target site. On the other hand, slow drug release allows for accumulation of the carrier at target sites with minimal drug loss and localized drug release.

Interestingly, the release rate of a drug from the polymer drug carrier is dependent on several factors similar to those affecting the loading capacity and micelle stability, however, having opposite effects. The influence of the drug loading capacity, molecular weight and the hydrophilic and the hydrophobic block length on drug release behaviour have been well documented.<sup>122</sup> Other factors affecting the release rate include the compatibility between the drug and polymer.<sup>118</sup> A strong interaction between the hydrophobic core- or bilayer membrane-forming block and the hydrophobic drug results in high loading capacity and slow drug release. This is due to the stronger interaction between the core or the bilayer and the drug molecules.

The location of the drug within the micelle or vesicle also determines the drug release.<sup>61</sup> For example, a hydrophobic drug that is present in the corona or at the interface of the corona and core of the micelles will be released more rapidly than drug present inside the core. Hydrophobic

drug molecules located in the hydrophobic core of micelles will have to diffuse through a longer path (larger core radius) resulting in slower release. Release kinetics often display an initial burst associated to the fast release of drug molecules located in the shell or at the core-shell interface followed by a slow release which corresponds to the diffusion of the drug from the core. The fast release can also be attributed to premature micelle disassembly which was confirmed in a study conducted by Chen *et al.*<sup>99</sup>

The physical state of both the hydrophobic block and the hydrophobic drug can also influence the release characteristics. If the glass transition temperature ( $T_g$ ) of the hydrophobic block is above that of the physiological condition (37 °C), the polymer is in solid-like phase or glassy state, therefore the diffusion of the drug is expected to be slower.<sup>123</sup> Furthermore, crosslinking of the hydrophobic core or vesicle membrane could also slow down the drug release from micelles.<sup>76</sup>

### 2.5.2 Cellular internalization

After the extravasation into the tumor tissue, the polymer carrier (micelles or vesicles) are internalized by the tumor cells (Figure 2.7). It has been observed that polymer carriers cannot diffuse through the cell membrane and instead are taken up by cells *via* a process called endocytosis (which is further divided into phagocytosis, macropinocytosis and/or (non) clathrin-mediated endocytosis).<sup>124</sup> Alternatively, in some cases the polymer carrier can release the drug close to the region of the cells and the drug can then be taken up by diffusion.

During the endocytosis process, the polymer carrier is internalized by the endosomes, which later fuse with lysosomes (Figure 2.7). During endocytosis the pH drops from physiological value (pH 7.4) to pH 6.5 – 5 in the endosomes and then to pH 4 in the lysosomes. In the acidic environment several of the lysosomal enzymes become active (for example nucleases, proteases, lipases).<sup>125</sup> Many studies have shown that the process is complex and details on the mechanism are not yet fully understood. To further complicate matters, it has been reported that endocytosis could be dependent on the molecular weight of the hydrophobic and hydrophilic blocks, concentration of the polymer, particle size of the nanoparticle carrier and the charge of the polymer carrier (which could interact with the cell membrane).<sup>126,127</sup>





### 2.5.3 Polymer drug carriers and multiple drug resistance (MDR)

Cells are able to gain resistance to drugs through a variety of mechanisms such as increased drug efflux, enzymatic deactivation and decreased cell permeability.<sup>133</sup> However, the use of polymer carriers has shown counteracting effects in multiple drug resistance (MDR). The MDR mechanism is associated with a number of efflux pumps including P-glycoprotein (P-gp). P-gp is a drug efflux transport protein that eliminates drugs from cancer cells and reduces the activity of the anticancer drug. Kabanov was the first to demonstrate that PEO-*b*-PPO copolymers (Pluronics) induce inhibition of the P-gp-mediated drug efflux system in cells.<sup>134</sup> For example an increase in DOX uptake by MDR cells with Pluronics was observed. This is believed to be caused by a Pluronic-induced deactivation of drug efflux pumps.<sup>135</sup>

Currently, numerous studies on polymer micelles to overcome MDR are being conducted.<sup>134,136</sup><sup>137</sup> The possible reasoning for polymer micelles to avoid recognition by the P-gp efflux pump is by means of the drug being enclosed in an endosome when entering the cell. This further results in higher intracellular drug concentrations inside the cells, compared to free drug which is easily pumped out.<sup>138</sup> The exact mechanism for polymer micelles in conjunction with MDR is not yet fully understood.

## 2.6 Conclusion

Polymer micelles and vesicles hold promise for the delivery of therapeutic agents. An important feature of these drug carriers is their amphiphilic character. Their core-shell or vesicular structure and physical properties makes them desirable carriers for hydrophobic drugs to target tumor sites in a controlled/triggered fashion. Currently, several polymer drug formulations have entered clinical trials with promising results.<sup>139,140</sup> However, researchers are faced with many challenges and more progress must be achieved to control the stability of the polymer drug carriers *in vitro* and *in vivo*. Perhaps future research in polymer chemistry and drug delivery will eventually lead to the discovery of the “Magic Bullet”, the ideal carrier for targeted drug delivery.<sup>141</sup>

## 2.7 References

- (1) Tong, R.; Cheng, J. *Polym. Rev.* **2007**, *47*, 345 - 381.
- (2) Duncan, R. *Nat. Rev. Drug Discovery* **2003**, *2*, 347 - 360
- (3) Duncan, R. *Nat. Rev. Cancer* **2006**, *6*, 688 - 701.
- (4) Duncan, R. *Curr. Opin. Biotechnol.* **2011**, *22*, 492 - 501.
- (5) Ringsdorf, H. *J. Polym. Sci.: Polym. Symp.* **1975**, *51*, 135 - 153.
- (6) York, A. W.; Kirkland, S. E.; McCormick, C. L. *Adv. Drug Deliv. Rev.* **2008**, *60*, 1018 - 1036.
- (7) Moad, G.; Rizzardo, E.; Thang, S. H. *Aust. J. Chem.* **2005**, *58*, 379 - 410.
- (8) Chiefari, J.; Chong, Y. K.; Ercole, F.; Krstina, J.; Jeffery, J.; Le, T. P. T.; Mayadunne, R. T. A.; Meijs, G. F.; Moad, C. L.; Moad, G.; Rizzardo, E.; Thang, S. H. *Macromolecules* **1998**, *31*, 5559 - 5562.
- (9) Yan, Y.; Zhang, W.; Qiu, Y.; Zhang, Z.; Zhu, J.; Cheng, Z.; Zhang, W.; Zhu, X. *J. Polym. Sci., Part A: Polym. Chem.* **2009**, *48*, 5206 - 5214.
- (10) Moad, G.; Rizzardo, E.; Thang, S. H. *Aust. J. Chem.* **2009**, *62*, 1402 - 1472.
- (11) Moad, G.; Thang, S. H. *Aust. J. Chem.* **2009**, *62*, 1379 - 1381.
- (12) Wakioka, M.; Baek, K.; Ando, T.; Kamigaito, M.; Sawamoto, M. *Macromolecules* **2002**, *35*, 330 - 333.
- (13) Iovu, M. C.; Matyjaszewski, K. *Macromolecules* **2003**, *36*, 9346 - 9354.
- (14) Wan, D. C.; Satoh, K.; Kamigaito, M.; Okamoto, Y. *Macromolecules* **2005**, *38*, 10397 - 10405.
- (15) Kamigaito, M.; Ando, T.; Sawamoto, M. *Chem. Rev.* **2001**, *101*, 3689 - 3745.
- (16) Hawker, C. J.; Bosman, A. W.; Harth, E. *Chem. Rev.* **2001**, *101*, 3661 - 3688.
- (17) Ray, B.; Kotani, M.; Yamago, S. *Macromolecules* **2006**, *39*, 5259 - 5265.
- (18) Wakioka, M.; Baek, K.; Ando, T.; Kamigaito, M.; Sawamoto, M. *Macromolecules* **2002**, *35*, 330 - 333.
- (19) Pound, G.; Aguesse, F.; McLeary, J. B.; Lange, R. F. M.; Klumperman, B. *Macromolecules* **2007**, *40*, 8861 - 8871.
- (20) Stenzel, M. H.; Cummins, L.; Roberts, G. E.; Davis, T. P.; Vana, P.; Barner-Kowollik, C. *Macromol. Chem. Phys.* **2003**, *204*, 1160 - 1168.

- (21) Barner, L.; Davis, T. P.; Stenzel, M. H.; Barner-Kowollik, C. *Macromol. Rapid Commun.* **2007**, *28*, 539 - 559.
- (22) Russum, J. P.; Barbre, N. D.; Jones, C. W.; Schork, F. J. *J. Polym. Sci., Part A: Polym. Chem.* **2005**, *43*, 2188 - 2193
- (23) Wakioka, M.; Baek, K.; Ando, T.; Kamigaito, M.; Sawamoto, M. *Macromolecules* **2002**, *35*, 330 - 333.
- (24) Debuigne, A.; Caille, J.; Willet, N.; Jérôme, R. *Macromolecules* **2005**, *38*, 9488 - 9496.
- (25) Debuigne, A.; Warnant, J.; Jérôme, R.; Voets, I.; de Keizer, A.; Stuart, M. A. C.; Detrembleur, C. *Macromolecules* **2008**, *41*, 2353 - 2360.
- (26) Kwak, Y.; Goto, A.; Fukuda, T.; Kobayashi, Y.; Yamago, S. *Macromolecules* **2006**, *39*, 4671 - 4679.
- (27) Ray, B.; Kotani, M.; Yamago, S. *Macromolecules* **2006**, *39*, 5259 - 5265.
- (28) Kaneyoshi, H.; Matyjaszewski, K. *Macromolecules* **2006**, *39*, 2757 - 2763.
- (29) Debuigne, A.; Willet, N.; Jérôme, R.; Detrembleur, C. *Macromolecules* **2007**, *40*, 7111 - 7118.
- (30) Fandrich, N.; Falkenhagen, J.; Weidner, S. M.; Pfeifer, D.; Staal, B.; Thunemann, A. F.; Laschewsky, A. *Macromol. Chem. Phys.* **2010**, *211*, 1678 - 1688.
- (31) Lipinski, C. *Amer. Pharm. Rev.* **2002**, *5*, 82 - 85.
- (32) Merisko-Liversidge, E. M.; Liversidge, G. G. *Toxicol. Pathol.* **2008**, *36*, 43 - 48.
- (33) Kim, S.; Shi, Y.; Kim, J. Y.; Park, K.; Cheng, J. *Expert Opin. Drug Deliv.* **2010**, *7*, 49 - 62.
- (34) Kim, K. T.; Meeuwissen, S. A.; Nolte, R. J. M.; van Hest, J. C. *Nanoscale* **2010**, *2*, 844 - 858.
- (35) Torchilin, V. P. *Expert Opin. Ther. Pat.* **2005**, *15*, 63 - 74.
- (36) Bader, H.; Ringsdorf, H.; Schmidt, B. *Angew. Makromol. Chem.* **1984**, *123/124*, 457 - 485.
- (37) Kataoka, K.; Kwon, G. S.; Yokoyama, M.; Okano, T.; Sakurai, Y. *J. Control. Rel.* **1993**, *24*, 119 - 132.
- (38) Kabanov, A. V.; Batrakova, E. V.; Alakhov, V. Y. *J. Control. Rel.* **2002**, *82*, 189 - 212.
- (39) Riess, G. *Prog. Polym. Sci.* **2003**, *28*, 1107-1170.
- (40) Choucair, A.; Eisenberg, A. *J. Am. Chem. Soc.* **2003**, *125*, 11993 - 12000.

- (41) Geng, Y.; Dalhaimer, P.; Cai, S.; Tsai, R.; Tewari, M.; Minko, T.; Discher, D. E. *Nature Nanotechnology* **2007**, *2*, 249 - 255.
- (42) Yu, K.; Eisenberg, A. *Macromolecules* **1996**, *29*, 6359 - 6361.
- (43) Shin, H.; Alani, A. W. G.; Rao, D. A.; Rockich, N. C.; Kwon, G. S. *J. Control. Rel.* **2009**, *140*, 294 - 300.
- (44) Gelderblom, H.; Verweij, J.; Nooter, K.; Sparreboom, A. *Eur. J. Cancer* **2001**, *37*, 1590 - 1598.
- (45) Soga, O.; van Nostrum, C. F.; Fens, M.; Rijcken, C. J. F.; Schiffelers, R. M.; Storm, G.; Hennink, W. E. *J. Control. Rel.* **2005**, *103*, 341 - 353.
- (46) Ponta, A.; Bae, Y. *Pharm. Res.* **2010**, *27*, 2330 - 2342.
- (47) Dua, J.; O'Reilly, R. K. *Soft Matter* **2009**, *5*, 3544 - 3561.
- (48) Meng, F.; Zhong, Z.; Feijen, J. *Biomacromolecules* **2009**, *10*, 197 - 209.
- (49) Allen, C.; Maysinger, D.; Eisenberg, A. *Colloids Surf., B* **1999**, *16*, 3 - 27.
- (50) Soundararajan, V.; Warnock, K.; Sasisekharan, R. *Macromol. Rapid Commun.* **2010**, *31*, 202 - 216.
- (51) Ahmed, F.; Pakunlu, R. I.; Brannan, A.; Bates, F.; Minko, T.; Discher, D. E. *J. Control. Rel.* **2006**, *116*, 150 - 158.
- (52) Du, J.; Tang, Y.; Lewis, A. L.; Armes, S. P. *J. Am. Chem. Soc.* **2005**, *127*, 17982 - 17983.
- (53) Maeda, H.; Wua, J.; Sawa, T.; Matsumura, Y.; Horic, K. *J. Control. Rel.* **2000**, *65*, 271 - 284.
- (54) Torchilin, V. P. *Pharm. Res.* **2007**, *24*, 1 - 16.
- (55) Nishiyama, N.; Kataoka, K. *Pharmacol. Ther.* **2006**, *112*, 630 - 648.
- (56) Lee, E. S.; Na, K.; Bae, Y. H. *J. Control. Rel.* **2003**, *91*, 103 - 113.
- (57) Lu, Y.; Low, P. S. *Adv. Drug Deliv. Rev.* **2002**, *54*, 675 - 693.
- (58) Bae, Y.; Jang, W.; Nishiyama, N.; Fukushima, S.; Kataoka, K. *Mol. BioSyst.* **2005**, *1*, 242 - 250.
- (59) Jones, M.; Ranger, M.; Leroux, J. *Bioconjugate Chem.* **2003**, *14*, 774 - 781.
- (60) Li, S.; Huang, L. *Mol. Pharm.* **2008**, *5*, 496 - 504.
- (61) Tyrrell, Z. L.; Shena, Y.; Radosza, M. *Prog. Polym. Sci.* **2010**, *35*, 1128-1143.
- (62) Croy, S. R.; Kwon, G. S. *Curr. Pharm. Des.* **2006**, *12*, 4669 - 4684.

- (63) Mikhail, A. S.; Allen, C. *J. Control. Rel.* **2009**, *138*, 214 - 223.
- (64) Torchilin, V. P.; Levchenko, T. S.; Whiteman, K. R.; Yaroslavov, A. A.; Tsatsakis, A. M.; Rizos, A. K.; Michailova, E. V.; Shtilman, M. I. *Biomaterials* **2001**, *22*, 3035 - 3044.
- (65) Kamada, H.; Tsutsumi, Y.; Yamamoto, Y.; Kihira, T.; Kaneda, Y.; Mu, Y.; Kodaira, H.; Tsunoda, S.; Nakagawa, S.; Mayumi, T. *Cancer Res.* **2000**, *60*, 6416 - 6420.
- (66) Kaneda, Y.; Tsutsumi, Y.; Yoshioka, Y.; Kamada, H.; Yamamoto, Y.; Kodaira, H.; Tsunoda, S.; Okamoto, T.; Mukai, Y.; Shibata, H.; Nakagawa, S.; Mayumi, T. *Biomaterials* **2004** *25*, 3259 - 3266.
- (67) Gaucher, G.; Asahina, K.; Wang, J.; Leroux, J. *Biomacromolecules* **2009**, *10*, 408 - 416.
- (68) Zhu, Z.; Li, Y.; Li, X.; Li, R.; Jia, Z.; Liu, B.; Guo, W.; Wu, W.; Jiang, X. *J. Control. Rel.* **2010**, *142*, 438 - 446.
- (69) Chen, X.; Qi, Z.; Huang, Y.; Pleton, R.; Ghosh, R. *Adv. Mat. Res.* **2008**, *47 - 50*, 1311 - 1314.
- (70) Hussain, H.; Tan, B. H.; Gudipati, C. S.; He, C. B.; Liu, Y.; Davis, T. P. *Langmuir* **2009**, *25*, 5557 - 5564.
- (71) Musacchio, T.; Laquintana, V.; Latrofa, A.; Trapani, G.; Torchilina, V. P. *Mol. Pharm.* **2009**, *6*, 468 - 479.
- (72) Batrakova, E. V.; Li, S.; Li, Y.; Alakhov, V. Y.; Elmquist, W. F.; Kabanov, A. V. *J. Control. Rel.* **2004**, *100*, 389 - 397.
- (73) Kataoka, K.; Matsumoto, T.; Yokoyama, M.; Okano, T.; Sakurai, Y.; Fukushima, S.; Okamoto, K.; Kwon, G. S. *J. Control. Rel.* **2000**, *64*, 143 - 153.
- (74) Tan, J. P. K.; Kim, S. H.; Nederberg, F.; Fukushima, K.; Coady, D. J.; Nelson, A.; Yang, Y. Y.; Hedrick, J. L. *Macromol. Rapid Commun.* **2010** *31*, 1187 - 1192.
- (75) Kim, S. Y.; Shin, I. G.; Lee, Y. M.; Cho, C. S.; Sung, Y. K. *J. Control. Rel.* **1998**, *51*, 13 - 22.
- (76) Zhang, W.; Li, Y.; Liu, L.; Sun, Q.; Shuai, X.; Zhu, W.; Chen, Y. *Biomacromolecules* **2010**, *11*, 1331 - 1338.
- (77) Chunga, T. W.; Cho, K. Y.; Lee, H.; Nah, J. W.; Yeo, J. H.; Akaike, T.; Cho, C. S. *Polymer* **2004**, *45*, 1591 - 1597
- (78) Benahmed, A.; Ranger, M.; Leroux, J. *Pharm. Res.* **2001**, *18*, 323 - 327.

- (79) Devasia, R.; Borsali, R.; Lecommandoux, S.; Bindu, R. L.; Mougin, N.; Gnanou, Y. *Polym. Prepr.* **2005**, *46*.
- (80) Liang, H.-F.; Chen, S.-C.; Chen, M.-C.; Lee, P.-W.; Chen, C.; Sung, H.-W. *Bioconjugate Chem.* **2006**, *17*, 291 - 299.
- (81) Hans, M.; Shimoni, K.; Danino, D.; Siegel, S. J.; Lowman, A. *Biomacromolecules* **2005**, *6*, 2708 - 2717.
- (82) Shuai, X.; Aia, H.; Nasongkla, N.; Kim, S.; Gao, J. *J. Control. Rel.* **2004**, *98*, 415 - 426.
- (83) Schilli, C. M.; Zhang, M.; Rizzardo, E.; Thang, S. H.; Chong, Y. K.; Edwards, K.; Karlsson, G.; Muller, A. H. E. *Macromolecules* **2004**, *37*, 7861 - 7866.
- (84) Li, G.; Song, S.; Guo, L.; Ma, S. *J. Polym. Sci., Part A: Polym. Chem.* **2008**, *46*, 5028 - 5035.
- (85) La, S. B.; Okano, T.; Kataoka, K. *J. Pharm. Sci.* **1996**, *85*, 86 - 90.
- (86) Kwon, G. S.; Naito, M.; Yokoyama, M.; Okano, T.; Sakurai, Y.; Kataoka, K. *Pharm. Res.* **1995**, *12*, 192 - 195.
- (87) Oh, I.; Lee, K.; Kwon, H. Y.; Lee, Y. B.; Shin, S. C.; Cho, C. S.; Kim, C. K. *Int. J. Pharm.* **1999**, *181*, 107 - 115
- (88) Adams, M. L.; Lavasanifar, A.; Kwon, G. S. *J. Pharm. Sci.* **2003**, *92*, 1343 - 1355.
- (89) Rapoport, N. *Prog. Polym. Sci.* **2007**, *32*, 962-990.
- (90) Kwon, G. S.; Yokoyama, M.; Okano, T.; Sakurai, Y.; Kataoka, K. *Langmuir* **1993**, *9*, 970 - 974.
- (91) Garrec, D. L.; Gori, S.; Luo, L.; Lessard, D.; Smith, D. C.; Yessine, M.-A.; Ranger, M.; Leroux, J.-C.; Ranger, M. *J. Control. Rel.* **2004**, *99*, 83 - 101.
- (92) Yokoyama, M.; Fukushima, S.; Uehara, R.; Okamoto, K.; Kataoka, K.; Sakurai, Y.; Okano, T. *J. Control. Rel.* **1998**, *50*, 79 - 92.
- (93) Opanasopita, P.; Yokoyama, M.; Watanabe, M.; Kawanoc, K.; Maitanic, Y.; Okano, T. *J. Control. Rel.* **2005**, *104*, 313 - 321.
- (94) Savic, R.; Azzam, T.; Eisenberg, A.; Maysinger, D. *Langmuir* **2006**, *22*, 3570 - 3578.
- (95) Herbert, K. E.; Coppock, J. S.; Griffiths, A. M.; Williams, A.; Robinson, M. W.; Scott, D. L. *Ann. Rheum. Dis.* **1987**, *46*, 734 - 740.
- (96) Carstens, M. G.; Van Nostrum, C. F.; Verrijck, R.; Leede, L. G. J. D.; Crommelin, D. J. A.; Hennink, W. E. *J. Pharm. Sci.* **2008**, *97*, 506 - 517.

- (97) Diezi, T. A.; Bae, Y.; Kwon, G. S. *Mol. Pharm.* **2010**, *7*, 1355 - 1360.
- (98) Li, S.; Garreau, H.; Pauvert, B.; McGrath, J.; Toniolo, A.; Vert, M. *Biomacromolecules* **2002**, *3*, 525 - 530.
- (99) Chen, H.; Kim, S.; He, W.; Wang, H.; Low, P. S.; Park, K.; Cheng, J. *Langmuir* **2008**, *24*, 5213 - 5217.
- (100) Lu, J.; Owen, S. C.; Shoichet, M. S. *Macromolecules* **2011**, *44*, 6002 - 6008.
- (101) Stolnik, S.; Daudali, B.; Arien, A.; Whetstone, J.; Heald, C. R.; Garnett, M. C.; Davis, S. S.; Iimun, L. *Biochimica et Biophysica Acta* **2001**, *1514*, 261 - 279.
- (102) Liu, X.; Wu, Z.; Zhou, F.; Li, D.; Chen, H. *Colloids Surf., B* **2010**, *79*, 452 - 459.
- (103) Wu, Z.; Chen, H.; Liu, X.; Zhang, Y.; Li, D.; Huang, H. *Langmuir* **2009**, *25*, 2900 - 2906.
- (104) O'Reilly, R. K.; Hawker, C. J.; Wooley, K. L. *Chem. Soc. Rev.* **2006**, *35*, 1068 - 1083.
- (105) Rijcken, C. J. F.; Schiffelers, R. M.; Van Nostrum, C. F.; Hennink, W. E. *J. Control. Rel.* **2008**, *132*, 33 - 35.
- (106) Wooley, K. L. *J. Polym. Sci., Part A: Polym. Chem.* **2000**, *38*, 1397 - 1407.
- (107) Wooley, K. L. *Chem. Eur. J.* **1997**, *3*, 1397 - 1399.
- (108) Yuan, C.; Xu, Y.; Deng, Y.; Chen, J.; Liu, Y.; Dai, L. *Soft Matter* **2009**, *5*, 4642 - 4646.
- (109) Hales, M.; Barner-Kowollik, C.; Davis, T. P.; Stenzel, M. H. *Langmuir* **2004**, *20*, 10809 - 10817.
- (110) Nardin, C.; Hirt, T.; Leukel, J.; Meier, W. *Langmuir* **2000**, *16*, 1035 - 1041.
- (111) Harada, A.; Kataoka, K. *Macromolecules* **1996**, *28*, 5294 - 5299.
- (112) Discher, D. E.; Eisenberg, A. *Science* **2002**, *297*, 967 - 973.
- (113) Yu, Y.; Eisenberg, A. *J. Am. Chem. Soc.* **1997**, *119*, 8383 - 8384.
- (114) Kwon, G.; Naito, M.; Yokoyama, M.; Okano, T.; Sakurai, Y.; Kataoka, K. *J. Control. Rel.* **1997**, *48*, 195 - 201.
- (115) Montazeri, H.; Afsane, A.; Lavasanifar, A. *Expert Opin. Drug Deliv.* **2006**, *3*, 139 - 162.
- (116) Fournier, E.; Dufresne, M.; Smith, D. C.; Ranger, M.; Leroux, J. *Pharm. Res.* **2004**, *21*, 962 - 968.
- (117) Nagarajan, R.; Barry, M.; Ruckenstein, E. *Langmuir* **1986**, *2*, 210 - 215.



- (118) Gaucher, G.; Dufresne, M.; Sant, V. P.; Kang, N.; Maysinger, D.; Leroux, J. J. *Control. Rel.* **2005**, *109*, 169 - 188.
- (119) Letchford, K.; Liggins, R.; Burt, H. *J. Pharm. Sci.* **2008**, *97*, 1179 - 1189.
- (120) Yokoyama, M.; Satoh, A.; Sakurai, Y.; Okano, T.; Matsumur, Y.; Kakizoe, T.; Kataoka, K. *J. Control. Rel.* **1998**, *55*, 219 - 229.
- (121) Musumeci, T.; Ventura, C. A.; Giannone, I.; Ruozi, B.; Montenegro, L.; Pignatello, R.; Puglisi, G. *Int. J. Pharm.* **2006**, *325*, 172 - 179.
- (122) Kim, S. Y.; Shin, G.; Lee, Y. M.; Cho, C. S.; Sung, Y. K. *J. Control. Rel.* **1998**, *51*, 13 - 22.
- (123) Teng, Y.; Morrison, M. E.; Munk, P.; Webber, S. E. *Macromolecules* **1998**, *31*, 3578 - 3587.
- (124) Hillaireau, H.; Couvreur, P. *Cell. Mol. Life Sci.* **2009**, *66*, 2873 - 2896.
- (125) Haag, R.; Kratz, F. *Angew. Makromol. Chem.* **2006**, *45*, 1198 - 1215.
- (126) Mahmud, A.; Lavasanifar, A. *Colloids Surf., B* **2005**, *45*, 82 - 89.
- (127) Savic, R.; Eisenberg, A.; Maysinger, D. *J. Drug Targeting* **2006**, *14*, 343 - 355.
- (128) Yan, J.; Ye, Z.; Luo, H.; Chen, M.; Zhou, Y.; Tan, W.; Xiao, Y.; Zhang, Y.; Lang, M. *Polym. Chem.* **2011**, *2*, 1331 - 1340.
- (129) Bae, Y.; Nishiyama, N.; Fukushima, S.; Koyama, H.; Yasuhiro, M.; Kataoka, K. *Bioconjugate Chem.* **2005**, *16*, 122 - 130.
- (130) Chan, Y.; Bulmus, V.; Zareie, M. H.; Byrne, F. L.; Barner, L.; Kavallaris, M. *J. Control. Rel.* **2006**, *115*, 197 - 207.
- (131) Ding, C.; Gu, J.; Qu, X.; Yang, Z. *Bioconjugate Chem.* **2009**, *20*, 1163 - 1170.
- (132) Rijcken, C. J. F.; Soga, O.; Hennink, W. E.; van Nostrum, C. F. *J. Control. Rel.* **2007**, *120*, 131 - 148.
- (133) Jabr-Milane, L. S.; van Vlerken, L. E.; Yadav, S.; Amiji, M. M. *Cancer Treat. Rev.* **2008**, *34*, 592 - 602.
- (134) Alakhov, V. Y.; Moskaleva, E. Y.; Batrakova, E. V.; Kabanov, A. V. *Bioconjugate Chem.* **1996**, *7*, 209 - 216.
- (135) Rapoport, N.; Pitt, W. G.; Sun, H.; Nelson, J. L. *J. Control. Rel.* **2003**, *91*, 85 - 95.

- (136) Kabanov, A. V.; Batrakova, E. V.; Alakhov, V. Y. *Adv. Drug Deliv. Rev.* **2002**, *54*, 759 - 779.
- (137) Lee, E. S.; Na, K.; Bae, Y. H. *J. Control. Rel.* **2005**, *103*, 405 - 418.
- (138) Cho, K.; Wang, X.; Chen, S. N. Z.; Shin, D. M. *Clin. Cancer Res.* **2008**, *14*.
- (139) Kim, T. Y.; Kim, D. W.; Chung, J. Y.; Shin, S. G.; Kim, S. C.; Heo, D. S.; Kim, N. K.; Bang, Y. J. *Clin. Cancer Res.* **2004**, *10*, 3708 - 3716.
- (140) Kim, D. W.; Kim, S. Y.; Kim, H. K.; Kim, S. W.; Shin, S. W.; Kim, J. S.; Park, K.; Lee, M. Y.; Heo, D. S. *Ann. Oncol.* **2007**, *18*, 2009 - 2014.
- (141) Kayser, O.; Lemke, A.; Hernández-Trejo, N. *Curr. Pharm. Biotechnol.* **2005**, *6*, 3 - 5.

### **Chapter 3**

## **Synthesis, characterization and self-assembly of poly(*N*-vinylpyrrolidone)-*b*-poly(vinyl acetate)**

### **Abstract**

Amphiphilic block copolymers of constant hydrophilic PVP block length and varying hydrophobic PVAc block length were synthesized via xanthate-mediated radical polymerization. In order to control the molecular weight of the hydrophilic PVP block, a xanthate chain transfer agent, *S*-(2-cyano-2-propyl) *O*-ethyl xanthate, was used. The PVP-*b*-PVAc block copolymer is composed of a hydrophilic and hydrophobic segment, which has the ability to self-assemble in aqueous solution. The PVP-*b*-PVAc block copolymers were characterized by <sup>1</sup>H NMR spectroscopy to confirm self-assembly behavior of PVP-*b*-PVAc block copolymers in water. The critical micelle concentration (CMC) was determined by a fluorescence technique. The CMC decreased with increasing PVAc block length, which can be attributed to the greater hydrophobicity of the PVAc segment of the PVP-*b*-PVAc block copolymer. A combination of dynamic light scattering (DLS), transmission electron microscopy (TEM) and static light scattering (SLS) was used to further characterize the block copolymers in water. DLS showed that the average particle size of the self-assembled block copolymers was 180 – 200 nm. The morphology of self-assembled PVP-*b*-PVAc block copolymer in water was examined by TEM, which showed spherical vesicles (bilayer-type structures) which was further confirmed by SLS. The stability of the PVP-*b*-PVAc block copolymers was evaluated using DLS under physiological conditions (pH 7.4, 37 °C) in the absence and presence of serum. Results showed that the block copolymers were stable in physiological conditions.

### 3.1 Introduction

In recent years, numerous novel drugs have been developed for the treatment of life-threatening and genetic diseases. However, these drugs are generally poorly soluble in water, which limits their application for intravenous administration.<sup>1</sup> As mentioned previously, solubilizing agents are often used to solubilize these drugs. However, these solubilizing agents have been associated with a number of adverse effects. Furthermore, most of the therapeutic drugs in current clinical treatments are small molecules, which generally spread throughout the body in the blood stream affecting healthy tissues. In addition, the small molecule drugs can be rapidly cleared by the kidneys, thus requiring high doses or continuous infusion for effective treatment. There is thus a need for drug delivery systems to overcome the above-mentioned issues. Research has shown that the use of drug delivery vehicles allows controlled and sustained delivery of drugs over a period of time, which further improves the efficacy of the drug.

Amphiphilic block copolymers have drawn great attention and shown great progress over the past years in the field of drug delivery.<sup>2-4</sup> Amphiphilic block copolymers consist of hydrophilic and hydrophobic segments that self-assemble in aqueous solution. The hydrophobic interactions are generally the main driving force behind the micellization process. Dependent on the molecular weight and hydrophilic/hydrophobic block ratios, these block copolymers can self-assemble into various structures such as spherical micelles, cylindrical micelles, worm-like micelles, or vesicles.<sup>5-7</sup> Discher and Eisenberg presented several studies based on the relationship between the block copolymer composition and the self-assembled morphologies.<sup>6</sup> They found that the self-assembled morphology was most simply a reflection of the hydrophilic-to-hydrophobic ratio. In their theory, spherical micelles are expected for block polymers with hydrophilic mass fraction ( $f$ ) greater than 45 %, whereas block copolymers with lower hydrophilic mass fraction ( $f$ ) typically self-assemble into vesicles. Many interesting reports have also been published on morphology transitions from spheres  $\rightarrow$  cylinders  $\rightarrow$  vesicles (also called “polymersomes”), induced by decreasing the relative length of the hydrophilic block.<sup>8</sup> Nevertheless, these self-assembled, nano-sized micelles or vesicles have applications in various fields such as water purification,<sup>9</sup> surface modification,<sup>10</sup> pharmaceuticals and in drug delivery.<sup>4,11,12</sup>

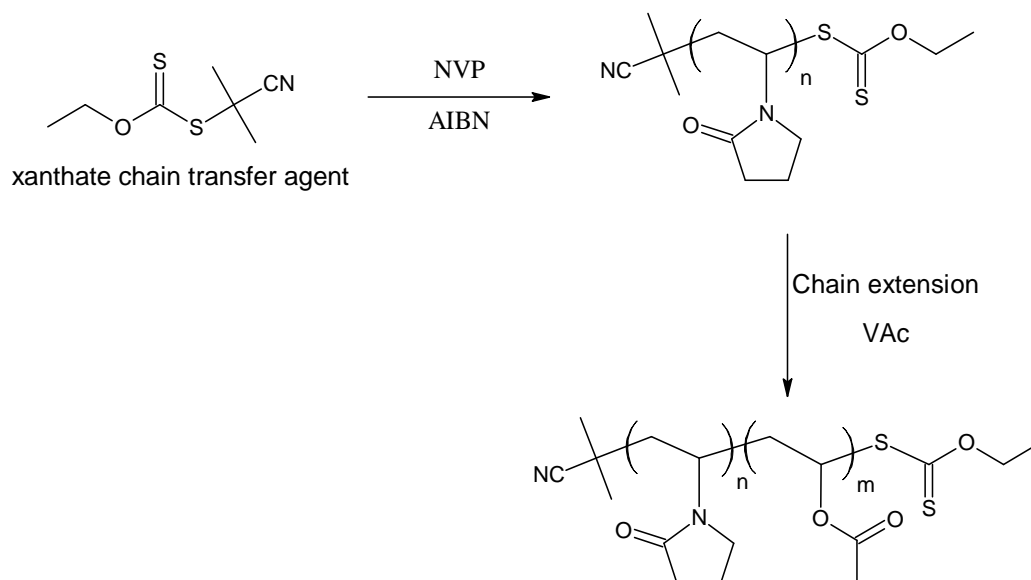
For their application in drug delivery, polymeric micelles have a hydrophobic core which can provide a depot for hydrophobic guest molecules such as hydrophobic drugs. On the other hand, vesicles can accommodate hydrophilic guest molecules in the hollow hydrophilic core and hydrophobic guest molecules within the hydrophobic bilayer or membrane. Ideally, these drug carriers should have long circulating properties after intravenous administration, without premature loss of the encapsulated drug. This allows the drugs to reach the targeted sites passively via the enhanced permeation and retention (EPR) effect. Therefore, an important property of the amphiphilic block copolymers is the CMC. The CMC of block copolymers is usually much lower than that of low molecular weight surfactants.<sup>4</sup> This is crucial for application in drug delivery as it ensures a good physical stability of the drug carrier against dilution after intravenous injection into the blood stream.

The rapid development of controlled radical polymerization (CRP) is increasingly being utilized to prepare well-defined homo-, gradient, di- and triblock copolymers for applications in drug, protein, and gene delivery for the treatment of infectious and genetic diseases.<sup>13</sup> The RAFT technique has proven to be a versatile tool for the synthesis of polymers used for drug delivery purposes. For the application of polymers in drug delivery, the chemical nature, chain architecture, the control of the molecular weight, and hydrodynamic size are important properties that contribute towards the stability, the drug loading, drug uptake and drug release of the drug carrier system.<sup>4</sup> RAFT is a versatile technique for a variety of functional monomers. Hydrophilic and hydrophobic monomers with suitable biocompatibility and chain transfer agents with reactive functionality further allow for bioconjugation of the polymers to drugs, peptides, proteins, targeting moieties and fluorescent dyes.<sup>14</sup> The evolution of CRP therefore allows for the design and facile preparation of tailor-made polymers for drug delivery applications.<sup>14</sup>

To date, poly(ethylene glycol) (PEG) is the preferred and most common choice for the hydrophilic segment of the amphiphilic block copolymers. In fact, most of the polymer drug carriers that have been examined in clinical trials are PEG-based.<sup>15,16</sup> However, PVP has shown improved properties compared to PEG and is attracting attention as an alternative to PEG.<sup>17,18</sup> PVP is an attractive biomaterial for drug delivery or tissue engineering since it is hydrophilic, non-toxic and biocompatible with living tissue. Studies have already shown prolonged *in vivo*

circulation time after intravenous administration for PVP-coated liposomes.<sup>19</sup> To date, PVP-based block copolymers such as PVP-*b*-poly(D,L-lactide) (PVP-*b*-PDLLA), PVP-*b*-poly( $\epsilon$ -caprolactone) (PVP-*b*-PCL) have been investigated for the self-assembly in micellar structures. However, their evaluation for drug delivery both *in vitro* and *in vivo* still needs to be explored further.

The purpose of the current study was to develop a PVP-*b*-PVAc drug carrier for hydrophobic anticancer drugs. Herein, the synthesis, characterization and self-assembly of amphiphilic PVP-*b*-PVAc block copolymers is presented. RAFT/MADIX polymerization was used for the synthesis of the block copolymers. PVP-*b*-PVAc diblock copolymers were synthesized via sequential monomer addition as illustrated in Scheme 1. The methodology used in this study comprises a two step process. The first step involves the synthesis of a starting block in bulk (referred to as the PVP macro-RAFT agent). Bulk polymerization was chosen as it only involves initiator, RAFT agent and monomer. Therefore, it minimizes the possibility of contamination and results in a high purity starting block. In order to control the molecular weight of the hydrophilic PVP block, a xanthate chain transfer agent, *S*-(2-cyano-2-propyl) *O*-ethyl xanthate, was chosen. In the second step, the starting block (macro-RAFT agent) is chain-extended upon further addition of a hydrophobic monomer, vinyl acetate (VAc). After the first step, the majority of the chains contain the active RAFT agent on the chain ends, making these potentially active for chain extension. Finally, the PVP-*b*-PVAc block copolymer is composed of a hydrophilic and hydrophobic segment, which has the ability to self-assemble in aqueous solution.



**Scheme 3.1:** Two-step reaction procedure for the synthesis of PVP-*b*-PVAc block copolymers

The self-assembly properties of the block copolymers were investigated using <sup>1</sup>H NMR spectroscopy, fluorescence spectroscopy, transmission electron microscopy (TEM) and light scattering techniques. These results can provide useful insight regarding the drug loading potential and hence the feasibility of PVP-*b*-PVAc block copolymers as a drug delivery vehicle for hydrophobic anti-cancer drugs.

## 3.2 Materials and methods

### 3.2.1 Materials

*N*-vinylpyrrolidone (Aldrich, 99 %) was dried over molecular sieves and distilled under reduced pressure. Vinyl acetate (Protea Chemicals, 99 %) was distilled under reduced pressure. AIBN (Riedel de Haen) was recrystallized from methanol. Dimethyl sulfoxide (Merck, 99 %) was used as received. Distilled deionized water was obtained using a Millipore Milli-Q purification system and used in all experiments. Phosphate buffer saline (PBS, pH 7.4, sterile) and fetal calf serum (FCS, sterile) were obtained from Sigma-Aldrich.

### 3.2.2 Synthesis of xanthate chain-transfer agent *S*-(2-cyano-2-propyl) *O*-ethyl xanthate

The xanthate agent was synthesized according to a procedure reported in the literature.<sup>20</sup> The purity of the xanthate was determined by <sup>1</sup>H NMR spectroscopy and was 98 %.

### 3.2.3 Synthesis of PVP macro-RAFT agent

The starting PVP blocks were synthesized via RAFT-mediated polymerization using a xanthate RAFT agent. The polymerizations were carried out as follows:

The xanthate RAFT agent (0.09 g,  $5 \times 10^{-4}$  mol), NVP (10 g,  $9 \times 10^{-2}$  mol) and AIBN (0.017g,  $1.03 \times 10^{-4}$  mol) were placed in a dry, pear-shaped 50 mL Schlenk flask and sealed using a rubber septum. The polymerization mixture was degassed via four freeze-pump-thaw cycles followed by introduction of ultra-high purity argon gas. The flask was immersed in an oil bath preheated at 60 °C. The polymerization reactions were stopped after 6 hours where the reaction mixture became very viscous and stirring was impaired. The polymerization mixture was diluted with dichloromethane (25 mL) and precipitate in diethyl ether (250 mL). The polymer was recovered by filtration and immediately dried under vacuum at ambient temperature.

### 3.2.4 Synthesis of PVP-*b*-PVAc block copolymers

For the synthesis of the diblock copolymers, the PVP macro-RAFT agent (starting block) was dissolved in methanol (2 mL) (a minimal amount of methanol was used in order to dissolve the PVP macro-RAFT agent in the hydrophobic VAc monomer). Vinyl acetate (7 g,  $8.3 \times 10^{-2}$  mol), AIBN (0.005 g,  $3 \times 10^{-5}$  mol) and the starting block (1 g) were placed in a Schlenk flask and



degassed via freeze-pump-thaw. The flask was immersed in an oil bath at 60 °C for 4 hours. The polymer was isolated by precipitation in diethyl ether and dried under vacuum at ambient temperature.

### 3.2.5 Polymer characterization

The block copolymers were characterized by  $^1\text{H}$  NMR spectroscopy using a 600 MHz spectrometer Varia<sup>Unity</sup> Inova instrument. Samples were dissolved in either deuterated dimethyl sulfoxide (DMSO- $d_6$ ), deuterated chloroform ( $\text{CDCl}_3$ ) or deuterium oxide ( $\text{D}_2\text{O}$ ).

The molecular weights were determined using size exclusion chromatography (SEC). The instrument setup consisted of a Shimadzu, LC-10AD pump, a column system fitted with a 50 x 8 mm guard column in series with three 300x8 mm, 10  $\mu\text{m}$  particle size GRAM columns (2 x 3000 Å and 100 Å) obtained from PSS, a Waters 2487 dual wavelength UV detector and a Waters 2414 differential refractive index (DRI) detector all in series. 100  $\mu\text{L}$  injection volumes are sampled individually with the oven temperature of the column and DRI detector kept at 40 °C. The solvent, dimethylacetamide (DMAc) used was stabilized with 0.05 % BHT (w/v) and 0.03 % LiCl (w/v). Polymer samples were filtered through 0.45  $\mu\text{m}$  GHP filters prior to analysis. Calibration was done using poly(methyl methacrylate) PMMA standard sets (Polymer Laboratories) ranging from 690 to  $1.2 \times 10^6$  g/mol.

HPLC was performed using a Waters 2690 separations Module (Alliance), a dual pump setup comprising a Agilent 1100 series variable wavelength UV detector, and PL-ELS 1000 detector. Data was recorded and processed using PSS WinGPC unity (Build 2019) software. A C18-grafted silica column was used (Luna RP C18 3  $\mu\text{m}$ , 150 mm, 4.60 mm, Phenomenex) at 30 °C. The ELSD nebulizer temperature was 70 °C. The flow rate was 0.5  $\text{mL min}^{-1}$ . For GPEC analysis, the mobile phase was acetonitrile/ deionized water (with 0.1 % formic acid) 65:35 (v/v). Prior to HPLC and GPEC analyses, PVP-*b*-PVAc were dialysed for 24 h in distilled water using SnakeSkin<sup>®</sup> pleated dialysis tubing (Pierce, 3.5 KDa MWCO). Samples were prepared in the same solvent composition as the mobile phase at concentrations of 5  $\text{mg mL}^{-1}$ . The injection

volume was 20  $\mu\text{L}$ . Homopolymers of PVP<sub>90</sub> ( $M_{n,\text{NMR}}$  8000  $\text{g}\cdot\text{mol}^{-1}$  (PMMA equivalents in DMAc,  $D = 1.3$ ) and PVAc<sub>200</sub> ( $M_{n,\text{SEC}}$  18 000  $\text{g}\cdot\text{mol}^{-1}$  (PS equivalents in THF,  $D = 1.2$ ) were prepared via xanthate-mediated polymerization and were used as a reference to estimate the elution volume of the PVP and PVAc homopolymers. Homopolymers and block copolymers were dissolved in 65:35 (v/v) acetonitrile/water. The gradient ranged from 65/35 acetonitrile/water to 100 % acetonitrile.

### 3.2.6 Self-assembly of PVP-*b*-PVAc block copolymers

Self-assembly of the PVP-*b*-PVAc block copolymers was achieved by the dialysis method. A typical procedure is as follows: PVP-*b*-PVAc block copolymer (50 mg) was dissolved in DMSO (5 mL). The solution was stirred for 15 minutes at room temperature. The homogeneous solution was dialyzed against distilled deionized water for 24 hours using Snakeskin<sup>®</sup> dialysis tubing (MWCO 3500 g/mol dextran equivalents). The water was replaced every 6 hours. The polymer was recovered by freeze-drying for 24 hours.

### 3.2.7 Determination of the critical micelle concentration (CMC) of PVP-*b*-PVAc block copolymers

The CMC of the block copolymers were determined using pyrene as probe. The fluorescence excitation spectra of pyrene were measured at varying PVP-*b*-PVAc concentrations using a Perkin Elmer Luminescence LS50B spectrometer using FL Winlab version 4.0 for data processing. Aqueous solutions of PVP-*b*-PVAc of varying concentration (0.0001 – 1 mg/mL) were prepared. 15  $\mu\text{L}$  of pyrene dissolved in acetone ( $1.8 \times 10^{-4}$  M) was added to 4.5 mL of the PVP-*b*-PVAc aqueous solutions of varying concentration (pyrene concentration  $6 \times 10^{-7}$  M). The polymer solutions containing pyrene were left for 24 hours at room temperature in the dark to equilibrate the partitioning of pyrene into the hydrophobic domain of the polymer. The excitation spectra were recorded from 300 nm to 360 nm with the emission wavelength at 390 nm. The spectra were recorded with a scan rate of  $250 \text{ nm min}^{-1}$ . The intensity ratio of  $I_{338}/I_{336}$  was plotted against the logarithm of the PVP-*b*-PVAc concentration to determine the CMC.

### *3.2.8 Size distribution and morphology of PVP-*b*-PVAc block copolymers*

The particle size and particle size distribution of the PVP-*b*-PVAc block copolymers were determined by dynamic light scattering (DLS) using a Malvern Instrument ZetaSizer Nano ZS90 equipped with a 4 mW He-Ne laser, operating at a wavelength of 633.0 nm. The scattered light was detected at a scattering angle of 90° at 25 °C or 37 °C. The final particle size and size distribution were obtained from three measurements, each comprising 10 – 15 sub-runs, and calculated via a CONTIN analysis.

TEM of the PVP-*b*-PVAc samples were carried out in order to observe the morphology of the self-assembled PVP-*b*-PVAc block copolymers. TEM micrographs were obtained using a LEO 912 microscope operating at an acceleration voltage of 120 kV. A drop of the sample solution was deposited onto a copper grid and dried at room temperature. The samples were negatively stained with uranyl acetate.

### *3.2.9 Multiangle static light scattering (MASLS)*

Multiangle static light scattering (MASLS) measurements were performed to determine the radius of gyration of the PVP-*b*-PVAc block copolymers in water. Measurements were performed on an ALV 7002 Correlator, ALV-SP/86 goniometer, RFIB263KF Photo Multiplier Detector with ALV 200 µm Pinhole detection system and a Cobolt Samba-300 DPSS laser. The wavelength was set to 532 nm, power to 300 mW and the temperature was controlled by a Haake Phoenix II – C30P thermostatic bath. All measurements were carried out at 25 °C. Toluene was used as a calibration standard.

Polymer solutions were prepared in Millipore water. All samples were passed through a 0.45 µm nylon filter prior to analysis. Then, samples were subjected to MASLS measurements using 6 angles ranging from 50° to 120° in 10° increments for four polymer concentrations above the CMC (0.25 to 2 mg/mL).

The  $R_h$  was determined by DLS which is based on the Stokes-Einstein equation

$$R_h = \frac{k_B T q^2}{6\pi\eta\Gamma}$$

in which  $k_B$  is the Boltzmann constant,  $T$  is the absolute temperature,  $\eta$  is the solvent viscosity, and  $\Gamma$  is the decay rate.  $q$  is the scattering vector and given by the equation

$$q = \frac{4\pi n_m}{\lambda} \sin \frac{\theta}{2}$$

with  $\theta$  being the measurement angle,  $n_m$  the refractive index of the solvent and  $\lambda$  the wavelength of the light in vacuum.

The weight-averaged molecular weight ( $M_w$ ), the radius of gyration ( $R_g$ ) and second virial coefficient ( $A_2$ ) were calculated based on the equation

$$\frac{K_R}{R(q)} = \frac{1}{M_w} \left( 1 + \frac{1}{3} R^2 q^2 \right) + 2A_2 c$$

where  $R$  is the solute Rayleigh ratio expressed by the equation

$$R = R_{tol,\theta} \left( \frac{n}{n_{tol}} \right)^2 \frac{I - I_0}{I_{tol}} \sin \theta$$

Here  $R_{tol,90}$  is the Rayleigh ratio of toluene at an angle of  $90^\circ$ ,  $n$  is the refractive index of the solvent,  $I$ ,  $I_0$  and  $I_{tol}$  are the scattering intensities of the solution, solvent, and toluene, respectively, and  $\theta$  is the measurement angle.  $K_R$  is the optical constant defined as

$$K_R = \frac{4\pi^2}{N_A \lambda^4} n_m^2 \left( \frac{dn}{dc} \right)^2$$

where  $dn/dc$  is the refractive index increment and  $N_A$  is Avogadro's constant. The  $dn/dc$  was calculated for each polymer based on the composition of the block copolymer and the  $dn/dc$  of PVP and PVAc in water at 25 °C.<sup>21</sup>

The data were analysed by the graphical method first reported by Zimm,<sup>22</sup> which involves the extrapolation of the scattering data to both zero angle and zero concentration, simultaneously. This can be achieved by plotting  $K_Rc/R_q$  vs.  $q^2 + (\text{constant } k)c$ , where  $k$ , an arbitrary mathematical constant with no physical significance is chosen to give a convenient spacing of the data points on the graph. The initial slope of the curve produced by points extrapolated to  $c = 0$  is proportional to  $R_g^2$ , whereas the slope of the curve of points extrapolated to  $\theta = 0$  is proportional to  $A_2$ . Extrapolation of  $c = 0$  and  $\theta = 0$  yields an intercept inversely proportional to  $M_w$ . However, due to the well-known problem of static light scattering analysis of block copolymers (which are polydisperse in composition and molecular weight) the quantities obtained by Zimm have to be treated only as apparent values.

#### *3.2.10 Stability of PVP-b-PVAc block copolymers in biological environment*

The stability of the block copolymers was assessed by DLS. The stability of the block copolymers was investigated in the systems mimicking biological fluids (PBS, pH 7.4) and PBS containing 20 % fetal calf serum (FCS). The PVP-*b*-PVAc samples were prepared as described in section 3.2.6. The solutions were incubated at 37 °C, and DLS measurements were recorded out at specific time intervals, at 37 °C.

### 3.3 Results and discussion

#### 3.3.1. Synthesis and characterization of PVP macro-RAFT-agent and PVP-*b*-PVAc block copolymers

PVP macro-RAFT agent was successfully synthesized using *S*-(2-cyano-2-propyl) *O*-ethyl xanthate. From Table 3.1 it is seen that the number average molecular weight ( $M_n$ ) of the homopolymerizations obtained by  $^1\text{H}$  NMR and SEC were closely in agreement to the theoretical  $M_n$ .

**Table 3.1:** Polymerization conditions, conversion and molecular weight of PVP macro-RAFT-agent

Polymer	$\alpha^a$ (%)	Reaction time (hr)	Reaction temperature	$M_{n,\text{theo}}$ (g/mol)	$M_{n,\text{SEC}}^b$ (g/mol)	$M_{n,\text{NMR}}^c$ (g/mol)	$D$
PVP macro-RAFT	60	6	60 °C	10 000	6500	9500	1.3

<sup>a</sup>conversion

<sup>b</sup> $M_{n,\text{SEC}}$  based on PMMA standards

<sup>c</sup> $M_{n,\text{NMR}}$  determined as the ratio of the xanthate signal to monomer backbone signal

A typical  $^1\text{H}$  NMR spectrum of the PVP macro-RAFT agent is shown in Figure 3.1. Peak assignments are indicated in Figure 3.1 and were made based on the expected structure. The peaks marked with an asteriks are diethyl ether. The signal at 4.60 ppm from the omega chain end and the polymer peaks between 4.0-3.5 ppm was used to calculate the number average molecular weight ( $M_n$ ) of the PVP macro-RAFT agent.

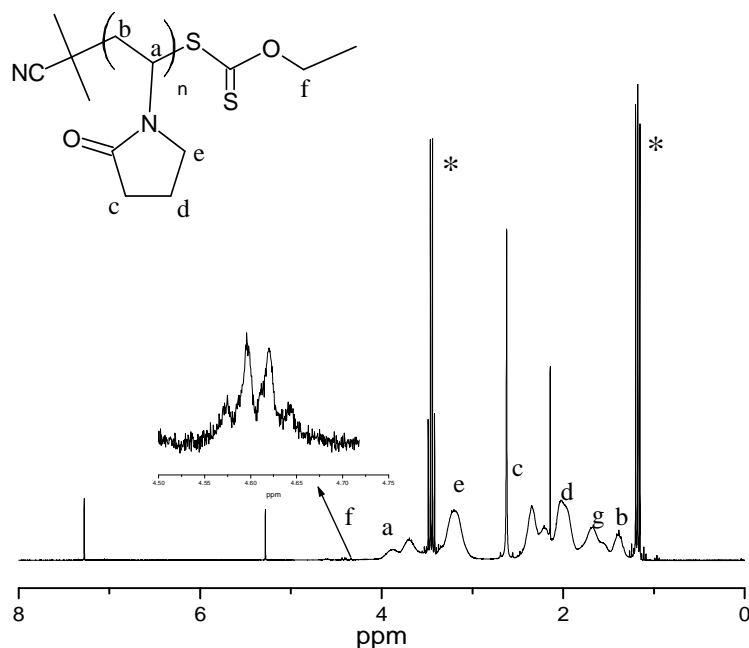


**Figure 3.1:**  $^1\text{H}$  NMR spectrum of PVP macro-RAFT agent in  $\text{CDCl}_3$

In a second step VAc is added to the PVP-macro RAFT agent (starting hydrophilic block) to obtain the corresponding PVP-*b*-PVAc block copolymer. The incorporation of the VAc units into the PVP macro-RAFT agent was evidenced by  $^1\text{H}$  NMR spectroscopy. A typical  $^1\text{H}$  NMR spectrum of PVP-*b*-PVAc is shown in Figure 3.2. Peak assignments are indicated in Figure 3.2 and were made based on the expected structure. The signals at 3 – 4 ppm are assigned to the monomer repeat units of PVP (a, e). The signal at 4.9 ppm is attributed to the methine peak of PVAc (g)

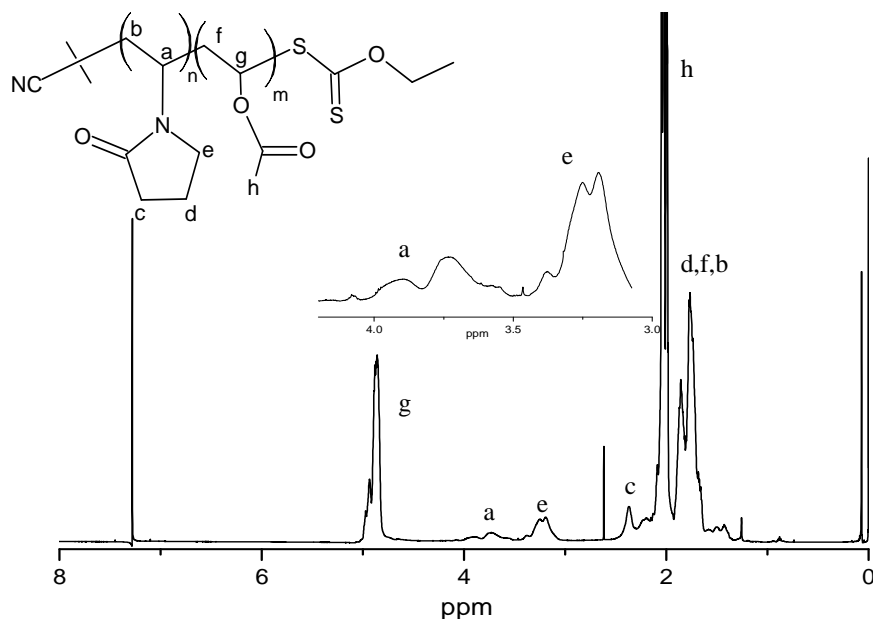


**Figure 3.2:**  $^1\text{H}$  NMR spectrum of PVP-*b*-PVAc in  $\text{CDCl}_3$

The various block copolymers of fixed hydrophilic PVP block length and varying hydrophobic PVAc block length are tabulated in Table 3.2. It must be mentioned that SEC data is likely not to reflect the true molar masses of the block copolymers due to the calibration based on PMMA standards. Furthermore, SEC analysis of block copolymers suffers inherent difficulties particularly when the blocks have a strongly differing polarity and interaction with the solvent and the column. This could perhaps explain the high  $M_n$  values obtained from SEC.



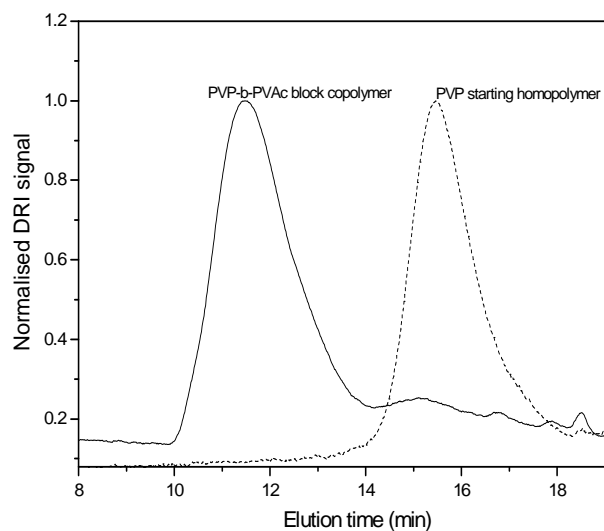
**Table 3.2:** Synthesis of PVP and PVP-*b*-PVAc block copolymers with different PVAc block length

Polymer	Experimental description	$M_{n,theor}^a$ (g/mol)	Theoretical (co)polymer composition	$M_{n,SEC}^b$ (g/mol)	$\mathcal{D}$
1	PVP <sub>90</sub> -xanthate-mediated diblock copolymerization of VAc	18000	PVP <sub>90</sub> - <i>b</i> -PVAc <sub>210</sub>	64100	1.6
2	PVP <sub>90</sub> -xanthate-mediated diblock copolymerization of VAc	22016	PVP <sub>90</sub> - <i>b</i> -PVAc <sub>256</sub>	74800	1.6
3	PVP <sub>90</sub> -xanthate-mediated diblock copolymerization of VAc	24900	PVP <sub>90</sub> - <i>b</i> -PVAc <sub>290</sub>	91000	1.7

<sup>a</sup>Number average molecular weight of vinyl acetate block based on initial molar ratios of the polymerization mixture and conversion

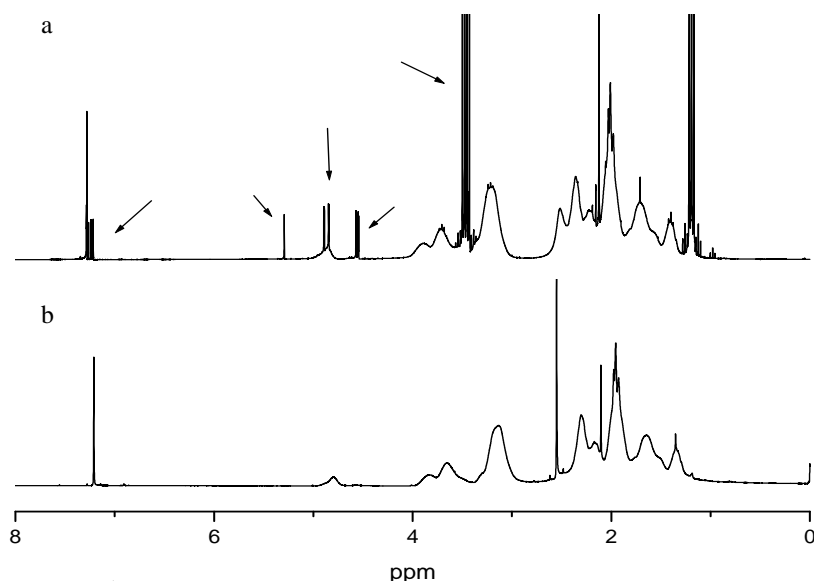
<sup>b</sup> $M_{n,SEC}$  based on PMMA standards

Figure 3.3 shows the SEC chromatogram for the chain extension of PVP-macro RAFT agent to vinyl acetate. An obvious peak shift of the PVP macro-RAFT to PVP-*b*-PVAc (*i.e.* low molecular weight to higher molecular weight) was seen. This indicated that propagation started from the initial xanthate end-functional PVP, and generated the PVP-*b*-PVAc diblock copolymer. The small tail seen at high elution time (*i.e.* low molecular weight) in the PVP-*b*-PVAc SEC chromatogram is ascribed to PVP homopolymer. These chains are dead or inactive chains that are unable to reinitiate in the second step. In the chain extension step, propagating chains are initiated either by primary radicals that originate from the azo-initiator (in this case AIBN) or by radicals from the leaving group of the RAFT agent. The polymeric radicals terminate by either reacting with the RAFT agent or with the same initiating group (initiator or leaving group of RAFT agent). Therefore, numerous different structures exist in these systems which could contribute towards the high  $M_n$  and dispersity ( $\mathcal{D}$ ) obtained. Indeed, the chains that contain the active RAFT agent are highly preferable since they can possibly be chain extended upon addition of PVAc monomer, resulting in block copolymer formation. Inherent to the mechanism of RAFT polymerization, PVAc homopolymer is inevitably formed.



**Figure 3.3:** Normalized SEC chromatograms for the chain extension of starting homopolymer chain-transfer agent (PVP macro-RAFT) with vinyl acetate

The purification of the block copolymers is important for their application as drug delivery carriers (Chapter 4). The dialysis method was implemented to purify the block copolymers. This method allows for low molecular weight contaminants (*e.g.* solvent, residual monomer and homopolymer) to be removed by diffusing through a dialysis membrane of a specific molecular weight cut-off (MWCO). The purification of the PVP-*b*-PVAc block copolymer via the dialysis method proved to be a very efficient purification technique. This is indicated in the  $^1\text{H}$  NMR spectra (Figure 3.4) where unpurified and purified PVP-*b*-PVAc block polymers are compared. Impurities are indicated by the arrows in the spectra.

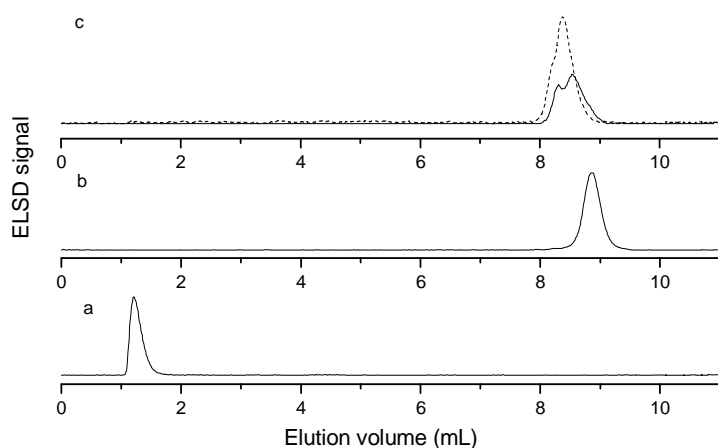


**Figure 3.4:**  $^1\text{H}$  NMR spectra of a) PVP-*b*-PVAc in  $\text{CDCl}_3$  not dialyzed (unpurified) b) PVP-*b*-PVAc in  $\text{CDCl}_3$  dialyzed (purified)

### 3.3.2 Gradient HPLC characterization of PVP-*b*-PVAc block copolymers

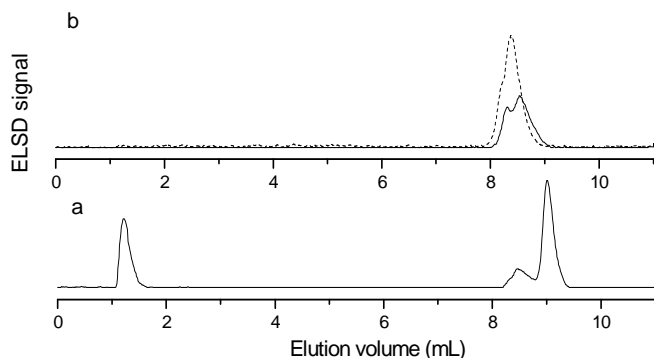
Previously in our group, Pound *et al.*<sup>23</sup> successfully separated double hydrophilic block copolymers of PEG-*b*-PVP and amphiphilic block copolymers of PEG-*b*-PVAc using gradient HPLC, also referred to Gradient Polymer Elution Chromatography (GPEC). In our study, the amphiphilic block copolymers of PVP-*b*-PVAc were therefore separated using the same method and conditions already developed. Acetonitrile and water were chosen as the eluent mixture which was able to dissolve all homo- and block copolymers. A dual detector system was used (ELSD detector to identify the macromolecular species and UV detection for the xanthate functionality). Homopolymers and block copolymers were dissolved in a 65/35 (v/v) ACN/water. Homopolymers of PVP<sub>90</sub> and PVAc<sub>200</sub> and block copolymers (PVP<sub>90</sub>-*b*-PVAc<sub>210</sub> and PVP<sub>90</sub>-*b*-PVAc<sub>290</sub>) were separated using GPEC with a gradient with increasing acetonitrile content. By increasing the hydrophobicity of the mobile phase, PVP-*b*-PVAc block copolymers eluted first followed by PVAc homopolymer.

Figure 3.5 shows the chromatograms of the homopolymers (Figure 3.5 (a) and (b)) and of PVP-*b*-PVAc with different PVAc length (Figure 3.5 (c), PVP<sub>90</sub>-*b*-PVAc<sub>290</sub> and PVP<sub>90</sub>-*b*-PVAc<sub>210</sub>). The PVP<sub>90</sub>-*b*-PVAc<sub>210</sub> and PVP<sub>90</sub>-*b*-PVAc<sub>290</sub> block copolymers present a broad peak with a bimodal distribution (shoulder), eluting earlier than PVAc, as expected. The shoulder could indicate the presence of PVAc homopolymer. PVP<sub>90</sub>-*b*-PVAc<sub>210</sub> eluted slightly earlier than PVP<sub>90</sub>-*b*-PVAc<sub>290</sub> due to the shorter PVAc block length. No trace of PVP homopolymer was detected (the presence of any short PVP chains was removed by dialysis). The chromatograms also show a slight overlap of the PVP-*b*-PVAc with PVAc homopolymer. This could indicate that most of the VAc was polymerized from the PVP starting block and that a small fraction of the block copolymer also consists of PVAc homopolymer. This is not unexpected, and in agreement with the theory for RAFT polymerization.



**Figure 3.5:** Gradient polymer elution chromatogram of a) PVP<sub>90</sub> prepared in bulk in the presence of *S*-2-(cyano-2-propyl) -(*O*-ethyl xanthate) b) PVAc<sub>200</sub> prepared in bulk in the presence of *S*-(2-ethylpropionate)-(*O*-ethyl xanthate) c) PVP<sub>90</sub>-*b*-PVAc<sub>290</sub> (-), PVP<sub>90</sub>-*b*-PVAc<sub>210</sub> (- -) block copolymers

An additional experiment was carried out whereby PVP<sub>90</sub>, PVAc<sub>200</sub> and PVP<sub>90</sub>-*b*-PVAc<sub>290</sub> were mixed together (ratio 1:1:1) in 65/35 (v/v) ACN/water. Figure 3.6 (a) shows the separation of the mixture of homopolymers and the block copolymers. As expected, PVP<sub>90</sub> eluted first followed by PVP<sub>90</sub>-*b*-PVAc<sub>256</sub> and PVAc<sub>200</sub>. Figure 3.6 (b) represents the chromatogram of only the PVP<sub>90</sub>-*b*-PVAc<sub>290</sub> and PVP<sub>90</sub>-*b*-PVAc<sub>210</sub> and confirms that the main structure was block copolymer.



**Figure 3.6:** Gradient polymer elution chromatogram of a) mixture of PVP<sub>90</sub>, PVAc<sub>200</sub> and PVP-*b*-PVAc<sub>290</sub> b) PVP-*b*-PVAc<sub>290</sub> (-) and PVP-*b*-PVAc<sub>210</sub> (- -) of varying PVAc block length

Based on the GPEC measurements it is difficult to get quantitative information regarding the presence of PVAc homopolymer contamination in the block copolymers. Further optimization including different mobile and stationary phases for this separation is recommended as future work.

### 3.3.3 Self-assembly behavior of PVP-*b*-PVAc block copolymers

<sup>1</sup>H NMR spectroscopy is a convenient characterization method to obtain a first indication of the self-assembly process of amphiphilic block copolymers in various solvents.<sup>24</sup> A comparison of the <sup>1</sup>H NMR spectra of PVP-*b*-PVAc in deuterated water (selective solvent for the PVP block) and in deuterated chloroform (a common solvent for both blocks) allows for the identification of the formation of aggregates.

Figure 3.7 (a and b) represents the <sup>1</sup>H NMR spectra of PVP-*b*-PVAc in CDCl<sub>3</sub> and PVP-*b*-PVAc in D<sub>2</sub>O. Figure 3.7 (a) shows the <sup>1</sup>H NMR spectrum of PVP-*b*-PVAc in CDCl<sub>3</sub>. Self-assembly of PVP-*b*-PVAc is not expected in CDCl<sub>3</sub> and all peaks of the hydrophilic PVP (3 – 4 ppm) and hydrophobic PVAc (2 – 2.1 ppm) were detected. The self-assembly of PVP-*b*-PVAc into either

micelles or vesicles was confirmed by  $^1\text{H}$  NMR in  $\text{D}_2\text{O}$ . The predominant peak is that of the PVP (protons from the repeat units of polymer backbone, 3 – 4 ppm) - the corona of the micelle- or vesicle-like structure - while the peaks of PVAc are suppressed (2 – 2.1 ppm) and not visible (5 ppm) due to the limited mobility of the PVAc-chains in the hydrophobic core or bilayer.

$^1\text{H}$  NMR spectroscopy confirmed that the PVP-*b*-PVAc block copolymers have the ability to self-assemble in aqueous media.

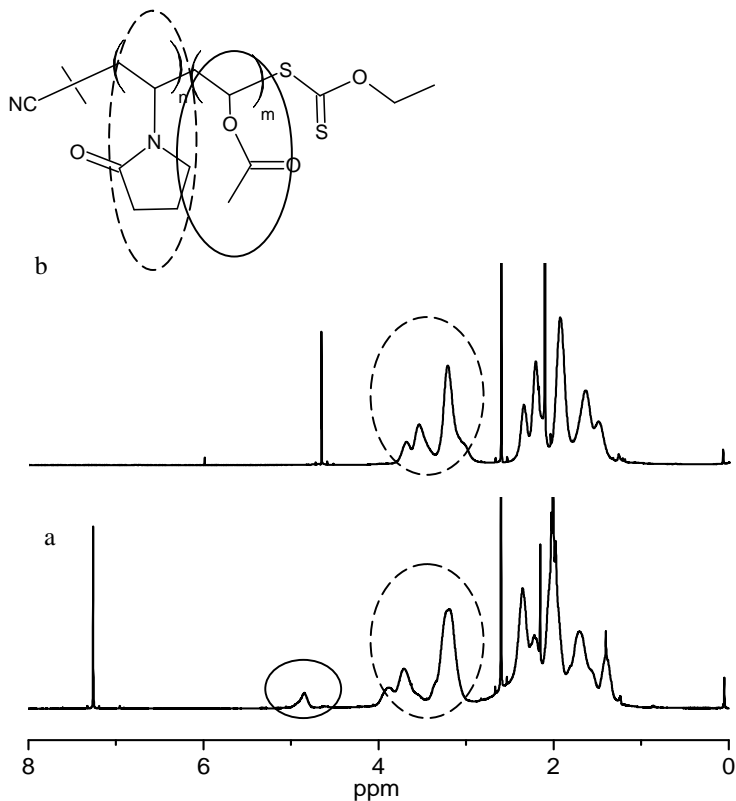


**Figure 3.7:**  $^1\text{H}$  NMR spectra of a) PVP<sub>90</sub>-*b*-PVAc<sub>290</sub> in  $\text{CDCl}_3$  b) PVP-*b*-PVAc in  $\text{D}_2\text{O}$

### 3.3.4 CMC of PVP-*b*-PVAc block copolymers

The thermodynamic stability of the block copolymer micelle upon dilution is an important factor for *in vivo* application. This is indicated by the CMC of the block copolymer. One of the requirements of a drug delivery carrier is its stability to be maintained at a very high dilution. This is crucial and therefore a low CMC is essential.

Several methods can be used to determine the CMC of amphiphilic block polymers. These include surface tension,<sup>25</sup> dye solubilisation,<sup>26,27</sup> light scattering and fluorescence spectroscopy.<sup>28</sup> The use of fluorescent probes, such as pyrene is the most common and accurate method used to determine the CMC.<sup>29</sup> Pyrene is a highly hydrophobic aromatic hydrocarbon and sensitive to the polarity of the surrounding environment. The self-aggregation behavior of PVP-*b*-PVAc block copolymers in aqueous environment were studied using pyrene as a fluorescent probe. The transfer of pyrene from a hydrophilic to a more hydrophobic environment results in a red shift in the excitation spectrum.<sup>30,31</sup>

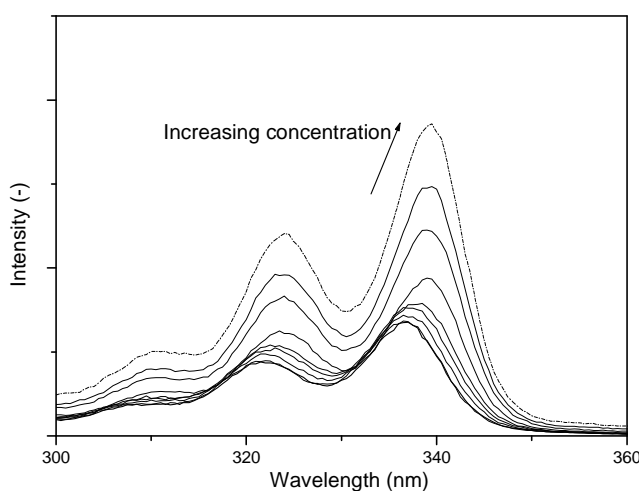


**Figure 3.8:** Fluorescence excitation spectra of pyrene ( $6.0 \times 10^{-7} M$ ) containing PVP<sub>90</sub>-*b*-PVAc<sub>290</sub> at different concentrations (0.0001 – 1 mg/mL)

The excitation spectra of pyrene is shown in Figure 3.8. A small change in the spectra is seen for the polymeric solutions for which the copolymer concentration is lower than the CMC. When the concentration increased above the CMC, an increase in the intensity and a red shift is seen. The CMC of the copolymers was calculated by the crossover point of the intensity ratio of  $I_{338 \text{ nm}}/I_{336 \text{ nm}}$  from the pyrene excitation spectra *versus* the logarithm of the concentration for the various PVP-*b*-PVAc copolymer solutions (Figure 3.9). The ratio  $I_{338 \text{ nm}}/I_{336 \text{ nm}}$  is almost constant at low polymer concentrations, but from a certain concentration, it starts to increase steadily, indicative of the incorporation of pyrene into the hydrophobic region of the vesicles. The CMC for PVP<sub>90</sub>-*b*-PVAc<sub>290</sub>, PVP<sub>90</sub>-*b*-PVAc<sub>256</sub> and PVP<sub>90</sub>-*b*-PVAc<sub>210</sub> were 0.0012 mg/mL, 0.0014 mg/mL and 0.0085 mg/mL, respectively, which is in agreement with the copolymer composition.

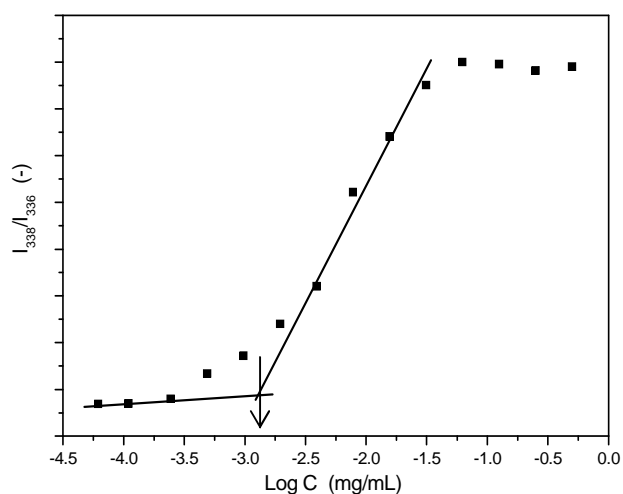


**Figure 3.9:** Fluorescence intensity ratio  $I_{338}/I_{336}$  for pyrene as a function of logarithm of concentration for PVP<sub>90</sub>-*b*-PVAc<sub>290</sub>. The CMC was calculated from the intersection of the horizontal line at low polymer concentration and the tangent of the curve at high polymer concentration

An increase in the hydrophobic block length serves to lower the CMC.<sup>32</sup> The results indicate that an increase in the molecular weight of the hydrophobic block decreases the CMC or, alternatively, the CMC of the block copolymer decreased with increasing PVAc block length, as expected. This indicates that the hydrophobic block length plays a critical role in the formation and the CMC of the polymer vesicles. Such extremely low CMC values obtained is an important factor for the structural stability of the PVP-*b*-PVAc block copolymers, which is necessary for long circulating polymer drug carriers in the body.<sup>33</sup>



### 3.3.5 Size distribution and morphology of PVP-*b*-PVAc

Measurements were carried out by DLS, TEM and SLS to further evaluate the properties of the block copolymers in terms of the particle size, the particle size distribution and the morphology. The results are tabulated in Table 3.3.

**Table 3.3:** Particle size of PVP-*b*-PVAc block copolymers of varying PVAc block length determined by DLS and TEM

Polymer	Particle size ( $Z_{ave}$ (nm))	PDI	Particle size (nm)
	DLS		TEM
PVP <sub>90</sub> - <i>b</i> -PVAc <sub>210</sub>	190 ± 1.8	0.09	120 – 150 nm
PVP <sub>90</sub> - <i>b</i> -PVAc <sub>256</sub>	180 ± 4.2	0.05	120 – 150 nm
PVP <sub>90</sub> - <i>b</i> -PVAc <sub>290</sub>	200 ± 3.5	0.05	90 – 200 nm

As mentioned earlier, the self-assembly of the PVP-*b*-PVAc block copolymers was carried out via the dialysis method. Here, the block copolymer is dissolved in a solvent (DMSO) followed by dialysis in which the water gradually replaces the solvent, which induces the self-assembly of the block copolymer. The particle size (diameter) of the self-assembled PVP-*b*-PVAc block copolymers in water was 180 – 200 nm with a monomodal size distribution as seen in Figure 3.10. No significant variation in particle size was seen for the various PVP-*b*-PVAc block copolymers of varying PVAc block length. The low polydispersity (< 0.1) strongly suggests the formation of monodisperse particles, which is usually the case for spherical micelles and also possible for vesicles. Note that DLS provides the hydrodynamic radius of the particles, at this stage no conclusion about the shape or morphology of the self-assembled PVP-*b*-PVAc block copolymers can be made.

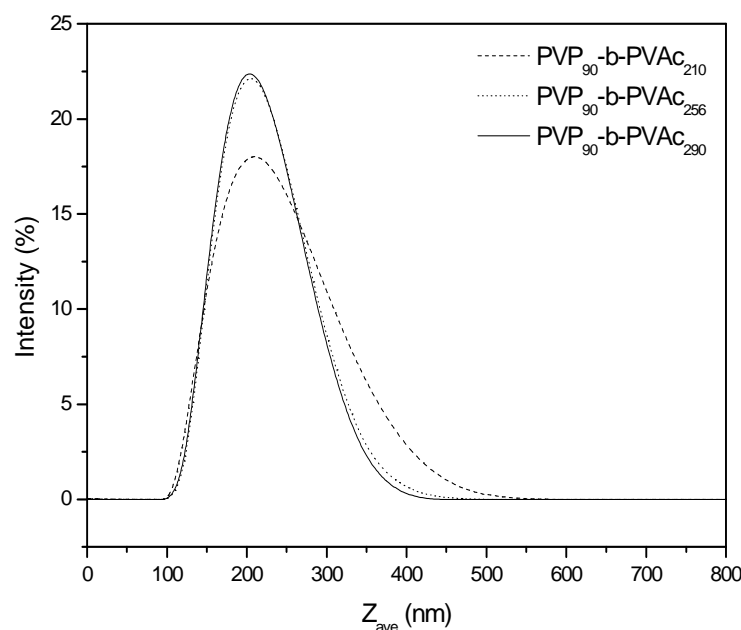


**Figure 3.10:** DLS size distributions of PVP-*b*-PVAc of varying PVAc block length

It has been reported in literature that the size of the particles is dependent on the polymer concentration. For example, Zhang and coworkers found that vesicles are preferentially formed at higher polymer concentrations compared to concentrations at which micelles are formed.<sup>34</sup> This is likely attributed to the higher probability of interpolymer aggregation at higher polymer concentration. The effect of different initial concentration of the PVP-*b*-PVAc block copolymer (10 mg/mL – 1 mg/mL) on the particle size was investigated. In our case, it was found that the particle size of the self-assembled PVP-*b*-PVAc remained between 160 – 200 nm at various polymer concentrations (data not shown).

In another study, Vangeyte *et al.*<sup>35</sup> investigated the influence of various preparation techniques and solvents used, on the particle size of poly(ethylene oxide)-*b*-poly( $\epsilon$ -caprolactone) (PEO-*b*-PCL) in water. The three preparation methods studied were the dialysis of the polymers in a common organic solvent against water, rapid addition of water to the polymer organic solutions, and rapid addition of the polymer organic solutions into water. Results indicated that direct dialysis of the copolymer solutions in an organic solvent against water resulted in large and polydisperse particles (> 1  $\mu$ m). On the other hand, the two other methods that consist of the rapid addition of the organic solution to water and vice versa resulted in well-defined, monodisperse particles (30 – 60 nm). However, the particle size was dependent on the organic

solvent used. The research group of Eisenberg also reported on the relationship between the morphology of poly(styrene)-*b*-(poly(acrylic acid)) (PS-*b*-PAA) block copolymers and the nature of the common solvent. It was found that the block copolymers yield only spherical micelle-like aggregates in DMF, while vesicles were obtained in THF.<sup>36</sup>

In the present study, the effect of the preparation method and solvent on the self-assembly of the PVP-*b*-PVAc block copolymers was not investigated. Self-assembly studies were only carried out via the dialysis method using only DMSO as organic solvent. Importantly, the self-assembly of PVP-*b*-PVAc block copolymers via the dialysis method was reproducible.

The morphology of the PVP-*b*-PVAc in water (5 mg/mL) was visualized by TEM. The self-assembled PVP-*b*-PVAc block copolymers were clearly distinguished as uniform, spherical structures as shown in Figure 3.11. Interestingly, we observed the characteristic feature for vesicle structures: a dark corona surrounding a light core. Eisenberg and Dischner<sup>6</sup> demonstrated the influence of the fraction of the hydrophilic block and the hydrophobic block on the molecular shape of the copolymer and particle morphology. The present observation is in line with their findings. Since the hydrophobic PVAc block is the dominant segment in the PVP-*b*-PVAc block copolymer, the formation of vesicles and bilayers is likely to be expected. The particle sizes obtained by TEM ranged from 150 – 200 nm with a few slightly smaller particles of 100 nm. The particle diameter derived from TEM was slightly smaller than that measured and compared to DLS. This is attributed to the dehydration and shrinkage of the particles during TEM sample preparation (drying process), as reported in previous studies.<sup>37</sup>

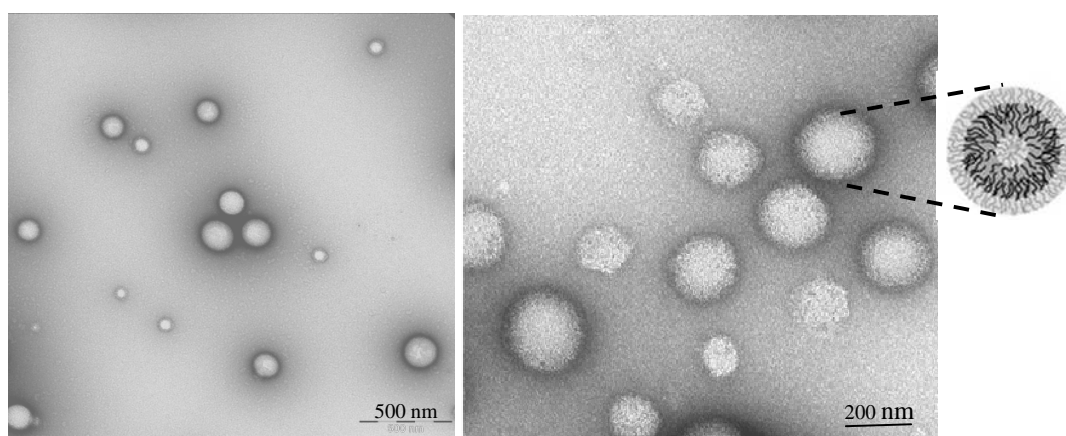


**Figure 3.11:** TEM image of PVP<sub>90</sub>-*b*-PVAc<sub>290</sub> block copolymer. Black corresponds to hydrophobic region (bilayer) and grey to hydrophilic regions. The insert is a schematic representation of the self-assembled, vesicular-like structure of the PVP-*b*-PVAc

In addition to DLS and TEM, SLS experiments were performed in water to confirm the structure of the PVP-*b*-PVAc block copolymers. From scattered light intensity measurements at various PVP-*b*-PVAc concentrations, we could determine the radii of gyration ( $R_g$ ) and the weight average molecular weight ( $M_w$ ) of the block copolymer aggregates. A typical Zimm plot of the scattering intensity versus the square of the scattering vector (including the extrapolation to zero concentration and zero angle) is given in Figure 3.12.

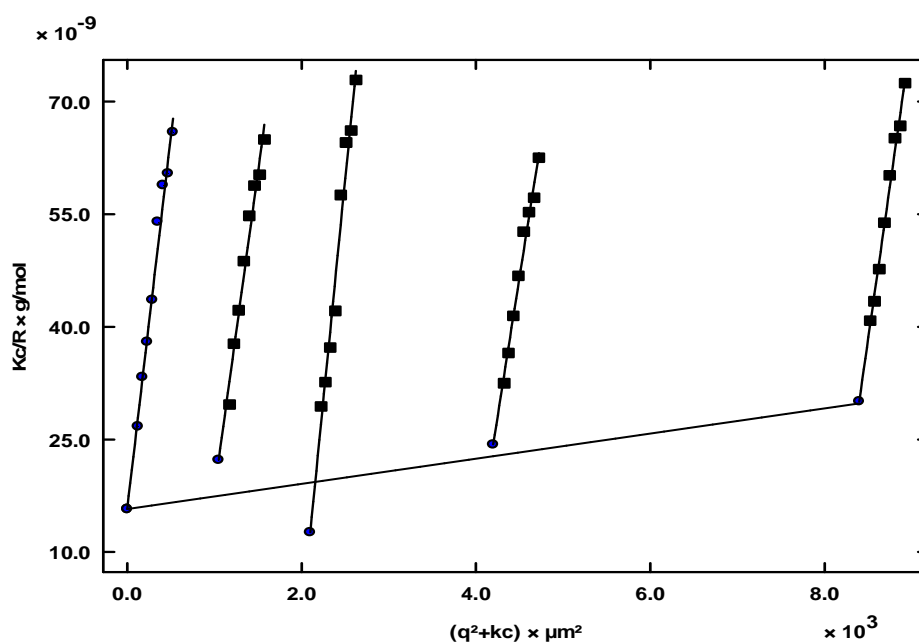


**Figure 3.12:** Zimm plot for PVP<sub>90</sub>-*b*-PVAc<sub>210</sub> extrapolated to zero angle and zero concentration in water at 25 °C. Squares represent experimental data, measurements at four different concentrations, from 50° – 120°. Circles represent simulated data

The ratio  $R_g/R_h$  is a characteristic value that depends on the morphology of the aggregates formed. From the  $R_g$  and  $R_h$  values obtained by DLS and SLS, we calculated the  $R_g/R_h$  ratio, which provided information on the structure of the PVP-*b*-PVAc in water. Table 3.4 summarizes the results obtained by combining DLS and SLS analysis for PVP<sub>90</sub>-*b*-PVAc<sub>290</sub> and PVP<sub>90</sub>-*b*-PVAc<sub>210</sub>.

**Table 3.4:** Physicochemical parameters of PVP-*b*-PVAc block copolymers obtained by SLS and DLS

PVP- <i>b</i> -PVAc	$R_h^a$ (nm)	$R_g^b$ (nm)	$R_g/R_h$	$M_{w(\text{particle})}^c$ (g.mol <sup>-1</sup> )	$\rho^d$ (g/cm <sup>3</sup> )	$N_{\text{agg}}^e$	$S/N_{\text{agg}}^f$ (nm <sup>2</sup> )
PVP <sub>90</sub> - <i>b</i> -PVAc <sub>290</sub>	105	119 (± 3.5)	1.15	$1.1 \times 10^8$	0.3	1200	52
PVP <sub>90</sub> - <i>b</i> -PVAc <sub>210</sub>	96	98.7 (± 5.1)	1.02	$6.3 \times 10^7$	0.1	1000	62

<sup>a</sup>Hydrodynamic radius ( $Z_{\text{ave}}/2$ ) determined by DLS. <sup>b</sup>Radius of gyration, extrapolated to zero concentration. <sup>c</sup> $M_{w(\text{particle})}$  weight average molecular weight of particles determined by SLS. <sup>d</sup> $\rho$  is the density of the particles calculated by  $\rho = M_{w(\text{particle})}/N_A V$ ,  $V$  is based on  $R_h$ . <sup>e</sup>Aggregation number was calculated by using the weight average molecular weight determined by SLS and number average molecular weight determined by SEC. <sup>f</sup>Surface area per PVP chain

The hydrodynamic radius ( $R_h$ ) was determined by DLS before the SLS measurements were started. DLS measurements give a  $R_h$  in the range of 95 – 100 nm for both PVP<sub>90</sub>-*b*-PVAc<sub>290</sub> and PVP<sub>90</sub>-*b*-PVAc<sub>210</sub>. Theoretical values for the  $R_g/R_h$  ratio are 0.78 for hard spheres, 1 for vesicles with a thin membrane, and values greater than 1.5 are for elongated structures or polymers with extended conformations (e.g. rod-like micelles).<sup>6,38,39</sup> For the reported block copolymers, the ratios of  $R_g/R_h$  from light scattering (Table 3.4) correspond well to the theoretical value for vesicles (~1). The results indicate that the PVP-*b*-PVAc block copolymers self-assembled predominantly into vesicular structures, which is consistent with the TEM images which show spherical bilayer structures. The density of the self-assembled structures were also calculated and found to be 0.3 g/cm<sup>3</sup> and 0.1 g/cm<sup>3</sup> for PVP<sub>90</sub>-*b*-PVAc<sub>290</sub> and PVP<sub>90</sub>-*b*-PVAc<sub>210</sub>. These values are reasonable for water-swollen yet solid polymer self-assembled structures. The aggregation number ( $N_{\text{agg}}$ ) was calculated to be 1200 and 1000 for PVP<sub>90</sub>-*b*-PVAc<sub>290</sub> and PVP<sub>90</sub>-*b*-PVAc<sub>210</sub>, respectively. These values are typical in the range for vesicles. As expected, the aggregation number increased with increasing hydrophobic PVAc block length and molecular weight.

It is necessary to point out that variables such as the preparation method, the nature and composition of the solvent mixture, the water content, the relative hydrophilic/hydrophobic block length and the molecular weight of the block copolymer, all provide control over the resulting particle size, the aggregation number and morphology of self-assembled block copolymers.<sup>8,40-43</sup> Therefore, depending on the type of system and conditions used, an entire range of morphologies can be obtained and only subtle changes in these variables can lead to

dramatic alterations in the physicochemical properties and morphologies of the self-assembled block copolymers.

Based on the DLS, TEM and SLS results, PVP-*b*-PVAc block copolymers self-assembled into spherical, vesicle structures of 180 – 200 nm in diameter. For the application of PVP-*b*-PVAc block copolymers as drug carrier, these particle sizes obtained are suitable for passive targeting via the EPR effect.

### 3.3.6 Stability of PVP-*b*-PVAc vesicles under physiological conditions

Upon intravenous administration, polymer drug carriers encounter blood cells and plasma proteins before reaching the target cells. Serum is a complex fluid that is made up of serum albumin, lipoproteins immuno-,  $\gamma$ - and macroglobulins. Serum proteins can bind to or penetrate in the drug carriers which can result in changes in their physicochemical properties such as the particle size.<sup>44-46</sup> The stability of PVP-*b*-PVAc was therefore investigated in physiological conditions (PBS, pH 7.4, 37 °C). Furthermore, *in vitro* studies are usually performed in the presence of serum (10 – 20 % FCS) (Chapter 5, Section 5.2.3). For this reason, the particle size stability of the PVP-*b*-PVAc carrier was also evaluated in PBS containing 20 % serum.

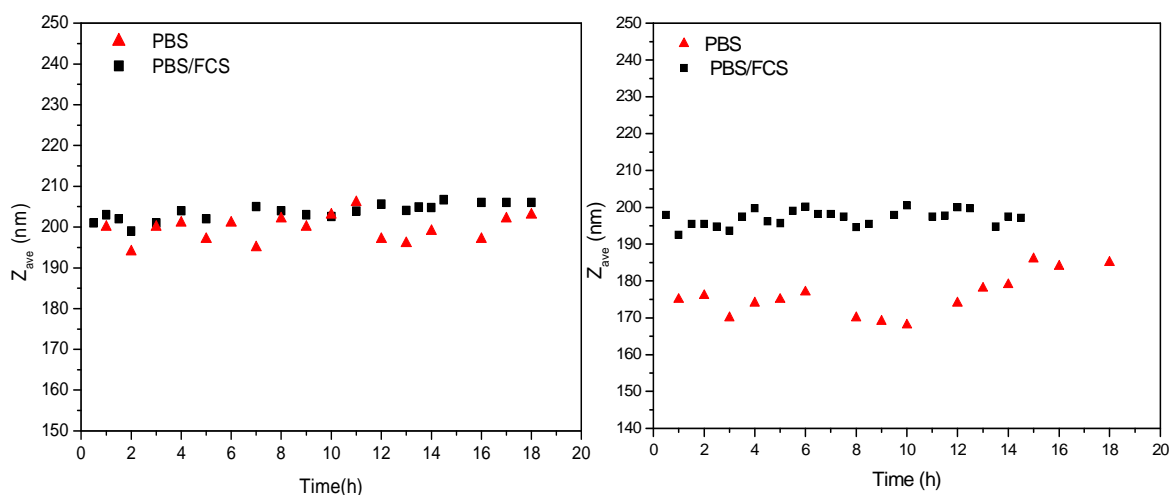


**Figure 3.13:** Stability of PVP<sub>90</sub>-*b*-PVAc<sub>290</sub> (left) and PVP-*b*-PVAc<sub>210</sub> (right) at 37 °C in PBS (pH 7.5) and PBS/FCS as determined by DLS

Figure 3.13 shows the particle size stability of the PVP-*b*-PVAc block copolymers (0.5 mg/mL) incubated with PBS (pH 7.4, 37 °C) or PBS containing 20 % serum. Prior to incubation studies in serum, a control experiment was carried out. As reported previously in the literature, DLS of biological fluids such as serum result in significant background signal (~ 60 nm) due to their heterogeneous nature.<sup>47</sup> As a control experiment, the background scattering of PBS/FCS (20 % serum) was measured alone and considered insignificant. PVP<sub>90</sub>-*b*-PVAc<sub>290</sub> and PVP<sub>90</sub>-*b*-PVAc<sub>210</sub> samples incubated in PBS were stable for more than 18 hours. For the PVP<sub>90</sub>-*b*-PVAc<sub>290</sub> block copolymer incubated in the presence of serum, the particle size remained constant over 16 hours. PVP<sub>90</sub>-*b*-PVAc<sub>210</sub> also showed stability over 18 hours in serum. The size stability of the vesicles is likely due to the PVP hydrophilic surface, which protects them from surface adsorption of serum components. High surface coverage of hydrophilic polymer chains is a favorable property for a drug carrier. This allows for prolonged blood circulation and protection of the carrier from protein adsorption.

### **3.4 Conclusion**

PVP-*b*-PVAc block copolymers of constant hydrophilic PVP block length and varying hydrophobic block length were synthesized via a CRP technique. The ability of the block copolymers to self-assemble in aqueous solution was confirmed by <sup>1</sup>H NMR, fluorescence spectroscopy, DLS, SLS and TEM. PVP-*b*-PVAc self-assembled into spherical vesicle-like structures ranging from 180 – 200 nm in aqueous solution. The low CMC values of the block copolymers should further allow for the PVP-*b*-PVAc carrier to maintain its vesicular morphology upon dilution. Furthermore, the stability of the PVP-*b*-PVAc carrier was maintained under physiological conditions in the presence and absence of serum. With these above mentioned properties, the PVP-*b*-PVAc block copolymer should be a versatile carrier for various hydrophobic and hydrophilic drugs.

### 3.5 References

- (1) Lipinski, C. *Amer. Pharm. Rev.* **2002**, 5, 82 - 85.
- (2) Zhang, H.; Bei, J.; Wang, S. *Biomaterials* **2009**, 30, 100-107.
- (3) Miguel, V. S.; Limer, A. J.; Haddleton, D. M.; Catalina, F.; Peinado, C. *Eur. Polym. J.* **2008**, 44, 3853 - 3863.
- (4) Riess, G. *Prog. Polym. Sci.* **2003**, 28, 1107-1170.
- (5) Wang, X. S.; Guerin, G.; Wang, H.; Wang, Y. S.; Manners, I.; Winnik, M. A. *Science* **2007**, 317, 644 - 647.
- (6) Discher, D. E.; Eisenberg, A. *Science* **2002**, 297, 967 - 973.
- (7) Yu, S. Y.; Azzam, T.; Rouiller, I. E.; Eisenberg, A. *J. Am. Chem. Soc.* **2009**, 131, 10557 - 10566.
- (8) Choucair, A.; Lavigueur, C.; Eisenberg, A. *Langmuir* **2004**, 20, 3894 - 3900.
- (9) Sidorov, S. N.; Bronstein, L. M.; Valetsky, P. M.; Hartmann, J.; Cölfen, H.; Schnablegger, H.; Antonietti, M. *J. Colloid Interface Sci.* **1999**, 212, 197 - 211.
- (10) Spatz, J. P.; Sheiko, S.; Möller, M. *Macromolecules* **1996**, 29, 3220 - 3226.
- (11) Kataoka, K.; Harada, A.; Nagasaki, Y. *Adv. Drug Deliv. Rev.* **2001**, 47, 113 - 131.
- (12) Torchilin, V. P. *Pharm. Res.* **2007**, 24, 1 - 16.
- (13) Zhang, L.; Nguyen, T. L. U.; Bernard, J.; Davis, T. P.; Barner-Kowollik, C.; Stenzel, M. H. *Biomacromolecules* **2007**, 8, 2890 - 2901.
- (14) York, A. W.; Kirkland, S. E.; McCormick, C. L. *Adv. Drug Deliv. Rev.* **2008**, 1018 - 1036.
- (15) Kim, D. W.; Kim, S. Y.; Kim, H. K.; Kim, S. W.; Shin, S. W.; Kim, J. S.; Park, K.; Lee, M. Y.; Heo, D. S. *Ann. Oncol.* **2007**, 18, 2009 - 2014.
- (16) Sparreboom, A.; Scripture, C. D.; Trieu, V. *Clin. Cancer Res.* **2005**, 11, 4136 - 4143.
- (17) Garrec, D. L.; Gori, S.; Luo, L.; Lessard, D.; Smith, D. C.; Yessine, M.-A.; Ranger, M.; Leroux, J.-C.; Ranger, M. *J. Control. Rel.* **2004**, 99 83 - 101.
- (18) Zhu, Z.; Li, Y.; Li, X.; Li, R.; Jia, Z.; Liu, B.; Guo, W.; Wu, W.; Jiang, X. *J. Control. Rel.* **2010**, 142, 438 - 446.
- (19) Torchilin, V. P.; Shtilman, M. I.; Trubetskoy, V. S.; Whiteman, K.; Milstein, A. M. *Biochimica et Biophysica Acta (BBA) - Biomembranes* **1994**, 1195, 181 - 184
- (20) Shi, L.; Chapman, T. M.; Beckman, E. J. *Macromolecules* **2003**, 36, 2563 - 2567.



- (21) Brandrup, J.; Immergut, E. H.; Grulke, E. A. *Polymer Handbook*; John Wiley and Sons, Inc, 1999.
- (22) Zimm, B. J. *J. Chem. Phys.* **1948**, *16*, 1099 - 1116.
- (23) Pound, G.; Aguesse, F.; McLeary, J. B.; Lange, R. F. M.; Klumperman, B. *Macromolecules* **2007**, *40*, 8861 - 8871.
- (24) Narrainen, A. P.; Pascual, S.; Haddleton, D. M. *J. Polym. Sci.* **2002**, *40*, 439.
- (25) Kaewsaiha, P.; Matsumoto, K.; Matsuoka, H. *Langmuir* **2005**, *21*, 9938 - 9945.
- (26) Patist, A.; Bhagwat, S. S.; Penfield, K. W.; Aikens, P.; Shah, D. O. *J. Surfactants Deterg.* **2000**, *3*, 53 - 58.
- (27) Chaibundit, C.; Ricardo, N. M. P. S.; Crothers, M.; Booth, C. *Langmuir* **2002**, *18*, 4277 - 4283.
- (28) Winnik, F. M.; Regismond, S. T. A. *Colloids Surf., A* **1996**, *118*, 1 - 39
- (29) Astafieva, I.; Zhong, X. F.; Eisenberg, A. *Macromolecules* **1993**, *26*, 7339 - 7352.
- (30) Jones, M.; Leroux, J. *Eur. J. Pharm. Biopharm.* **1999**, *48*, 101 - 111.
- (31) Kalyanasundaram, K.; Thomas, J. K. *J. Am. Chem. Soc.* **1977**, *7*, 2039 - 2044.
- (32) Astafieva, I.; Zhong, X. F.; Eisenberg, A. *Macromolecules* **1993**, *26*, 7339 - 7352.
- (33) Opanasopit, P.; Yokoyama, M.; Watanabe, M.; Kawano, K.; Maitani, Y.; Okano, T. *Pharm. Res.* **2004**, *11*, 2001 - 2008.
- (34) Zhang, L.; Eisenberg, A. *Macromol. Symp.* **1997**, *113* 221-232.
- (35) Vangeyte, S.; Gautier, S.; Jérôme, R. *Colloids Surf. A: Physicochem. Eng. Aspects* **2004**, *242*, 203 - 211.
- (36) Yu, Y.; Eisenberg, A. *J. Am. Chem. Soc.* **1997**, *119*, 8383 - 8384.
- (37) Matter, Y.; Enea, R.; Casse, O.; Lee, C. C.; Baryza, J.; Meier, W. *Macromol. Chem. Phys.* **2011**, *212*, 937 - 949.
- (38) Burchard, W. *Adv. Polym. Sci* **1986**, *48*, 1 - 124.
- (39) Dou, H. J.; Jiang, M.; Peng, H. S.; Chen, D. Y.; Hong, Y. *Angew. Chem., Int. Ed.* **2003**, *42*, 1516 -1519.
- (40) Stenzel, M. H.; Barner-Kowollik, C.; Davis, P.; Dalton, H. M. *Macromol. Biosci.* **2004**, *4*, 445.
- (41) Yang, Z.; Yuan, J.; S. Cheng, J. *Eur. Polym. J.* **2005**, *42*, 267 - 274.
- (42) Garnier, S.; Laschewsky, A. *Macromolecules* **2005**, *38*, 7580 - 7592.

- (43) Hussain, H.; Tan, B. H.; Gudipati, C. S.; He, C. B.; Liu, Y.; Davis, T. P. *Langmuir* **2009**, *25*, 5557 - 5564.
- (44) Diezi, T. A.; Bae, Y.; Kwon, G. S. *Mol. Pharm.* **2010**, *7*, 1355 - 1360.
- (45) Kim, S.; Shi, Y.; Kim, J. Y.; Park, K.; Cheng, J. *Expert Opin. Drug Deliv.* **2010**, *7*, 49 - 62.
- (46) Lu, J.; Owen, S. C.; Shoichet, M. S. *Macromolecules* **2011**, *44*, 6002 - 6008.
- (47) van Gaal, E. V. B.; Spierenburg, G.; Hennink, W. E.; Crommelin, D. J. A.; Mastrobattista, E. *J. Control. Rel.* **2010**, *141*, 328 - 338.

## Chapter 4

### **Poly(vinylpyrrolidone)-*b*-poly(vinyl acetate): A potential drug carrier**

#### **Abstract**

Poly(*N*-vinylpyrrolidone)-*b*-poly(vinyl acetate)) (PVP-*b*-PVAc) block copolymers of varying molecular weight and hydrophobic block lengths were synthesized via controlled radical polymerization and investigated as carriers for the solubilization of highly hydrophobic riminophenazine compounds. These compounds have recently been shown to exhibit a strong activity against a variety of cancer types. PVP-*b*-PVAc self-assembles into polymer vesicles in aqueous media, and the dialysis method was used to load the water-insoluble drug (clofazimine) into these polymer vesicles. The polymer vesicles were characterized by <sup>1</sup>H NMR spectroscopy to confirm vesicle formation and the incorporation of the anti-cancer drugs into the polymer vesicles. Dynamic light scattering was used to determine the particle size and particle size distribution of the drug-loaded vesicles as well as the stability of the vesicles under physiological conditions. The size of the polymer vesicles did not increase upon loading with clofazimine, and the particle size of 180 – 200 nm and the narrow particle size distribution were maintained. The morphology of the vesicles was examined by transmission electron microscopy. The drug loading capacity and the encapsulation efficiency of the polymer vesicles were determined by UV/Vis spectroscopy. The polymer vesicles had a relatively high drug loading capacity of 20 wt %. The results indicate that the present PVP-*b*-PVAc block copolymer could be a potential candidate as a drug carrier for hydrophobic drugs.

#### **4.1 Introduction**

To date, various drug delivery and drug targeting systems have been developed or are currently under development for poorly water-soluble drugs. Many of the existing potent therapeutic agents such as anti-cancer drugs are restricted to being used intravenously due to their poor water solubility.<sup>1</sup> Currently, conventional solubilizing agents (e.g. Cremophor EL<sup>®</sup>/ethanol) are used for the formulation in order to improve the solubility. However, these solubilizing agents have undesirable toxic side-effects such as hypersensitivity, neurotoxicity and nephrotoxicity.<sup>2,3</sup> Research focuses on the development of formulations that avoid the use of Cremophor EL<sup>®</sup> to allow an improved control of the toxicity and the pharmacological interactions caused by these anti-cancer agents. As an alternative approach for the solubilization of poorly water-soluble drug molecules, the use of amphiphilic block copolymers is currently the focus of interest in nanopharmaceuticals.<sup>4</sup>

Polymer micelles used in drug delivery are formed from amphiphilic block copolymers consisting of a hydrophilic and a hydrophobic biodegradable and/or biocompatible polymer chain. In aqueous medium, amphiphilic block copolymers self-assemble into distinct structures comprised of a hydrophilic outer shell and a hydrophobic inner core. The hydrophobicity of the micellar core provides a host for the incorporation and solubilization of anti-cancer agents, which are mostly hydrophobic.<sup>5</sup> The hydrophilic shell stabilizes the micelle structure and protects it from biological surroundings. Consequently, both the hydrophilic corona and the hydrophobic core of the micelle carriers control the physicochemical and biological properties of the drug delivery system. On the other hand, amphiphilic block copolymers, if made with suitable amphiphilic proportions, can also self-assemble into vesicular structures. In this case, the hydrophobic blocks self-assemble into bilayer structure whereas the hydrophilic block faces the inner and outer aqueous phases. The hydrophobic bilayer membrane can incorporate hydrophobic drugs while the hydrophilic core can incorporate hydrophilic drugs.

Polymer micelles and vesicles have emerged as versatile drug carriers during the past decades because of their attractive properties.<sup>6-8</sup> As drug vehicles, they present numerous advantages, such as the reduction of side effects of anti-cancer drugs, minimization of drug degradation and of loss upon administration, prevention of harmful or undesirable side-effects, and enhancement of the drug bioavailability. In addition, their nanoscale size (10 – 200 nm in diameter) prevents them from uptake by the reticulo-endothelial system (RES) and allows for higher accumulation at the target site through the enhanced permeation and retention (EPR) effect.<sup>9,10</sup> The biocompatible hydrophilic corona provides these micelles or vesicles with “stealth” properties. The low critical micelle concentration (CMC) makes them relatively stable, prevents them from rapid dissociation, and further allows for the drug to be retained over a longer period of time in the blood stream. This is crucial for the *in vitro* and *in vivo* application of polymer drug carriers.

Clofazimine [3-(4-chloroanilino)-10-(4-chlorophenyl)-2,10-dihydro-2-(isopropylimino)phenazine] is a riminophenazine compound with anti-mycobacterial and anti-inflammatory activity (Figure 4.1).<sup>11</sup> It is one of the most active antimycobacterial agents in this class of compounds (the riminophenazines). In 1957, Barry *et al.*<sup>12</sup> investigated the antituberculosis activity of clofazimine. To date, clofazimine has primarily been used in the treatment of mycobacterial diseases such as leprosy and drug-resistant tuberculosis. It has also been used in the treatment of *Mycobacterium avium* infections in AIDS patients.<sup>13</sup> Recently clofazimine has also been reported to inhibit the growth of various cancer cell types.<sup>14,15</sup>

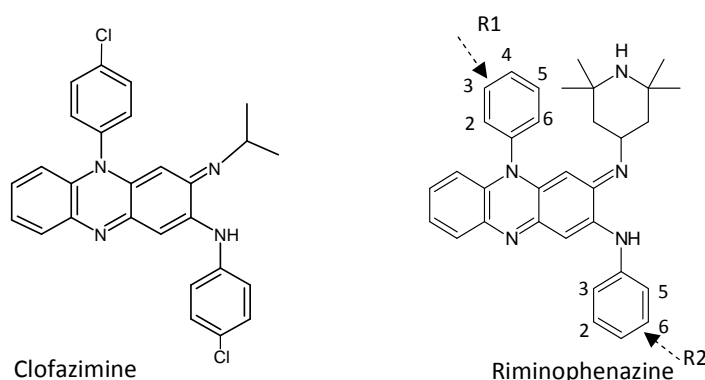


**Figure 4.1:** Chemical structure of parent compound clofazimine and its derivatives (riminophenazines) R1 and R2 are chlorine substituted rings

Like many anti-cancer drugs, clofazimine is a highly hydrophobic drug (water-solubility below 0.225 mg/L (virtually insoluble)), which limits its potential therapeutic value. O'Reilly *et al.*<sup>16</sup> investigated systems of sodium cholate and sodium cholate/fatty acid mixtures to improve the solubility of clofazimine. A 60-fold increase of clofazimine solubility was observed. Attempts of modifying the chemical structure of clofazimine have been proven to be unsuccessful.<sup>17</sup> To enhance the solubility and bioavailability of clofazimine, the use of cyclodextrins, which are water-soluble cyclic oligosaccharides composed of glucose units, has been reported by Salem *et al.*<sup>17</sup> The modified cyclodextrin could be used to solubilise riminophenazines. The solubility of clofazimine increased by about 4000-fold. Hernandez-Valdepena and coworkers recently, synthesized nanoaggregates formed by randomly hydrophobised polyacids derived from poly(methyl vinyl ether-*alt*-maleic acid) (PMVEMAc), which were able to solubilize clofazimine in neutral aqueous media.<sup>18</sup> The encapsulation of clofazimine into liposomes has also been reported to solubilise the drug and furthermore improve the overall therapeutic efficacy. Mehta *et al.*<sup>19</sup> showed that clofazimine can be effectively encapsulated in liposomes with an efficiency of 95 to 100 %. *In vitro* and *in vivo* studies have demonstrated that liposome-encapsulated clofazimine is much less toxic than free clofazimine. This is advantageous as the encapsulated drug could be administered at higher doses than free drug due to the water-insolubility of the drug.

In this study, PVP-*b*-PVAc block copolymers were evaluated as possible carriers for the hydrophobic drug, clofazimine. Drug-loaded vesicles were prepared via physical encapsulation as illustrated in Figure 4.2. The drug-loaded vesicles were characterized for drug loading efficiency, morphology and stability as potential carriers for hydrophobic drugs.

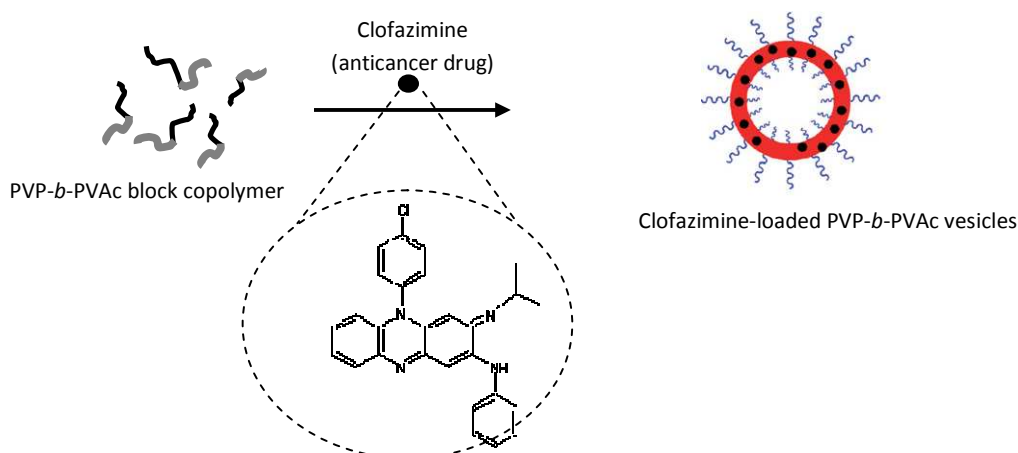


**Figure 4.2** Schematic representation of the encapsulation of clofazimine into PVP-*b*-PVAc polymer vesicles

## 4.2. Materials and methods

### 4.2.1 Chemicals

Dimethyl sulfoxide (Merck, 99 %) was used as received, clofazimine (B663) was obtained from the University of Pretoria. Dulbecco's modification of Eagles Medium (DMEM) (sterile) was purchased from Sigma Aldrich. Distilled deionized water was obtained using a Millipore Milli-Q purification system and used in all the experiments. Fetal calf serum (FCS) (sterile) and phosphate buffer saline (PBS) (pH 7.5, sterile) were purchased from Sigma-Aldrich. Block copolymers of PVP-*b*-PVAc were synthesized as described in Chapter 3.

### 4.2.2 Loading of clofazimine into PVP-*b*-PVAc block copolymers

Clofazimine was incorporated into PVP-*b*-PVAc block copolymers via the dialysis method. A typical procedure for the preparation of the drug-loaded vesicles is as follows. PVP-*b*-PVAc (50 mg), and the hydrophobic drug, clofazimine (10 mg) were dissolved in DMSO (5 mL). The solution was stirred for 10 minutes at room temperature. The homogeneous solution was dialyzed against distilled water for 24 hours using a dialysis membrane (MWCO 3500 g/mol). The water was replaced every 6 hours. The resultant solution was lyophilized to obtain dry drug-loaded PVP-*b*-PVAc samples for long-term storage.

### 4.2.3 <sup>1</sup>H NMR measurements of block copolymers

<sup>1</sup>H NMR measurements were performed on PVP-*b*-PVAc block copolymers. The <sup>1</sup>H NMR spectra were recorded on a Varian 600 MHz Inova spectrometer (Varian Associates Inc. NMR Instruments). The self-assembly of the block copolymers and drug incorporation were confirmed using <sup>1</sup>H NMR spectra in DMSO-*d*<sub>6</sub> and in D<sub>2</sub>O.

### 4.2.4 Size distribution and morphology of clofazimine-loaded PVP-*b*-PVAc

The size and size distribution of the loaded and unloaded vesicles were determined by DLS using a Malvern ZetaSizer Nano instrument (ZS90) fixed at an angle of 90 degrees, equipped with a 4 mW He-Ne laser operating at a wavelength of 633 nm. Time correlation functions were analysed using the CONTIN analysis software provided by Malvern, to obtain the hydrodynamic diameter of the particles ( $Z_{ave}$ ) and the particle size distribution. TEM of the drug-loaded and unloaded PVP-*b*-PVAc samples were carried out in order to observe the morphology of the vesicles. TEM

micrographs were obtained using a LEO 912 microscope operating at an acceleration voltage of 120 kV. A drop of the sample solution was deposited onto a copper grid and dried at room temperature. The sample solution was negatively stained with uranyl acetate.

#### *4.2.5 Evaluation of the drug loading capacity and encapsulation efficiency of clofazimine-loaded PVP-*b*-PVAc*

The drug loading capacity and the encapsulation efficiency of clofazimine-loaded PVP-*b*-PVAc of different vesicle formulations were determined spectrophotometrically. A Perkin Elmer Lambda 20 photodiode array spectrophotometer was used to measure the UV-Vis spectra. It consisted of a holographic monochromator, pre-aligned deuterium and halogen lamps and a photodiode array detector. UV Winlab (version 2.0) software was used for data acquisition and processing.

The drug encapsulation efficiency is defined as the ratio of the weight of the drug encapsulated in the vesicles to the weight of the drug initially used, while the drug loading content is the weight ratio of the drug encapsulated in the vesicles to that of the weight of the polymer vesicles. The loading capacity and the encapsulation efficiency are calculated using the following equations:

$$\text{Drug loading capacity (DLC) \%} = \frac{\text{mass of drug in vesicles}}{\text{mass of polymer vesicles}} \times 100\%$$

$$\text{Drug encapsulation efficiency (EE) \%} = \frac{\text{mass of drug in vesicles}}{\text{mass of drug initially used}} \times 100\%$$

The obtained vesicle solution was filtered to remove free drug and then lyophilized to obtain dry clofazimine-loaded PVP-*b*-PVAc samples. The samples were dissolved in methanol to determine the drug loading content and encapsulation efficiency of the vesicles. The clofazimine content was determined by UV/Vis spectrometry. The concentration of the clofazimine was measured using a standard calibration curve (correlation coefficient 0.998) experimentally obtained from clofazimine/methanol solutions. Clofazimine has two UV absorbance peaks at 280 nm and 460 nm. The clofazimine content was determined by measuring the absorbance at 460 nm to minimize the interference of the polymer with an absorbance at ~280 nm. The calibration curve is linear over the range of 0.5 – 75  $\mu\text{g.mL}^{-1}$ .



#### 4.2.6 Stability studies of clofazimine-loaded PVP-*b*-PVAc

The particle size stability of drug-loaded vesicles was studied in PBS and in PBS/serum under physiological conditions (pH 7.4, 37 °C). The clofazimine-loaded PVP-*b*-PVAc solution (prepared as described in Section 4.2.2), was diluted in phosphate buffer solution (1:9 (v/v) vesicle solution/PBS) at pH 7.4 (concentration of PVP-*b*-PVAc 0.5 mg/mL). For systems mimicking biological fluids, the stability of the vesicles was assessed in PBS containing 20 % (v/v) serum. Drug-loaded PVP-*b*-PVAc as prepared in Section 4.2.2 was diluted in buffer solutions containing FCS. The particle sizes of the vesicles were measured as a function of time at 37 °C by DLS.

Clofazimine-loaded vesicles were incubated at physiological conditions (pH 7.4, 37 °C) and the concentration of the drug was monitored over time. 100 µL of a 20 % (w/w) clofazimine-loaded vesicle solution was added to 900 µL of PBS buffer at pH 7.4 and incubated at 37 °C. 20 µL aliquots were withdrawn at specific time intervals and the drug concentration analyzed by UV/Vis spectroscopy.

### 4.3. Results and discussion

#### 4.3.1 Preparation and characterization of clofazimine-loaded PVP-*b*-PVAc block copolymers

Clofazimine is a poorly water-soluble drug (water solubility 0.225 mg/L).<sup>20</sup> This is illustrated in Figure 4.3 (A) which clearly shows the flaky, undissolved drug particles in water. To overcome the solubility issue, the drug was physically entrapped into PVP-*b*-PVAc via the dialysis method. PVP-*b*-PVAc and clofazimine were dissolved in DMSO and dialyzed against distilled deionized water (DMSO was chosen as solvent due to the solubility of clofazimine in this solvent). The gradual replacement of DMSO by water triggered the micellization of the copolymer and the incorporation of drug in the hydrophobic bilayer membrane and resulted in an orange, homogeneous dispersion as seen in Figure 4.3 (B). Clofazimine was successfully loaded into PVP-*b*-PVAc block copolymers and no drug precipitation was observed during the encapsulation procedure. Drug-loaded PVP-*b*-PVAc could either be stored in solution or in freeze-dried form.

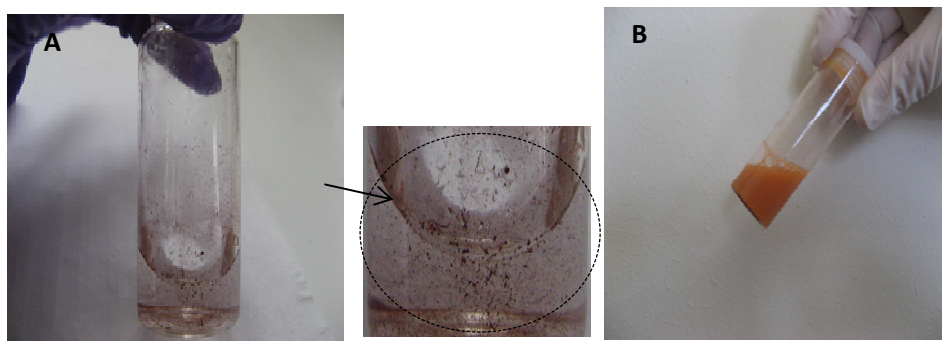


**Figure 4.3:** A) Clofazimine insoluble in aqueous media B) Clofazimine physically encapsulated in PVP-*b*-PVAc in aqueous media

The encapsulation of clofazimine into the hydrophobic PVAc bilayer membrane was confirmed by  $^1\text{H}$  NMR. Figure 4.4 shows the  $^1\text{H}$  NMR spectra of clofazimine-loaded PVP<sub>90</sub>-*b*-PVAc<sub>210</sub> block copolymers in different environments. Figure 4.4 (a) represents clofazimine-loaded PVP<sub>90</sub>-*b*-PVAc<sub>210</sub> block copolymer aggregates in DMSO-*d*<sub>6</sub>. Figure 4.4 (b) represents the  $^1\text{H}$  NMR spectra of clofazimine-loaded PVP<sub>90</sub>-*b*-PVAc<sub>210</sub> in deuterium oxide (D<sub>2</sub>O). For clofazimine-loaded PVP<sub>90</sub>-*b*-PVAc<sub>210</sub> in DMSO-*d*<sub>6</sub> (Figure 4.4 (a)) vesicle formation is not expected and all peaks of the hydrophilic (PVP) and hydrophobic (PVAc) segments were detected. Proton peaks of clofazimine were also detected (6 – 7.8 ppm as indicated with a circle on the  $^1\text{H}$  NMR spectrum). The formation of clofazimine-loaded PVP<sub>90</sub>-*b*-PVAc<sub>210</sub> vesicles was confirmed by  $^1\text{H}$  NMR spectroscopy in D<sub>2</sub>O (Figure 4.4 (b)). The predominant peak is that of the PVP (3 – 4 ppm) - the corona of the vesicle-like structure - while the peaks of PVAc are suppressed. This is due to the limited mobility of the PVAc-chains in the hydrophobic bilayer membrane of the vesicle. The intensity of the PVAc peak is reduced compared to that in Figure 4.4 (a) where the vesicles are not expected to be present. No peaks of clofazimine are present. This is due to the drug being incorporated within the vesicle bilayer membrane which restricts the mobility of the drug molecules resulting in suppressed proton resonances.  $^1\text{H}$  NMR indicated that amphiphilic block copolymer self-assembled into vesicular structures in water, comprised of a hydrophobic membrane (PVAc) and a hydrophilic outer shell (PVP) and that clofazimine is contained in the hydrophobic bilayer membrane of the amphiphilic block copolymer.

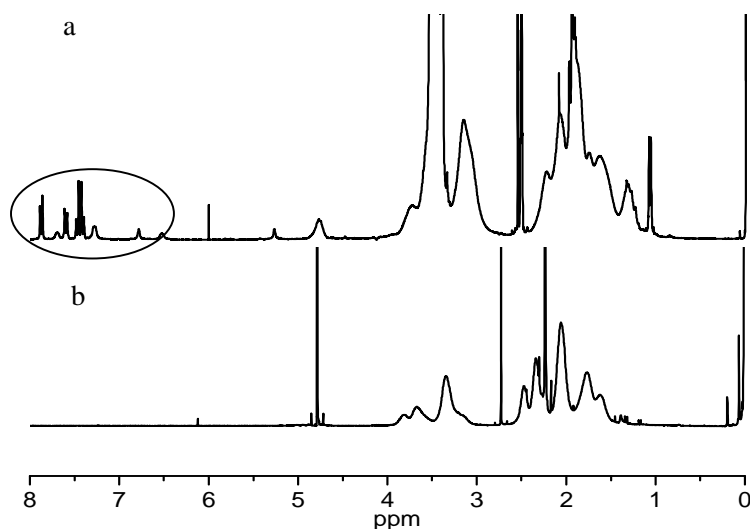


**Figure 4.4:**  $^1\text{H}$  NMR spectra of a) clofazimine-loaded  $\text{PVP}_{90}\text{-}b\text{-PVAc}_{210}$  in  $\text{DMSO-}d_6$  b) clofazimine-loaded  $\text{PVP}_{90}\text{-}b\text{-PVAc}_{210}$  in  $\text{D}_2\text{O}$

#### 4.3.2 Size distribution and morphology of clofazimine-loaded $\text{PVP-}b\text{-PVAc}$ block copolymers

The particle size and the size distribution of drug-loaded vesicles were measured by DLS. The average particle size of the drug-loaded  $\text{PVP-}b\text{-PVAc}$  was 180 – 210 nm for the samples in water (Table 4.1).

**Table 4.1:** Particle sizes of unloaded and drug-loaded  $\text{PVP-}b\text{-PVAc}$  (20 % (w/w) clofazimine/ $\text{PVP-}b\text{-PVAc}$ ) measured by DLS analysis

Polymer sample	Unloaded $\text{PVP-}b\text{-PVAc}$ $Z_{\text{ave}}$ (nm)	PDI	Loaded $\text{PVP-}b\text{-PVAc}$ $Z_{\text{ave}}$ (nm)	PDI
$\text{PVP}_{90}\text{-}b\text{-PVAc}_{210}$	$180 \pm 3.1$	0.09	$190 \pm 2.2$	0.09
$\text{PVP}_{90}\text{-}b\text{-PVAc}_{256}$	$205 \pm 2.1$	0.06	$200 \pm 3.2$	0.09
$\text{PVP}_{90}\text{-}b\text{-PVAc}_{290}$	$200 \pm 2.5$	0.09	$210 \pm 2.5$	0.09

Reasonably narrow size distributions and monomodal pattern ( $\text{PDI} < 0.1$ ) for the different block copolymers were obtained as presented in Figure 4.5. After loading of clofazimine, the particle size did not increase considerably for the different block copolymers of varying PVAc block length. Furthermore, the size distribution of the drug-loaded  $\text{PVP-}b\text{-PVAc}$  block copolymers was

approximately the same as that before drug loading. Since the optimal size of a drug carrier for efficient delivery of an antitumor agent to a tumor is around 100 – 200 nm, the particle sizes for the drug-loaded PVP-*b*-PVAc obtained are acceptable and meet the requirements for passive targeting via the EPR effect.<sup>9</sup>

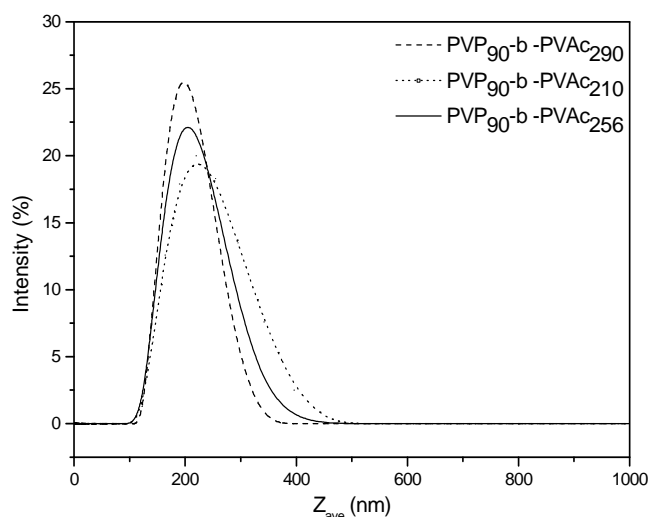


**Figure 4.5:** Size distribution of clofazimine-loaded PVP-*b*-PVAc of varying PVAc block length

In the literature, the possibility that block copolymer vesicles can transform into micelles with increasing amount of solubilized hydrophobic molecules has been theoretically predicted.<sup>21</sup> In a study conducted by Li *et al.*<sup>22</sup>, the effect of the amount of hydrophobic drug loaded into the vesicles on the particle size was investigated. It was observed that with increasing amount of hydrophobic drug the particle size of the vesicles decreased. They hypothesised that a transformation from vesicles to micelles had occurred. It is likely that increasing amounts of drug results in unfavourable stretching of the hydrophobic chains which eventually results into micellization of the vesicles.

In order to determine whether the drug content has an effect on the particle size of the PVP-*b*-PVAc carrier, different drug feed ratios were investigated. Figure 4.6 shows the relationship between different drug feed ratios on the particle size of the PVP-*b*-PVAc carrier. All samples were prepared using the same procedure (Section 4.2.2). It was observed that the PVP-*b*-PVAc carrier sizes for the different drug formulations (5 – 20 (w/w) % drug/polymer) were in the range

of 190 – 210 nm. No significant change was observed. Therefore the increase in the drug content had no major effect on the particle size of the carrier. In the case of 30 %, drug precipitation was seen in the dialysis tubing and therefore samples were not analyzed.

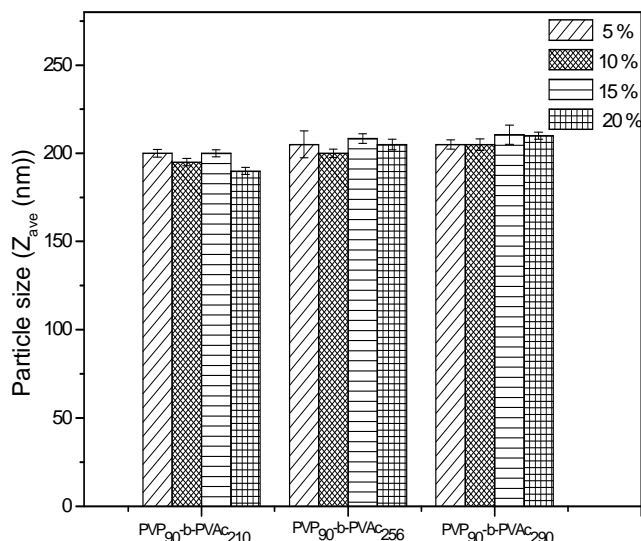


**Figure 4.6:** The effect of different drug feed ratios (% (w/w) clofazimine/polymer) on the particle size of clofazimine-loaded PVP-*b*-PVAc of varying PVAc block length. Error bars represent the standard deviation ( $n = 3$ )

The morphology of the drug-loaded PVP-*b*-PVAc vesicles was visualized by TEM. As depicted in Figure 4.7, the average diameters of the drug-loaded PVP-*b*-PVAc vesicles were 150 – 200 nm. The characteristic dark outer layer (representing the membrane bilayer or vesicle wall) and lighter inner core (representing the hydrated core) are clearly evident. TEM results are in fairly good agreement with those determined by DLS. The presence of slightly smaller particles is as a result of shrinkage of the particles which is consistent with similar reports studying polymer vesicles via TEM in the dried state.<sup>23</sup>

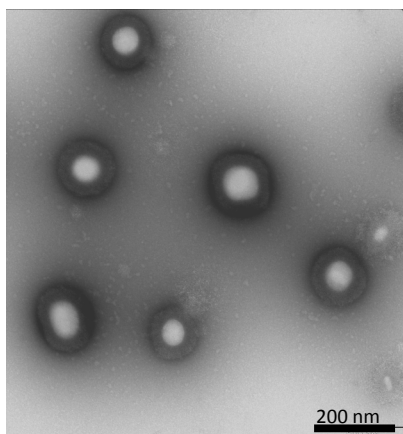


**Figure 4.7:** TEM image of clofazimine-loaded PVP<sub>90</sub>-b-PVAc<sub>290</sub> showing the vesicular structure

#### 4.3.3 Drug loading capacity and encapsulation efficiency

For any drug formulation, the drug loading capacity and efficiency are important parameters. As outlined in Chapter 2, the loading capacity and the encapsulation efficiency of a polymer drug carrier is influenced by several factors. The nature of the hydrophobic core (of micelles) or bilayer membrane (of vesicles), the block length of the hydrophobic core or bilayer membrane, the size or thickness of the core or the bilayer membrane and the degree of hydrophobicity of the drug are all important factors to be considered.<sup>24,25</sup>

In order to find an optimal drug to polymer ratio for the PVP-*b*-PVAc drug carrier, a series of clofazimine-loaded PVP-*b*-PVAc with different weight ratios of clofazimine to polymer (5 %, 10 %, 15 %, 20 % and 30 %) were prepared. The effect of the hydrophobic block length and the drug/polymer weight ratio on the drug loading capacity and encapsulation efficiency were investigated.

Figure 4.8 represents the drug loading capacity and the encapsulation efficiency of clofazimine-loaded PVP-*b*-PVAc of different drug feed ratios (using a constant amount of polymer).

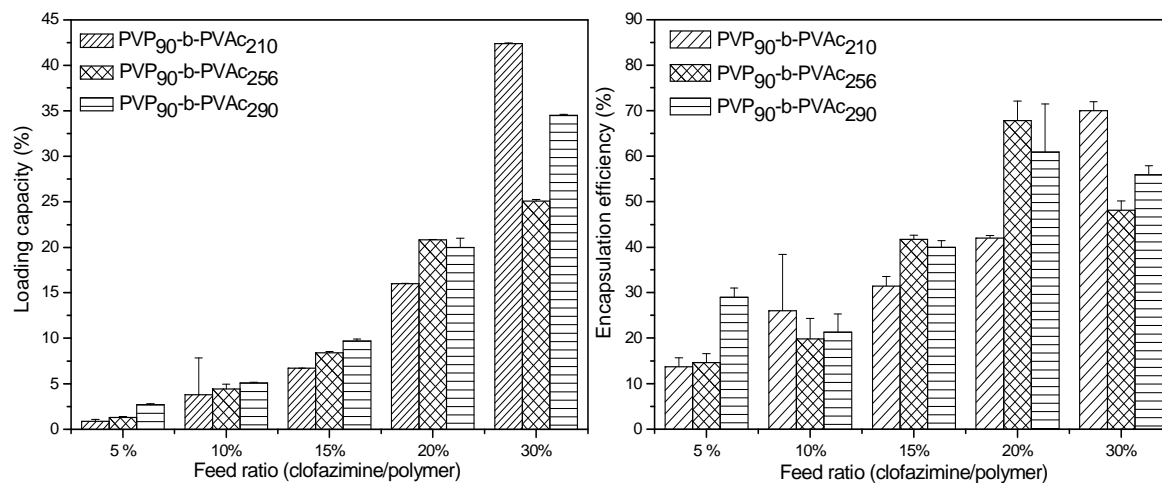


**Figure 4.8:** Drug loading capacity and encapsulation efficiency of clofazimine-loaded PVP-*b*-PVAc of different hydrophobic PVAc block length. Feed ratios were 5, 10, 20, or 30 weight percentage (% w/w) of clofazimine relative to PVP-*b*-PVAc. Error bars represent the standard deviation ( $n = 3$ )

Clofazimine-loaded PVP-*b*-PVAc of longer hydrophobic PVAc block length (PVP<sub>90</sub>-*b*-PVAc<sub>290</sub> and PVP<sub>90</sub>-*b*-PVAc<sub>256</sub>) resulted in a higher drug loading capacity and encapsulation efficiency (having the same amount of drug) compared to PVP<sub>90</sub>-*b*-PVAc<sub>210</sub> of shorter PVAc block length. The results follow the general trend: the loading capacity and the encapsulation efficiency of the polymer carrier increase with increasing hydrophobic chain length. The loading capacity of polymer vesicles is dependent on the molecular weight of the hydrophobic block, since copolymers with larger hydrophobic molecular weight can form thicker hydrophobic bilayer membranes. The thicker membrane can therefore accommodate more hydrophobic drug.<sup>22</sup> It is also possible that the longer the hydrophobic PVAc block, the stronger the hydrophobic interaction between the drug and the hydrophobic bilayer membrane resulting in higher drug loading capacities and higher encapsulation efficiencies.

The effect of the feed weight ratio on the drug loading capacity and encapsulation efficiency was also studied. The drug loading capacity and encapsulation efficiency increased with increasing initial drug feed (constant amount of polymer). As the feed amount of clofazimine increased from 5 – 20 %, the drug loading capacity increased from 2.7 wt % to 20 wt %, for PVP<sub>90</sub>-*b*-PVAc<sub>290</sub> and 1.4 wt % to 20 wt % for PVP<sub>90</sub>-*b*-PVAc<sub>256</sub>. In the case of the more hydrophilic

block copolymer, clofazimine-loaded PVP<sub>90</sub>-*b*-PVAc<sub>210</sub>, the drug loading capacity increased from 5 wt % to 42 wt %. The encapsulation efficiency also increased with increasing drug feed amount. The encapsulation efficiency increased from 20 wt % to 60 wt % for clofazimine-loaded PVP<sub>90</sub>-*b*-PVAc<sub>290</sub>, from 13 wt % to 40 wt % for clofazimine-loaded PVP<sub>90</sub>-*b*-PVAc<sub>210</sub>, and 14 wt % to 60 wt % for clofazimine-loaded PVP<sub>90</sub>-*b*-PVAc<sub>256</sub>. A decrease in the encapsulation efficiencies for clofazimine-PVP<sub>90</sub>-*b*-PVAc<sub>290</sub> and PVP<sub>90</sub>-PVAc<sub>256</sub> was seen when a 30 % (w/w) drug/polymer ratio was used. This corresponded to drug precipitation that was observed in the dialysis tubing during the loading process, which indicated that the vesicles had reached their maximum loading capacity. Therefore the maximum drug/polymer feed ratio for clofazimine is 20 %, above this value clofazimine overloading of the system occurs. Exceeding the solubilization capacity of the vesicles, results in release in the aqueous phase, followed by crystallization or precipitation of the drug as reported previously in the literature.<sup>22,26</sup> Interestingly, for the more hydrophilic block copolymer, the drug loading capacity reached a maximum loading capacity of 40 wt % with an encapsulation efficiency of 70 wt % when a 30 % (w/w) drug/polymer ratio was used. No drug precipitation was observed during dialysis, however, the sample was unable to maintain its stability upon storage. The colloidal stability of the drug-loaded carrier often becomes lower as the drug loading increases due to the enhanced hydrophobicity of the carrier after loading with hydrophobic drug.<sup>27</sup>

The drug loading capacity and encapsulation efficiency is also dependent on the miscibility between the polymers and the hydrophobic drugs.<sup>28</sup> In a study conducted by Letchford *et al.*<sup>28</sup>, the solubilization of five model hydrophobic drugs by methoxy poly(ethylene glycol)-*b*-poly( $\epsilon$ -caprolactone) diblock copolymers (MePEG-*b*-PCL) was investigated. Indomethacin, showed the best solubility in the MePEG-*b*-PCL micelles, having a higher loading capacity and encapsulation efficiency than the poorly solubilized etoposide. Additionally, a higher PCL block length also resulted in better loading capacity.

For comparative purposes, paclitaxel (PTX), a commonly used anti-cancer drug (water solubility 5.5 mg/L) was selected to evaluate the loading capacity and encapsulation efficiency of the polymer vesicles. PVP-*b*-PVAc copolymers were loaded with PTX using the same procedure as for clofazimine-loaded samples (Section 4.2.2).



The loading capacity and encapsulation efficiency obtained for the PTX-loaded PVP<sub>90</sub>-*b*-PVAc<sub>290</sub> and PTX-loaded PVP<sub>90</sub>-*b*-PVAc<sub>210</sub> is presented in Figure 4.9. Similarly to clofazimine-loaded vesicles, the longer hydrophobic PVAc block provided a higher PTX loading capacity and encapsulation efficiency as expected. PVP<sub>90</sub>-*b*-PVAc<sub>290</sub> (10 % (w/w) PTX/polymer) showed the highest drug loading levels of 15 wt % and encapsulation efficiency of 62 wt %. A further increase in the initial drug feed to a 20 % (w/w) PTX/polymer did not result in a greater drug loading level or encapsulation efficiency. Rather a decrease in encapsulation efficiency was seen as a result of PTX precipitation that was found inside the dialysis membrane tube. At a feed ratio of 20 % (w/w) PTX/polymer, no precipitation was observed for PVP<sub>90</sub>-*b*-PVAc<sub>210</sub>, however, the sample was unstable upon storage.

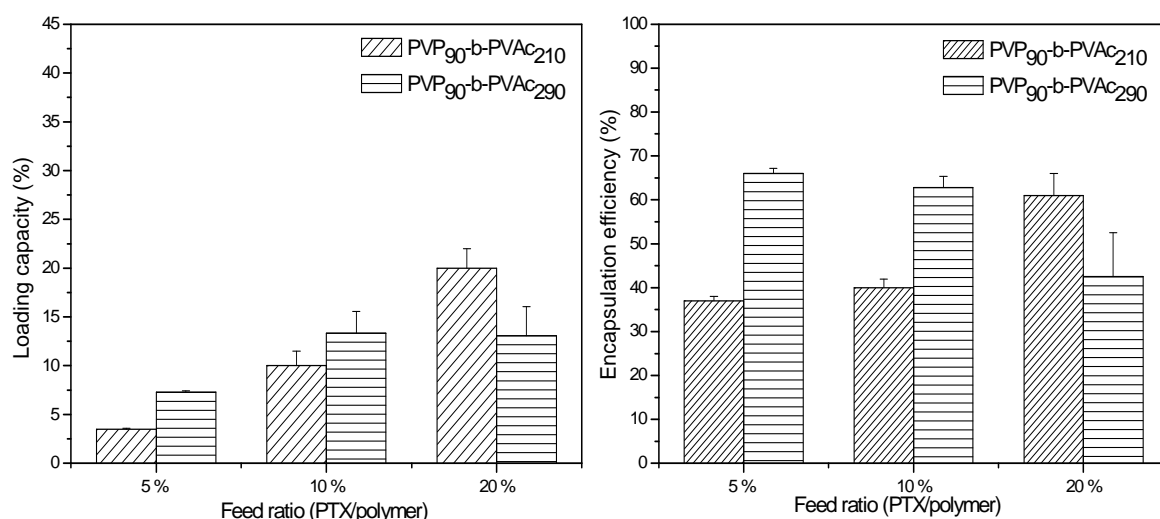


**Figure 4.9:** Drug loading capacity and encapsulation efficiency of paclitaxel-loaded PVP-*b*-PVAc of different hydrophobic PVAc block length. Feed ratios were 5, 10, or 20, weight percentage (% w/w) of PTX relative to PVP-*b*-PVAc. Error bars present the standard deviation ( $n = 3$ )

The results clearly demonstrate that the loading capacity and encapsulation efficiency of the PVP<sub>90</sub>-*b*-PVAc<sub>*n*</sub> vesicles is dependent on the hydrophobicity (PVAc block length) and the drug feed ratio. In addition, differences in the hydrophobicity of the drugs and/or compatibility with the PVAc domain are also important factors which could explain the differences in the loading capacity and encapsulation efficiency for clofazimine and PTX. However, to prove the above assumption solubility studies, polymer-drug compatibility parameters and partition coefficients will need to be determined, which at this point is beyond the scope of the study.

Other factors such as the structural properties of the drugs can also have an impact on the loading capacity and efficiency. For drugs with bulky groups and high molecular weight, it is more difficult for high concentrations to become encapsulated in the core or the bilayer membrane due to steric hindrance which prevents the close stacking of the drug molecules, resulting in lower encapsulation efficiencies.

Our final optimized formulation of clofazimine and PTX-loaded PVP-*b*-PVAc had a composition of 20 % (w/w) clofazimine/PVP-*b*-PVAc and 10 % PTX/PVP-*b*-PVAc. Due to the longer hydrophobic block length, PVP<sub>90</sub>-*b*-PVAc<sub>290</sub> showed the highest loading capacity and encapsulation efficiency for both drugs. Furthermore, this polymer gave the lowest CMC (0.0012 mg/mL) which is important for its application. PVP<sub>90</sub>-*b*-PVAc<sub>290</sub> showed to be the best candidate for drug loading and was, therefore, further used for *in vitro* cytotoxicity studies (Chapter 5).

#### 4.3.4 Stability studies of clofazimine-loaded PVP-*b*-PVAc block copolymers

The particle size stability of the polymer vesicles in biological fluids is important for *in vitro* and *in vivo* applications. The particle size stability of 20 % (w/w) clofazimine-loaded PVP<sub>90</sub>-*b*-PVAc<sub>290</sub> vesicles (polymer concentration 0.5 mg/mL) in physiological conditions (PBS, pH 7.4, 37 °C) was investigated using DLS. The particle sizes of clofazimine-loaded PVP<sub>90</sub>-*b*-PVAc<sub>290</sub> vesicles in PBS/FCS were also investigated.

Figure 4.10 (a) shows that the average particle size of the PVP<sub>90</sub>-*b*-PVAc<sub>290</sub> vesicles in PBS were 210 – 220 nm, and stable up to 16 hours. No precipitation was observed. The same sample was incubated in PBS, pH 7.4 at 37 °C. At designated time intervals, the concentration of the drug was monitored by UV/Vis spectroscopy. The concentration of the drug in the drug-loaded PVP-*b*-PVAc sample remained constant over 24 hours. After 30 hours the concentration decreased by 20 % due to leakage of drug from the vesicles (data not shown). For free drug incubated in PBS (50/50 (v/v) ethanol/PBS, pH 7.4), the formation of fluffy-like precipitate was visible after 24 hours. This is not unexpected due to the low solubility of the drug in aqueous media. Similar results have also been observed for other hydrophobic cancer drugs.<sup>29</sup>

For clofazimine-loaded PVP<sub>90</sub>-*b*-PVAc<sub>290</sub> in PBS/FCS, the average particle sizes were similar to the vesicles in PBS. In addition, the vesicle sizes remained stable for 15 hours in PBS/FCS. No drug precipitation was observed during the incubation time. Clofazimine-loaded PVP<sub>90</sub>-*b*-PVAc<sub>210</sub> also showed stability in PBS and PBS/FCS. Particle sizes of 180 – 190 nm (in PBS) and 170 nm (in PBS/FCS) were maintained over 16 hour incubation. No drug precipitation was observed. This indicates that the hydrophilic PVP segment (the corona of the vesicles) was able to stabilize and protect the vesicles from non-specific surface adsorption of serum components.

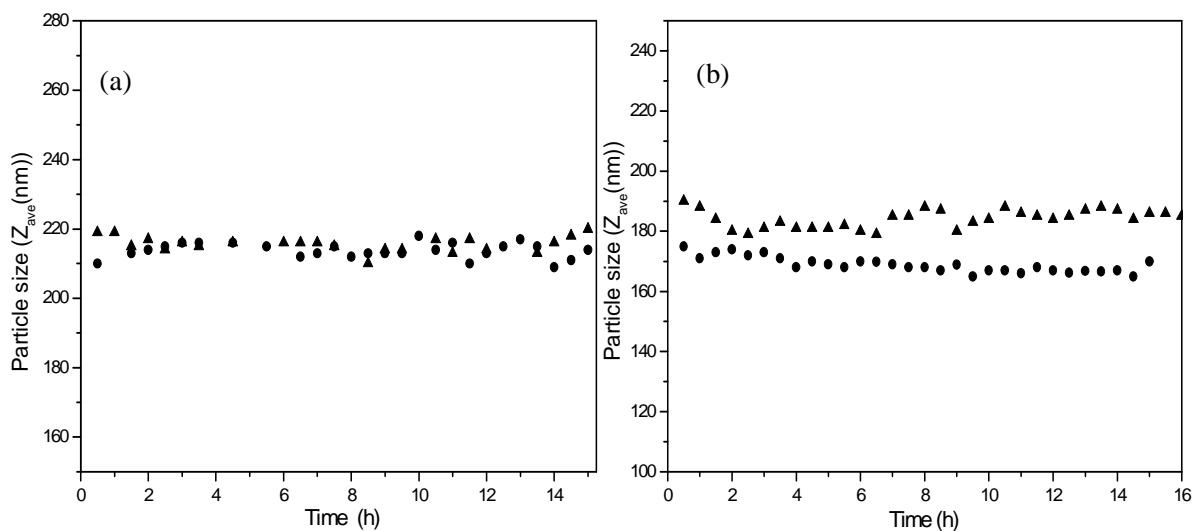


**Figure 4.10:** Particle size ( $Z_{ave}$ ) of clofazimine-loaded (a) PVP<sub>90</sub>-*b*-PVAc<sub>290</sub> (b) PVP<sub>90</sub>-*b*-PVAc<sub>210</sub> in (▲) PBS pH 7.4 and (●) PBS/FCS pH 7.4, as a function of time at 37°C

#### **4.4 Conclusion**

PVP-*b*-PVAc block copolymers of constant hydrophilic block length and varying hydrophobic block length were loaded with clofazimine, via the dialysis method. The polymer could effectively solubilize the hydrophobic drug. <sup>1</sup>H NMR spectroscopy confirmed the self-assembly of the PVP-*b*-PVAc block copolymers and the localization of the drug within the hydrophobic PVAc bilayer. The obtained drug-loaded vesicles had diameters from of 180 – 210 nm with narrow size distributions. The optimal clofazimine-loaded PVP-*b*-PVAc vesicle formulation was prepared using a 20 % drug/polymer feed ratio, having of a particle size of 200 nm which remained stable in physiological conditions. Overall, PVP-*b*-PVAc vesicles could be a potential candidate as a drug carrier for hydrophobic drugs.

#### 4.5 References

- (1) Lipinski, C. A. *J. Pharmacol. Toxicol. Methods* **2000**, *44*, 235 - 249.
- (2) Gelderblom, H.; Verweij, J.; Nooter, K.; Sparreboom, A. *Eur. J. Cancer* **2001**, *37*, 1590 - 1598.
- (3) Singla, A. K.; Garg, A.; Aggarwal, D. *Int. J. Pharm.* **2002**, *235*, 179 - 192.
- (4) Mikhail, A. S.; Allen, C. *J. Control. Rel.* **2009**, *138*, 214 - 223.
- (5) Lasic, D. D. *Nature* **1992**, *355*, 279 - 280.
- (6) Torchilin, V. P. *J. Control. Rel.* **2001**, *73*, 137 - 172.
- (7) Kim, S.; Shi, Y.; Kim, J. Y.; Park, K.; Cheng, J. *Expert Opin. Drug Deliv.* **2010**, *7*, 49 - 62.
- (8) Tyrrell, Z. L.; Shena, Y.; Radosza, M. *Prog. Polym. Sci.* **2010**, *35*, 1128-1143.
- (9) Maeda, H.; Wua, J.; Sawa, T.; Matsumura, Y.; Horic, K. *J. Control. Rel.* **2000**, *65*, 271 - 284.
- (10) Kwon, G. S.; Okano, T. *Adv. Drug Deliv. Rev.* **1996**, *21*, 107 - 116.
- (11) Reddy, V. M.; O'Sullivan, J. F.; Gangadhram, P. R. *J. Antimicrob. Chemother.* **1999**, *43*, 615 - 623.
- (12) Barry, V. C.; Belton, J. G.; Conalty, M. L.; Denny, J. M.; Edward, D. W.; O'Sullivan, J. F.; Twomey, D.; Winder, F. *Nature* **1957**, *179*, 1013 - 1015.
- (13) Fournier, S.; Burguière, A. M.; Flahault, A.; Vincent, V.; Treilhou, M. P.; Eliasiewicz, M. *Eur. J. Clin. Microbiol. Infect. Dis.* **1999**, *18*, 16 - 22.
- (14) Pourgholami, M. H.; Lu, Y.; Wang, L.; Stephens, R. W.; Morris, D. L. *Cancer Lett.* **2004**, *207*, 37 - 47.
- (15) Van Rensburg, C. E. J.; Van Staden, A. M.; Anderson, R. *Cancer Res.* **1993**, *53*, 318 - 323.
- (16) O'Reilly, J. R.; Corrigan, O. L.; O'Driscoll, C. M. *Int. J. Pharm.* **1994**, *109*, 147 - 154.
- (17) Salem, I. I.; Steffan, G.; Düzgünes, N. *Int. J. Pharm.* **2003**, *260*, 105 - 114.
- (18) Hernandez-Valdepena, I.; Domurado, M.; Coudane, J.; Braud, C.; Baussard, J.; Domurado, M. V. D. *Eur. J. Pharm. Sci.* **2009**, *39*, 345 - 351.
- (19) Mehta, R. T.; Keyhani, A.; McQueen, T. J.; Rosenbaum, B.; Rolston, K. V.; Tarrand, J. *J. Antimicrob. Agents Chemother.* **1993**, *37*, 2584 - 2587.

- (20) Feng, P. C.; Fenselau, C. C.; Jacobson, R. R. *Drug Metab. Dispos.* **1982**, *10*, 286 - 288.
- (21) Nagarajan, R. *Curr. Opin. Colloid In* **1997**, *2*, 282 - 293.
- (22) Li, S.; Byrne, B.; Welsh, J.; Palmer, A. F. *Biotechnol. Prog.* **2007**, *23*, 278 - 285.
- (23) Fernyhough, C.; Ryan, A. J.; Battaglia, G. *Soft Matter* **2009**, *5*, 1674 - 1682.
- (24) Lin, W. J.; Juang, L. W.; Lin, C. C. *Pharm. Res.* **2003**, 668 - 673
- (25) Carstens, M. G.; de Jong, P. H. J. L. F.; van Nostrum, F. C.; Kemmink, J.; Verrijk, R.; de Leede, L. G. J.; Crommelin, D. J. A.; Hennink, W. E. *Eur. J. Pharm. Biopharm.* **2008**, *68*, 596 - 606.
- (26) Torchilin, V. P. *Pharm. Res.* **2007**, *24*, 1 - 16.
- (27) Burt, H. M.; Zhang, X.; Toleikis, P.; Embree, L.; Hunter, W. L. *Colloids Surf., B* **1999**, *16*, 161 -171.
- (28) Letchford, K.; Liggins, R.; Burt, H. *J. Pharm. Sci.* **2008**, *97*, 1179 - 1189.
- (29) Soga, O.; van Nostrum, C. F.; Fens, M.; Rijcken, C. J. F.; Schiffelers, R. M.; Storm, G.; Hennink, W. E. *J. Control. Rel.* **2005**, *103*, 341 - 353.

## **Chapter 5**

### ***In vitro* cytotoxicity and cellular uptake of PVP-*b*-PVAc**

#### **Abstract**

*In vitro* cytotoxicity studies of poly((*N*-vinylpyrrolidone)-*b*-poly(vinyl acetate)) (PVP-*b*-PVAc) and drug-loaded PVP-*b*-PVAc were investigated against MDA-MB-231 multi-drug-resistant breast epithelial cancer cells and MCF12A normal breast epithelial cells. *In vitro* experiments demonstrated that the PVP-*b*-PVAc drug carrier showed no cytotoxicity, confirming the biocompatibility of the PVP-*b*-PVAc drug carrier. *In vitro* cellular uptake of fluorescently labeled PVP-*b*-PVAc was studied using fluorescence microscopy. The PVP-*b*-PVAc carrier was taken up by the cancer cells after 6 hours and localized in both the cytoplasm and in the perinuclear region. From these results, we could conclude that the present PVP-*b*-PVAc block copolymer could potentially be useful as a drug carrier for hydrophobic drugs.

## 5.1 Introduction

One of the essential requirements of a drug carrier or a drug delivery system is that they have no inherent cytotoxicity.<sup>1</sup> Prior to *in vivo* work, drug delivery systems are subjected to *in vitro* studies in order to determine the biocompatibility of the polymer drug carrier and the efficacy of the drug carrier. *In vitro* cytotoxicity assays and various screening assays are widely used in drug development to study the effect of novel compounds/drugs, drug carriers or drug delivery systems on healthy cells or cancer cells.<sup>2</sup> Thus, *in vitro* investigation can provide preliminary evidence to show the advantages of a drug carrier system in drug delivery application. However, it must be mentioned that although *in vitro* studies are beneficial, they are not a true representation of *in vivo* conditions.

A prerequisite for an effective polymer drug carrier, is the need for the drug to be delivered intracellularly to exert its therapeutic action inside the cytoplasm or into the nucleus or other specific organelles. *In vitro* cellular uptake and internalisation studies, therefore, provide essential information regarding the intracellular pathway and cellular distribution of the drug delivery carrier.

In recent years, fluorescence microscopy has become an important tool for studying the *in vitro* cellular internalization and localization of polymer drug carriers.<sup>3,4</sup> In order to confirm that the drug carrier has successfully delivered the drug to the target site, it is necessary to track a polymer drug carrier on its cellular journey. The attachment of a fluorescent label to the polymer backbone is a convenient way to trace the polymer.<sup>5</sup> Commonly used fluorescent labels include rhodamines,<sup>6</sup> and fluorescein dyes - sulfhydryl-reactive or amine-reactive fluorescein dyes *e.g.* fluorescein isothiocyanate (FITC)<sup>7-9</sup>, which can be conjugated to polymers having appropriate reactive functional groups. For example, Eisenberg and coworkers showed internalization of micelles through bioconjugation of a rhodamine fluorescent probe onto poly(ethylene glycol)-*b*-poly( $\epsilon$ -caprolactone) (PEG-*b*-PCL) micelles.<sup>10</sup> In a subsequent study, Savic *et al.*<sup>11</sup> used a triple-labeling approach where the nucleus, the PCL-*b*-PEO micelles, and the plasma membrane were individually labeled and selectively visualized. Fluorescence results indicated that the micelles were predominantly localized in the cytoplasm and distributed within several cytoplasmic organelles, but not in the nucleus.



In some cases, the drug molecules themselves consist of aromatic ring systems exhibiting inherent fluorescence (e.g. doxorubicin).<sup>12</sup> Therefore, if fluorescently labeled micelles are combined with a drug (which exhibits fluorescence) then the fate of both the micelles and the drug can be detected independently. However, in order to distinguish between the drug delivery carrier and the drug, it is imperative that they emit fluorescence at different wavelengths (*i.e.* different colours).

The versatility of the RAFT technique has previously been addressed in Chapter 2. Not only does it allow for the synthesis of well-defined end-functional polymers, but it also allows for postmodification of otherwise inert polymers.<sup>13,14</sup> Thiol-ene chemistry is the most widely used and easiest accessible route to post-polymerization polymer modification on polymers synthesized via the RAFT technique.<sup>15,16</sup> Thiol groups lend themselves to thiol-ene processes for polymer bioconjugation resulting in polymers that can be used for pharmaceuticals, drug delivery and biomedical imaging applications.<sup>17,18</sup>

Several procedures for the removal of the RAFT thiocarbonyl thio end-group, yielding thiol end-group polymers have been thoroughly documented by Moad *et al.*<sup>19</sup> There are several types of thiol-reactive dyes reported in the literature, including iodoacetamides, disulfides, maleimides, vinyl sulfones and various electron-deficient aryl halides and sulfonates. Iodoacetamides and maleimides are by far the most popular thiol-reactive moieties. Thiol-based polymers are therefore the preferred targets for these specific thiol-reactive fluorescent labels. The use of thiol-maleimide coupling reactions has been documented in the literature.<sup>20-22</sup> Li *et al.*<sup>23</sup> described the first example of sequential thiol-ene reactions, involving thiol-maleimide coupling. Poly(*N*-isopropylacrylamide) (PNIPAm) prepared by a trithiocarbonate RAFT agent, when reacted with 2-ethanolamine in the presence of tributylphosphine in 1,4-dioxane, yielded the thiol-terminated homopolymer, PNIPAm-SH. This further reacted with bismaleimidodiethyleneglycol to yield maleimide end-functional PNIPAm. Similarly, Scales *et al.*<sup>24</sup> synthesized fluorescently labeled PNIPAM polymers. End groups were cleaved with sodium borohydride (NaBH<sub>4</sub>). The thiol-terminated polymer reacted with *N*-(1-pyrene) maleimide in the presence of a catalytic amount of ethylenediamine in DMF, which resulted in fluorescent ω-chain-end modified PNIPAm.

With the advancement in polymer chemistry, the development of fluorescent polymers has also found use in various applications in medicine, including *in vitro* and *in vivo* trafficking in drug delivery. This is an alternative approach to track the cellular pathway and distribution of the polymer drug carrier *in vitro*. The attachment of fluorescent labels to polymers is often restricted due to the limited availability of fluorescent labels with specific functional groups for conjugation to the polymer. In addition, the attachment of the fluorescent dyes to the polymers can alter the physicochemical properties of the drug carrier, which could further affect the route of internalisation and the intracellular distribution.<sup>11</sup> To circumvent this, fluorescent amphiphilic polymers have particularly gained interest.<sup>14,25</sup> For example, Perrier and coworkers<sup>25</sup> synthesized a fluorescent, thermosensitive, amphiphilic poly(*N*-isopropyl-acrylamide-co-*N*-vinylcarbazole) conjugated to pH responsive poly(2-(*N,N*-dimethylamino))ethyl acrylate, (PNIPAm-co-PNVC)-*b*-PDMAEA. These polymers could be useful to gain insight and understand the *in vivo* fate of the drug delivery vehicle. In addition to fluorescent polymers, the development of fluorogenic polymers (polymers bearing a fluorogenic label, whose fluorescence is revealed only upon cellular uptake) for cellular internalization and trafficking studies have also been investigated.<sup>26</sup>

In the present study, we evaluated the toxicity of the PVP-*b*-PVAc drug carrier. Furthermore, we investigated the cytotoxicity of drug-loaded PVP-*b*-PVAc to evaluate its potential as a drug delivery vehicle. The attachment of a fluorescent label to the PVP-*b*-PVAc carrier allowed for *in vitro* cellular uptake studies using fluorescence microscopy. Clofazimine has no inherent fluorescence, therefore, we considered perylene red (Exalite 613), a hydrophobic fluorescent probe to mimic the hydrophobic drug, clofazimine. Perylene red was physically entrapped into the fluorescently labeled PVP-*b*-PVAc using the same method as for the hydrophobic drug, clofazimine. The cellular uptake of the resulting fluorescently labeled perylene red-loaded PVP-*b*-PVAc vesicles was explored *in vitro* and compared with free perylene red.

## 5.2 Materials and Methods

### 5.2.1 Materials

*n*-butyl amine, dichloromethane (DCM, 99 %), diethyl ether, dimethyl formamide (DMF, 98 %), dimethyl sulfoxide (DMSO, 99 %), Dulbecco's Modified Eagle's Medium (DMEM, sterile), tris(2-carboxyethyl)phosphine (TCEP.HCl) were purchased from Sigma Aldrich. Fluorescein maleimide was obtained from Sigma-Aldrich. Perylene red laser dye (Exalite 613) was obtained from Exciton (USA). Multi-drug-resistant (MDR) MDA-MB-231 and MCF12A cell lines were obtained from the Department of Physiology, University of Stellenbosch. Amphiphilic block copolymer, PVP<sub>90</sub>-*b*-PVAc<sub>290</sub> was used in all cytotoxicity experiments.

### 5.2.2 Cell culture and culture conditions

MCF12A normal breast epithelial cells and MDR MDA-MB-231 breast epithelial cancer cells were seeded in 96-well plates with  $5 \times 10^4$  cells/well and maintained in DMEM supplemented with 1 % penicillin/streptomycin (PS), 10 % fetal calf serum and 1 % L-glutamine at 37 °C in a 5 % CO<sub>2</sub> humidified atmosphere.

### 5.2.3 In vitro cytotoxicity assay

The MTT assay is a routine, quantitative assay used to assess the response of different cell lines to drugs.<sup>2</sup> This quantitative calorimetric assay is based on a yellow water-soluble tetrazolium salt, (4,5-dimethylthiazol-2-yl)-2,5-diphenyltetrazolium bromide (MTT), which is reduced when in contact with viable cells. The reduction reaction is facilitated by the mitochondrial reductase enzymes, thus the conversion is directly related to the number of viable cells. In the MTT assay, the yellow MTT is converted to purple, insoluble formazan crystals which are solubilised by organic solvents (*e.g.* DMSO) and the resulting samples are measured by a spectrometer. The absorbance is proportional to the concentration of the formazan solution which is proportional to the number of live cells.<sup>27</sup>

To determine the cytotoxicity of clofazimine and clofazimine-loaded PVP-*b*-PVAc, *in vitro* MTT assays were conducted on a MDA-MB-231 breast cancer epithelial cell line and a MCF12A healthy breast epithelial cell line. Cells were seeded in 96-well plates and cultured

overnight at 37 °C at a 5 % CO<sub>2</sub> humidified atmosphere. All glassware was autoclaved (steam sterilized at 121 °C for 20 minutes) prior to use. The clofazimine-loaded PVP-*b*-PVAc was sterilized by filtration using 0.22 µm Millipore-Millex syringe filters. Clofazimine was dissolved in DMSO (0.1 %) and diluted in DMEM. Serial dilutions were made from the stock solution to yield final concentrations of 0.6 – 10 µg/mL of free drug. For clofazimine-loaded PVP-*b*-PVAc, the clofazimine concentration for each formulation was prepared by serial dilutions in the cell culture medium, to obtain final concentrations of 0.6 – 10 µg/mL. The cells were then incubated in DMEM containing free clofazimine and clofazimine-loaded PVP-*b*-PVAc for 24 hours.

After treatment of the cells, 20 µL of MTT assay was added. The plates were incubated for a further 4 hours after which the medium was aspirated and the precipitated formazan was extracted with 200 µL of DMSO. The absorbance was measured at 570 nm using a microplate reader. Experiments were done in triplicate. The relative cell viability of the unloaded and drug-loaded polymer was compared to the control cell culture in complete DMEM.

Cell viability was calculated by the following equation

$$\text{Cell viability (\%)} = \frac{\text{Int}_{\text{sample}}}{\text{Int}_{\text{control}}} \times 100 \%$$

where Int<sub>sample</sub> is the fluorescence intensity the sample in the cells and Int<sub>control</sub> is the fluorescence intensity of the cells incubated in culture medium (positive control). The IC<sub>50</sub> values of the drug and drug-loaded PVP-*b*-PVAc was calculated from the cell viability data. The concentration of drug required for 50 % inhibition of cell viability was determined from the dose-response curves (logarithmic concentration of drug or drug-loaded PVP-*b*-PVAc) versus % viability).

#### *5.2.4 Synthesis of fluorescently labeled PVP-*b*-PVAc*

##### *Aminolysis of PVP-*b*-PVAc*

PVP-*b*-PVAc (1.2 g, 0.2 mmol) was dissolved in DCM (10 mL). After complete dissolution of the polymer, *n*-butylamine (0.073 g, 1.0 mmol, 5-fold molar excess) was added to the reaction mixture. The reaction was carried out for 2 hours at room temperature. The polymer was recovered and purified by precipitation from diethyl ether.

*Conjugation of fluorescein maleimide to PVP-b-PVAc-SH*

PVP-*b*-PVAc-SH was dissolved in dry DMF (3 mL) and flushed under argon for 10 minutes. A solution of TCEP.HCl in DMF was added (150:1 mole ratio of TCEP to polymer). The reaction mixture was stirred for 2 hours at room temperature under argon flow. 100  $\mu$ L of fluorescein maleimide (10 mM in DMF) was added to the reaction mixture after 2 hours. The reaction mixture was then stirred at room temperature in the dark for 24 hours. The resulting reaction mixture was dialyzed against water (MWCO 3.5 KDa) for 7 days at 4 °C and protected from light, to remove residual or unreacted fluorescein maleimide. The water was changed three times per day. The purified polymer was recovered by freeze-drying, stored at 4 °C and protected from light.

*5.2.5 Preparation of perylene red-loaded PVP-b-PVAc*

Perylene red-loaded PVP-*b*-PVAc was prepared using the same method reported previously for clofazimine-loaded PVP-*b*-PVAc. Briefly, 10 mg of fluorescently labeled PVP-*b*-PVAc was dissolved in DMSO (1 mL) and perylene red (0.5 mg). The solution was stirred for 10 minutes and then dialyzed against distilled deionized water for 24 hours. The water was changed every 6 hours. The micelle solution was filtered through a microsyringe filter (0.22  $\mu$ m) to remove aggregates and free (precipitated) dye. Dynamic light scattering (DLS) was used to determine the particle size ( $Z_{Ave}$ ) and the particle size distribution (PSD) of the perylene red-loaded PVP-*b*-PVAc.

*5.2.6 Cellular uptake*

15 000 cells were seeded into 8-well chambered coverglasses (Nunc<sup>TM</sup>) and utilized for fluorescence microscopy upon reaching 80 % confluency. Nuclei were stained by using Hoechst 33342 in a final concentration of 50  $\mu$ g/mL.

Perylene red-loaded PVP-*b*-PVAc (polymer concentration 5 mg/mL) was added to the cells and images were acquired immediately thereafter. Samples were observed on an Olympus Cell<sup>®</sup> system attached to an IX-81 inverted fluorescence microscope equipped with a F-view-II cooled CCD camera (Soft Imaging Systems). Using a Xenon-Arc burner (Olympus Biosystems GMBH) as light source, images were excited with the 360 nm, 472 nm or 572 nm excitation filter. Emission was collected using a UBG triple-

bandpass emission filter cube. For the z-stack image frame acquisition, a step width of 0.5  $\mu\text{M}$ , an Olympus Plan Apo N 100x/1.4 Oil objective and the Cell<sup>®</sup> imaging software have been used.

Images were processed and background-subtracted using the Cell<sup>®</sup> software. The time lapse images were recorded with a cycle time of 10 s for a duration of 3 minutes. Images were processed and background-subtracted, volume rendered and projected by using the Cell<sup>®</sup> software.

## **5.3 Results and discussion**

### *5.3.1 In vitro cytotoxicity studies*

Many chemotherapeutic agents are limited in clinical application. This is not only ascribed to the poor delivery of the therapeutic drugs to the targeted sites, but also its toxicity and undesirable side effects on normal tissue or cells. As discussed previously, the purpose for polymer drug carriers is to enhance the delivery and uptake of the drug to the target sites, and to reduce the toxicity and side effects of the drug to normal cells. In order to achieve this effect, it is essential that the drug carrier system itself is non-toxic to human cells.<sup>28</sup>

Prior to cell culture studies on MDA-MB-231 breast cancer epithelial cells, cytotoxicity studies of PVP-*b*-PVAc were performed on MCF12A healthy breast epithelial cells. Figure 5.1 represents the cell viability results of various concentrations of PVP-*b*-PVAc on MCF12A cells. PVP-*b*-PVAc block copolymers showed no cytotoxicity (cell viability greater than 80 %) for concentrations 10 – 1000  $\mu\text{g/mL}$ . Clofazimine-loaded PVP-*b*-PVAc and free drug (clofazimine) of different concentrations are shown to be nontoxic to normal cells (Figure 5.1 (b)). These results enhance the appeal of using PVP-*b*-PVAc block copolymers as drug carriers for hydrophobic drugs.

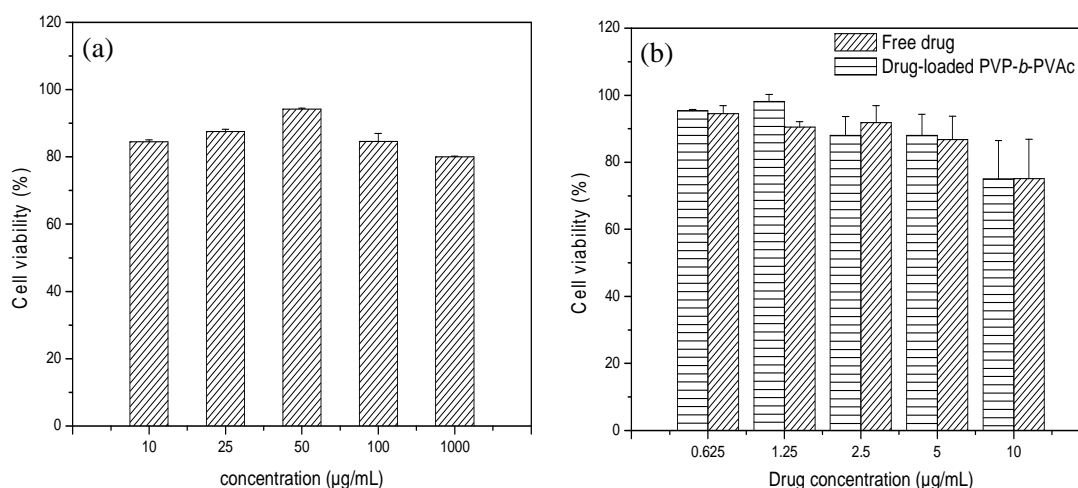


**Figure 5.1:** Cell viability (MTT) assays of (a) PVP-*b*-PVAc (b) clofazimine-loaded PVP-*b*-PVAc against MCF12A breast cell line (Mean  $\pm$ SD  $n=3$ ) after 24 hours

In order to discriminate between drug and polymer toxicity, the cytotoxicity of “unloaded” PVP-*b*-PVAc was evaluated on a MDA-MB-231 drug-resistant breast cancer cells prior to free drug and clofazimine-loaded PVP-*b*-PVAc. The cells were exposed to different concentrations of unloaded PVP-*b*-PVAc for 24 hours (Figure 5.2). The cell viability was above 90 % for polymer concentrations 1 – 50 µg/mL for cells treated with various concentrations of PVP-*b*-PVAc for 24 hours, indicating that that polymer is non-toxic to the cells.

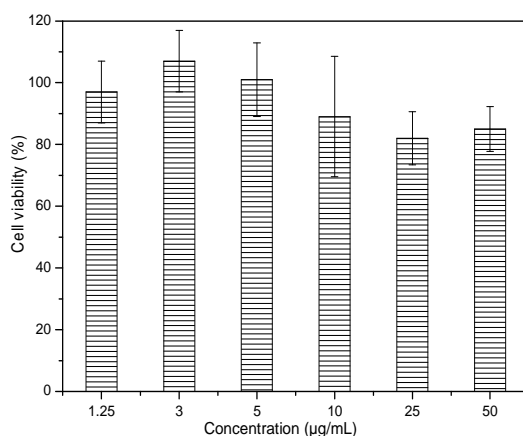


**Figure 5.2:** Cell viability (MTT) assay of PVP-*b*-PVAc against MDR MDA-MB-231 breast cancer cell line (Mean  $\pm$ SD  $n=3$ ) after 24 hours

The cytotoxicity of free drug and clofazimine-loaded PVP-*b*-PVAc of various drug concentrations (1.25 – 20  $\mu\text{g/mL}$ ) are shown in Figure 5.3. It was found that increasing the clofazimine concentration decreased the viability of the cells. At low concentration of clofazimine, the cytotoxicity of free drug and drug-loaded PVP-*b*-PVAc is not obvious. However, at higher concentrations of clofazimine, a difference was observed. Cells incubated for 24 hours with different clofazimine-loaded PVP-*b*-PVAc formulations showed higher cytotoxicity compared to free clofazimine. It must be pointed out that at these drug concentrations, the polymer is above the CMC therefore the drug is present inside the vesicles rather than in free form. In addition, PVP-*b*-PVAc showed no obvious cytotoxicity (over 90 % viability, Figure 5.2), which confirms that the enhanced cytotoxicity was not due to the presence of the PVP-*b*-PVAc carrier. The  $\text{IC}_{50}$  value for the cytotoxicity experiment is the concentration of drug required for 50 % inhibition of cell viability. If the PVP-*b*-PVAc carrier has a negligible cytotoxic effect on cells, then any change in the  $\text{IC}_{50}$  value when treated with PVP-*b*-PVAc/clofazimine formulations, is as a result of increased uptake of the drug or due to an enhanced therapeutic effect. The  $\text{IC}_{50}$  value of drug-loaded PVP-*b*-PVAc (9  $\mu\text{g/mL}$ ) is much lower if compared to the free drug (30  $\mu\text{g/mL}$ ) after 24 hours incubation. It has been reported that polymer drug carriers often reduce the  $\text{IC}_{50}$  through improved drug solubility, more efficient uptake and improved drug trafficking within the cell.<sup>29,30</sup> The lower  $\text{IC}_{50}$  confirms the synergistic action of the clofazimine-loaded PVP-*b*-PVAc formulation *in vitro*.

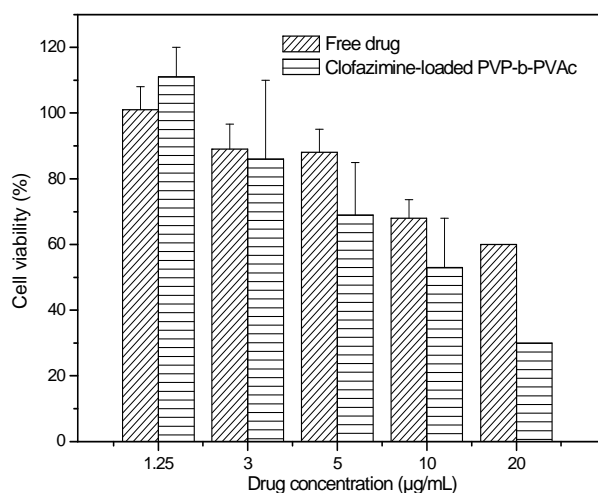


**Figure 5.3:** Cell viability (MTT) assays of free drug and clofazimine-loaded PVP-*b*-PVAc against MDR MDA-MB-231 breast cancer cell line (Mean  $\pm$ SD  $n=3$ ) after 24 hours



PTX is a widely used anticancer drug in the clinic and exhibits strong cytotoxic activity against various cancer types, especially breast and ovarian cancer.<sup>31</sup> The cytotoxicity of free paclitaxel and paclitaxel-loaded PVP-*b*-PVAc formulations were evaluated using MDA-MB-231 cells, and compared to clofazimine. The potency of PTX was clearly demonstrated by the low concentration of the IC<sub>50</sub> value of pure paclitaxel compared to pure clofazimine having the same concentration in MDA-MB-231 cells. Figure 5.4 shows that PTX-loaded PVP-*b*-PVAc demonstrated the same cytotoxicity (40 – 45 %) as free PTX when incubated at low concentrations in MDA-MB-231 cells for 24 hours. At higher PTX concentrations, the cytotoxicity was higher in PTX-loaded PVP-*b*-PVAc than free PTX. The calculated IC<sub>50</sub> value of PTX-loaded PVP-*b*-PVAc is 0.42 µg/mL, which is lower than that of the free drug, which has an IC<sub>50</sub> of 1.58 µg/mL.

When the cells were incubated for 24 hours with several PTX-loaded PVP-*b*-PVAc formulations, the same trend (in which drug-loaded PVP-*b*-PVAc showed higher cytotoxicity than free drug) was observed as for clofazimine-loaded PVP-*b*-PVAc formulations.

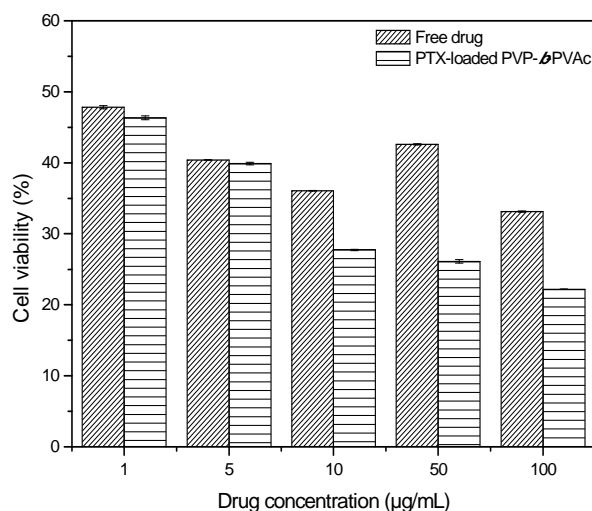


**Figure 5.4:** Cell viability (MTT) assays of free drug and PTX-loaded PVP-*b*-PVAc against MDR MDA-MB-231 breast cancer cell line (Mean  $\pm$ SD n=3 ) after 24 hours

At this stage, the reason for the observed cytotoxicity is not exactly known but could possibly be explained by the mechanism of cell entry (endocytosis for polymer micelles *vs.* drug permeation for free drug).<sup>32</sup> It is speculated that the PVP-*b*-PVAc drug carrier could facilitate the

intracellular uptake of the drug, resulting in a higher concentration of drug in the cytoplasm which further improves the drug efficacy. Polymeric self-assemblies have previously been shown to enhance the *in vitro* cellular uptake of anticancer drugs.<sup>33</sup> For example, Danhier and coworkers<sup>33</sup> loaded poly(ethylene glycol)-*b*-poly( $\epsilon$ -caprolactone-*co*-trimethylenecarbonate) with PTX, which was exposed to cervix epithelial carcinoma cells for 24 hours. Results indicated that PTX-loaded formulations showed lower IC<sub>50</sub> values than free PTX, which suggests that the polymer carrier enhanced the cellular uptake of the PTX. Similarly, Burt *et al.*<sup>34</sup> loaded PTX into the hydrophobic bilayer of poly(butadiene)-poly(ethylene oxide) (PB-PEO) polymer vesicles. PTX-loaded PB-PEO vesicles also showed higher cytotoxicity compared to free PTX against human breast cells. In addition, the vesicles showed an increase in storage stability, beyond the 3 hour half-life of PDLLA-PEG micelles.

Polymer drug carriers have also been reported to overcome drug resistance in multidrug-resistant cancer cells which are overexpressed with efflux transporters and numerous other multidrug-resistant associated proteins in the plasma membranes.<sup>35</sup> The efflux pumps play an important role in protecting tissues and organs from toxic molecules.<sup>36</sup> Among several mechanisms of drug resistance, P-glycoprotein (P-gp) is the best known and most extensively investigated. P-gp, a membrane associated glycoprotein preferentially effluxes hydrophobic compounds from the inside of the cell back to the extracellular space. In tumor cells, the P-gp efflux pump is believed to transport more than 50 % of anti-cancer drugs out of the cell membrane and contributes to the multidrug resistance phenomenon (MDR). Of course, other efflux transporters also contribute to this phenomenon and should not be ruled out.

The effectiveness of a drug is dependent on its intracellular concentration. Free drug diffuses through the cell membrane and slowly gets transported out of the cell by efflux transporters (for more precise details on drug binding, drug efflux and the P-gp action, the reader is referred to the references)<sup>37,38</sup>. This results in a low concentration of drug in the cytoplasm, below the cell-killing threshold which results in limited efficacy. In this way, efflux systems confer resistance to drugs because they reduce the intracellular concentration of the drug. On the other hand, drug encapsulated in a polymer carrier (being enclosed in an endosome when entering the cell) is not

recognized by the efflux pumps. This results in higher intracellular drug concentrations, thereby improving the efficacy of the drug. However, the mechanism of the effect of polymer carriers on the P-gp drug efflux system still remains unclear. Further research is needed to elucidate the exact mechanisms of the effect of drug carriers on the P-gp efflux system.

### 5.3.2 Cellular uptake studies of fluorescently labeled PVP-*b*-PVAc

PVP-*b*-PVAc-fluorescein maleimide was synthesised via a thiol-maleimide reaction as shown in Figure 5.5. An important feature specific to RAFT polymerization is the preparation of polymers bearing terminal thiocarbonyl thio groups, which can easily be aminolysed with primary or secondary amines,<sup>39</sup> producing terminal thiol groups. A general aminolysis procedure was applied to the xanthate end-functional PVP-*b*-PVAc block copolymer to reduce the omega-terminal thiocarbonyl thio chain-ends yielding thiol-terminal PVP-*b*-PVAc. The oxidative coupling of the thiol-functionality (resulting in disulfide formation) was minimized by conducting the conjugation reaction under an inert atmosphere in the presence of a reducing agent, tris(2-carboxyethyl)phosphine (TCEP.HCl). The thiol end-group remained as a ‘‘chemical handle’’ that was conjugated to the maleimide-functionalized dye, fluorescein maleimide.

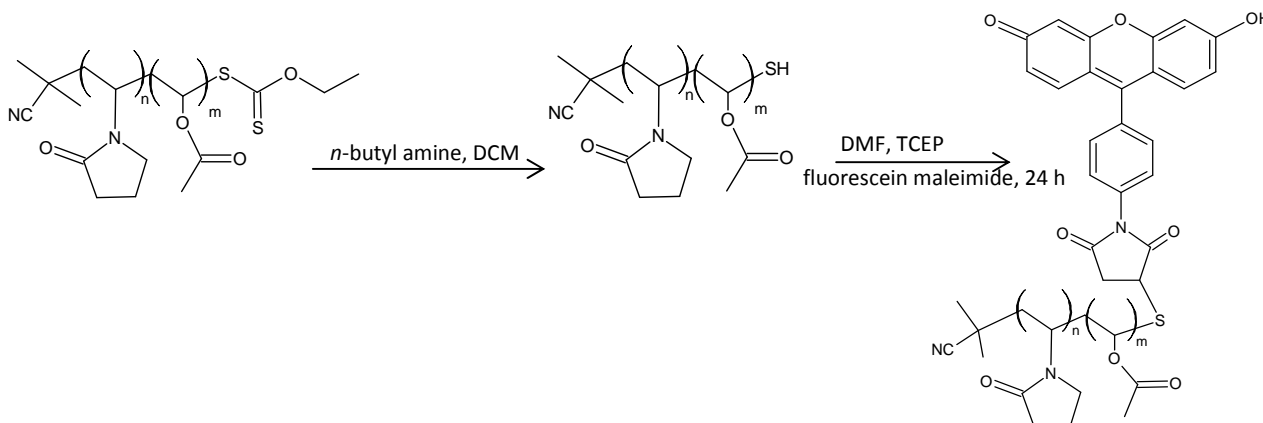


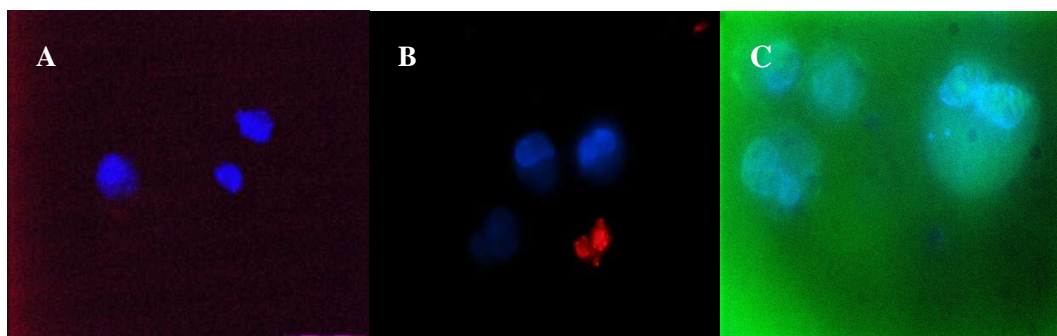
**Figure 5.5:** Reaction scheme for the attachment of fluorescein maleimide, a thiol-reactive fluorescein dye, to PVP-*b*-PVAc

In order to determine whether the fluorescein maleimide was attached to the polymer, the fluorescently labeled PVP-*b*-PVAc polymer fraction that eluted at a specific retention time from size exclusion chromatography (SEC) was collected. The fluorescence spectrum of the fraction was recorded on a luminescence spectrometer (Perkin Elmer Model LS50B) at an excitation

wavelength of 480 nm. The polymer fraction showed an emission at 512 nm, which confirms the presence of the fluorescent tag on the polymer. The efficiency of the conjugation reaction was however not determined and the amount of free dye was not quantified. It was assumed that most free dye was removed after extensive dialysis for 7 days followed by filtration. Perylene red (Exciton 613), a hydrophobic laser dye was encapsulated into the fluorescently labeled PVP-*b*-PVAc via the dialysis method. The cellular uptake of the resulting perylene-loaded fluorescently labeled PVP-*b*-PVAc was explored *in vitro* and compared with free label (fluorescein maleimide and perylene red).

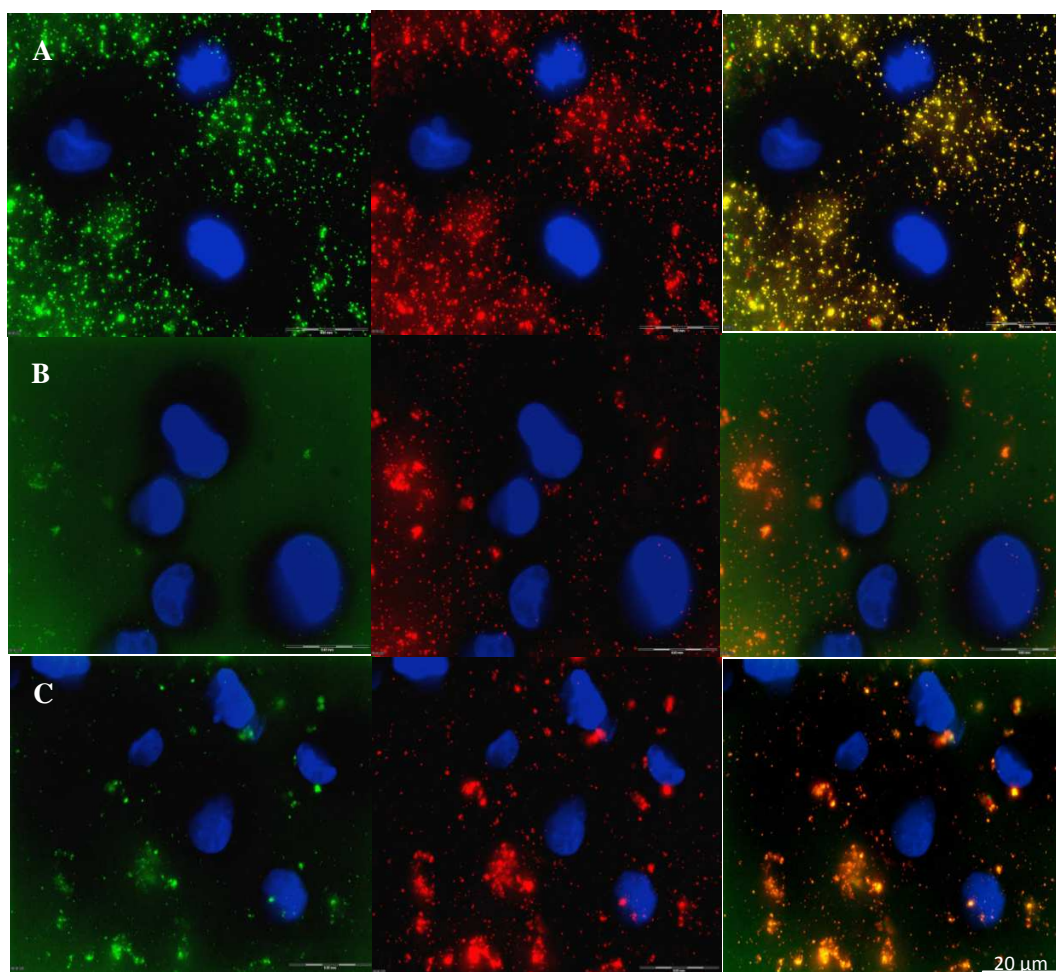
The cellular uptake of fluorescently labeled PVP-*b*-PVAc encapsulated with perylene red was visualized using fluorescence microscopy. Cell nuclei were labeled with Hoechst 33342. Fluorescently labeled perylene red-loaded PVP-*b*-PVAc ( $Z_{ave}$  (DLS) 160 nm, PDI 0.09) were incubated with MDA-MB-231 breast epithelial cancer cells grown on glass cover slips and observed under fluorescence microscopy for 6 hours. At specific time intervals, images were taken to study the time-dependent uptake of the PVP-*b*-PVAc carrier.

Incubation of breast epithelial cancer cells with “free” hydrophobic perylene red dye in PBS (0.1 % DMSO) at 37 °C, as control, showed almost no or minimal fluorescence signal at  $t = 0$  (Figure 5.6 (A)). After 1 hour and 6 hours of incubation, no obvious fluorescence or particle signal was detected in the intracellular or in the perinuclear region of the cells, strongly indicating that the free perylene red was not taken up by the cells. After 6 hours of incubation, some aggregation of the perylene dye far from the vicinity of the cells was observed (Figure 5.6 (B)). No fluorescent image was observed for the free dye inside the cells, which could be ascribed to the hydrophobicity of the dye and its limited solubility in aqueous media, resulting in no cellular uptake. Control experiment for cells incubated with “free” hydrophilic fluorescein maleimide in PBS (Figure 5.6 (C)) resulted in instantaneous uptake into the cells.



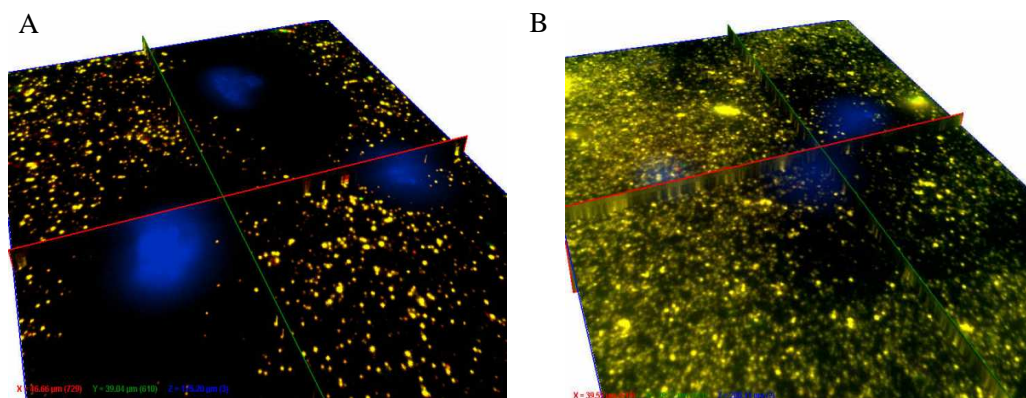
**Figure 5.6:** Fluorescence micrographs of MDA-MB-231 breast cancer cells incubated with perylene red (control) for A)  $t = 0$  hr B)  $t = 6$  hr C) Fluorescein maleimide (control)

Figure 5.7 displays the fluorescence micrographs of cells in contact with perylene red-loaded vesicles at  $t = 0$ ,  $t = 3$  hours and  $t = 6$  hours incubation time. Real-time imaging over the first five minutes of incubation showed fluorescent nano-sized particles (which represent the vesicles) throughout the outside region of the cells. Figure 5.7 (A), (overlay plot), clearly shows the distinct, well-defined black region (representing the inside region of the cell) with no detectable fluorescent signal indicating that no uptake has occurred. Strongly fluorescent particles were detected outside the cell region. The overlay of the fluorescently labeled PVP-*b*-PVAc (green) encapsulated with perylene red, results in yellow, indicating that the vesicles were intact. At this stage no vesicles were taken up by the cells. The real-time imaging over the first few minutes showed significant motion of the vesicles outside the cells with some vesicles aligning themselves around the cell membrane and interacting with the cell membrane. This interaction is said to be the initial step of endocytosis. Figure 5.7 (B) shows a low fluorescence signal observed in the cytoplasm, indicating that a small fraction of vesicles were taken up by the cells after 3 hours. Strong fluorescence was still detected outside the cell wall, indicating that most of the vesicles still remained outside the cell. With extended incubation time, 6 hours at 37 °C, enhanced fluorescence was seen with a larger fraction of vesicles accumulating in the intracellular region with some of the vesicles in very close proximity to the cell nucleus (Figure 5.7(C)).



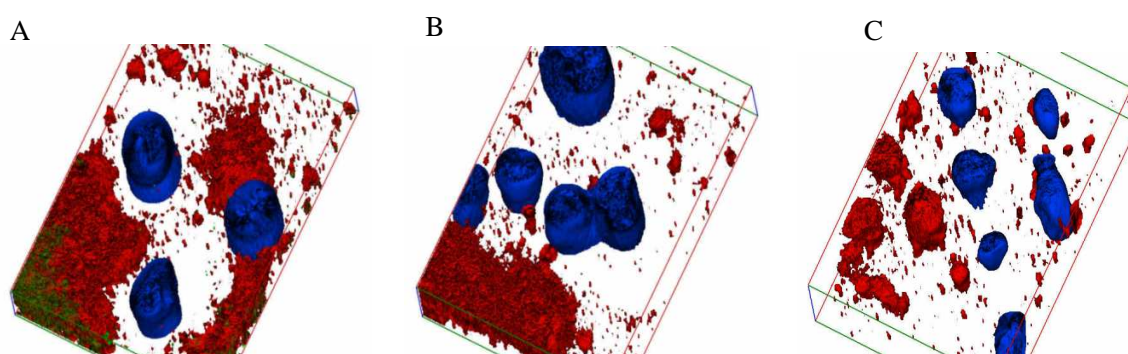
**Figure 5.7:** Fluorescence micrographs of MDA-MB-231 breast cancer cells incubated with: (A) fluorescently labeled perylene red-loaded PVP-*b*-PVAc at 0 hr. (B) after 3h (C) after 6h. For each panel, images from left to right show the cells with nuclear staining by Hoechst 33342 and fluorescein-maleimide labeled PVP-*b*-PVAc, perylene red-labeled PVP-*b*-PVAc, and the overlays of both images. Scale bars correspond to 20  $\mu\text{m}$

Figure 5.8 represents the slice viewer plot, where each slice corresponds to an X, Y or Z-axis position inside the cell. By viewing the volume slices, a more complete three dimensional view of the cell region is seen. Figure 5.8 (A), better illustrates the absence of the vesicles in the cytoplasmic and the perinuclear region at incubation time  $t = 0$  as seen in Figure 5.7 (A). In Figure 5.8 (B) after 6 hours of incubation, the distinct cell membrane is less defined compared to time  $t = 0$ , (Figure 5.8 (A)) indicating that vesicles were internalized and localized in the cytoplasm.



**Figure 5.8:** Slice viewer plots of fluorescently labeled PVP-*b*-PVAc loaded with perylene red in MDA-MB-231 breast cancer cells (A)  $t = 0$  (B)  $t = 6$  hr

Figure 5.9 represents the iso-surface projection plots of the perylene red-loaded PVP-*b*-PVAc at the different time intervals. These plots clearly show the intracellular distribution of the vesicles. The iso-surface projection plot, Figure 5.9 (B) compared to Figure 5.9 (A), clearly shows the distribution of the small fraction of vesicles which have been taken up by the cells and localized in the cytoplasm and not in the nucleus. The iso-surface projection plot after 6 hours (Figure 5.9 (C)) strongly indicates a distinctly different fluorescence distribution showing that the vesicles are more evenly distributed inside the cell cytoplasm and in the perinuclear region.



**Figure 5.9:** Iso-surface projection plots of fluorescently labeled PVP-*b*-PVAc loaded with perylene red in MDA-MB-231 breast cancer cells (A)  $t = 0$  (B)  $t = 3$  hr (C)  $t = 6$  hr.

The results showed that the PVP-*b*-PVAc carrier was capable of entering the cells and carrying the hydrophobic dye to the cells. Furthermore, during the incubation no obvious morphological abnormalities of the cells or cytotoxicity of the PVP-*b*-PVAc carrier were observed. This

indicated that the PVP-*b*-PVAc carrier was well tolerated by the cells and is non-toxic. This result is in agreement with our previous *in vitro* cytotoxicity experiments (Section 5.2) which showed that the carrier is non-toxic.

Although the fluorescence results provided no information regarding the release of the hydrophobic dye during the 6 hour incubation time, evidence that the PVP-*b*-PVAc carrier was taken up by the cells and located in both the cytoplasm and the perinuclear region was clear. The improved solubility and efficient cellular uptake of the dye, in the dye-loaded PVP-*b*-PVAc (which mimics the drug-loaded PVP-*b*-PVAc to a certain extent), could further support the reasoning for the enhanced cytotoxicity of the drug-loaded PVP-*b*-PVAc compared to free drug, observed in the *in vitro* cytotoxicity experiments. Based on the observations for the dye-loaded PVP-*b*-PVAc, similar behavior is anticipated for the drug-loaded PVP-*b*-PVAc. If this is the case, then we hypothesize that for drug-loaded PVP-*b*-PVAc, subsequent degradation or dissociation of the PVP-*b*-PVAc carrier (most likely as a result of interaction with proteins and serum components) would result in the release of the hydrophobic drug in high concentrations within the cytoplasmic region. This would further improve the efficacy of the drug, compared to free drug, which is transported into the cells via a passive diffusion mechanism.<sup>40</sup>

It must be pointed out that there are numerous factors that contribute towards the cellular internalization of polymer carriers. Cellular internalization of polymer carriers is a time, energy, temperature and concentration dependent process.<sup>41</sup> In addition, the chemical composition and the physicochemical properties of polymeric carrier (*e.g.* the ratio of hydrophilic and hydrophobic block lengths, charge, particle size) play an important role.<sup>42</sup> Mahmud *et al.*<sup>43</sup> demonstrated the effect of block length and molecular weight of the poly(ethylene glycol)-*b*-poly( $\epsilon$ -caprolactone) (mPEG-*b*-PCL) carrier. Results showed that hydrophilic PEO block length had a more profound effect on cellular internalization compared to PCL core forming block. The effect of the core-forming block on the internalization of polymer carriers by different cells has not been fully investigated in the literature. Furthermore, the internalization of carriers is also dependent on the type of cell line in which the studies are carried out.<sup>44</sup> As a result of all the above mentioned factors that need to be taken into account, a comparison of the cellular uptake results observed for the PVP-*b*-PVAc carrier with those of other carrier systems previously



reported in the literature is rather difficult. Importantly, fluorescence data showed that the PVP-*b*-PVAc carrier is capable of rapid entry into the cells, an important requirement for any drug delivery system.

#### **5.4 Conclusion**

Cytotoxicity assays confirmed the biocompatibility of the PVP-*b*-PVAc carrier. The *in vitro* MTT assays showed that PVP-*b*-PVAc had no toxic effect on healthy breast epithelial cells and breast cancer epithelial cells. On the other hand, clofazimine-loaded PVP-*b*-PVAc showed significant advantages in achieving higher cytotoxicity and smaller IC<sub>50</sub> value over free drug (clofazimine and PTX). Cellular uptake of the PVP-*b*-PVAc carrier was clearly evidenced by fluorescence microscopy. PVP-*b*-PVAc vesicles were readily taken up by the breast epithelial cancer cells and localized in the cytoplasmic region. From the *in vitro* studies it is anticipated that PVP-*b*-PVAc is a promising drug carrier to improve the efficacy of hydrophobic drugs.

## 5.5 References

- (1) Choksakulnimitr, S.; Masuda, S.; Tokuda, H.; Takakura, Y.; Hashida, M. *J. Control. Rel.* **1995**, *34*, 233 - 241.
- (2) Li, A. P. *Drug Discov. Today* **2005**, *2*, 179 - 185.
- (3) Torchilin, V. P. *Adv. Drug Deliv. Rev.* **2005**, *95* - 109.
- (4) Kim, Y.; Pourgholami, M. H.; Morris, D. L.; Stenzel, M. H. *J. Mater. Chem.* **2011**, *21*, 12777 - 12783.
- (5) Maysinger, D.; Lovric, J.; Eisenberg, A.; Savic, R. *Eur. J. Pharm Biopharm* **2007**, *65*, 270 - 281.
- (6) Rijcken, C. J. F.; Soga, O.; Hennink, W. E.; van Nostrum, C. F. *J. Control. Rel.* **2007**, *120*, 131 - 148.
- (7) Zhang, W.; Li, Y.; Liu, L.; Sun, Q.; Shuai, X.; Zhu, W.; Chen, Y. *Biomacromolecules* **2010**, *11*, 1331 - 1338.
- (8) Yan, J.; Ye, Z.; Luo, H.; Chen, M.; Zhou, Y.; Tan, W.; Xiao, Y.; Zhang, Y.; Lang, M. *Polym. Chem.* **2011**, *2*, 1331 - 1340.
- (9) Duong, T. T.; Marquis, C. P.; Whittaker, M.; Davis, T. P.; Boyer, C. *Macromolecules* **2011**, *44*, 8008 - 8019.
- (10) Luo, L. B.; Tam, J.; Maysinger, D.; Eisenberg, A. *Bioconjugate Chem.* **2002**, *13*, 1259 - 1265.
- (11) Savic, R.; Luo, L. B.; Eisenberg, A.; Maysinger, D. *Science* **2003**, *300*, 615 - 618.
- (12) Ahmed, F.; Pakunlu, R. I.; Brannan, A.; Bates, F.; Minko, T.; Discher, D. E. *J. Control. Rel.* **2006**, *116*, 150 - 158.
- (13) Moad, G.; Rizzardo, E.; Thang, S. H. *Aust. J. Chem.* **2005**, *58*, 379 - 410.
- (14) Beija, M.; Charreyre, M.; Martinho, J. M. G. *Prog. Polym. Sci.* **2010**, *36*, 568 - 602.
- (15) Lowe, A. B. *Polym. Chem.* **2010**, *1*, 17 - 36.
- (16) Roth, P. J.; Boyer, C.; Lowe, A. B.; Davis, T. P. *Macromol. Rapid Commun.* **2011**, *32*, 1123 - 1143.
- (17) Zelikin, A. N.; Such, G. K.; Postma, A.; Caruso, F. *Biomacromolecules* **2007**, *8*, 2950 - 2953.
- (18) Zelikin, A. N.; Li, Q.; Caruso, F. *Chem. Mater.* **2008**, *20*, 2655 - 2661.

- (19) Moad, G.; Rizzardo, E.; Thang, S. H. *Polym. Int.* **2011**, *60*, 9 - 25.
- (20) Ghosh, S. S.; Kao, P. M.; McCue, A. W.; Chappelle, H. L. *Bioconjugate Chem.* **1990**, *1*, 71 - 76.
- (21) Kakwere, H.; Perrier, S. *J. Am. Chem. Soc.* **2009**, *131*, 1889 – 1895.
- (22) Pounder, R. J.; Stanford, M. J.; Brooks, P.; Richards, S. P.; Dove, A. P. *Chem. Commun.* **2008**, 5158 - 5160.
- (23) Li, M.; De, P.; Gondi, S. R.; Sumerlin, B. S. *J. Polym. Sci., Part A: Polym. Chem.* **2008**, *46*, 5093 - 5100
- (24) Scales, C. W.; Convertine, A. J.; McCormick, C. L. *Biomacromolecules* **2006**, *7*, 1389 - 1392.
- (25) Suchao-in, N.; Chirachanchai, S.; Perrier, S. *Polymer* **2009**, *50*, 4151 - 4158.
- (26) Mangold, S. L.; Carpenter, R. T.; Kiessling, L. L. *Org. Lett.* **2008**, *14*, 2997 - 3000.
- (27) Croy, A. H.; Owen, T. C.; Bartlop, J. A.; Cory, J. G. *Cancer Commun.* **1991**, *3*, 207 - 212.
- (28) De Jong, W. H.; Borm, P. J. A. *Int. J. Nanomedicine* **2008**, *3*, 133 - 149.
- (29) Lee, E. S.; Na, K.; Bae, Y. H. *Nano Lett.* **2005**, *5*, 325 - 329.
- (30) Thanou, M.; Duncan, R. *Curr. Opin. Invest. Drugs* **2003**, *4*, 701 - 709.
- (31) Panchagnula, R. *Int. J. Pharm.* **1998**, *172*, 1 - 15.
- (32) Torchillan, V. P. *Eur. J. Pharm. Biopharm.* **2000**, *11*, S81 - S91.
- (33) Danhier, F.; Magotteaux, N.; Ucakar, B.; Lecouturier, N.; Brewster, M.; Préat, V. *Eur. J. Pharm. Biopharm.* **2009**, *73*, 230 - 238.
- (34) Burt, H. M.; Zhang, X.; Toleikis, P.; Embree, L.; Hunter, W. L. *Colloids Surf., B* **1999**, *16*, 161 -171.
- (35) Gottesman, M. M.; Fojo, T.; Bates, S. E. *Nat. Rev. Cancer* **2002**, *2*, 48 - 58.
- (36) Leslie, E. M.; Deeley, R. G.; Cole, S. P. C. *Toxicol. Appl. Pharmacol.* **2005**, *204*, 216 - 237.
- (37) Sharom, F. J. *Pharmacogenomics* **2009**, *9*, 105 - 127.
- (38) Ambudkar, S. V.; Kim, I. W.; Sauna, Z. E. *Eur. J. Pharm. Sci.* **2006**, *27*, 392 - 400.
- (39) Castro, E. A. *Chem. Rev.* **1999**, *99*, 3505 - 3524
- (40) Lee, Y.; Park, S. Y.; Mok, H.; Park, T. G. *Bioconjugate Chem.* **2008**, *19*, 525 - 531.

- (41) Liaw, J.; Aoyagi, T.; Kataoka, K.; Sakurai, Y.; Okano, T. *Pharm. Res.* **1999**, *16*, 213 - 220.
- (42) Savic, R.; Eisenberg, A.; Maysinger, D. *J. Drug Targeting* **2006**, *14*, 343 - 355.
- (43) Mahmud, A.; Lavasanifar, A. *Colloids Surf., B* **2005**, *45*, 82 - 89.
- (44) Zauner, W.; Farrow, N. A.; Haines, A. M. R. *J. Control. Rel.* **2001**, *71*, 39 - 51.

## Chapter 6 Summary and Perspectives

### 6.1 Summary

Amphiphilic block copolymers have been used extensively in drug and gene delivery research. Their applications in drug delivery include drug solubilization, controlled drug release and drug targeting. A feature unique to amphiphilic block copolymers is their self-assembly behaviour in aqueous environment. This attractive feature allows for the encapsulation of highly hydrophobic anti-cancer drugs to increase the effective solubility of these therapeutic agents. Furthermore, it permits drugs to be more effectively administered, transported, and eventually delivered to the desired targeted site through the blood stream, which consists mostly of water.

The results presented in this dissertation describe the potential application of the amphiphilic block copolymer, poly((vinylpyrrolidone)-*b*-poly(vinyl acetate)) (PVP-*b*-PVAc) as an effective drug carrier for hydrophobic anti-cancer drugs. In this chapter the results of the dissertation are summarized and future perspectives are given.

In **Chapter 1**, a general introduction, the aim of the study and structure of the dissertation is given. The primary objective of this study was to develop a PVP-*b*-PVAc polymer drug carrier and explore its potential as a drug carrier. The physicochemical properties, formulation stability and anti-cancer activity of the carrier were examined.

A general overview of amphiphilic block copolymers in drug delivery is presented in **Chapter 2**. The chapter discusses the properties of drug carriers (*e.g.* particle size, size distribution, drug loading capacity, drug release, stability) which determine their ability to deliver drugs. The chapter also highlights the various key factors that primarily influence these properties.

The synthesis, characterization and self-assembly of PVP-*b*-PVAc is described in **Chapter 3**. The amphiphilic block copolymers were synthesized via the RAFT/MADIX technique. PVP-*b*-PVAc block copolymers may be synthesized by a two-step sequential monomer addition polymerization procedure. The methodology consisted of growing the PVAc chain from a xanthate end-functional PVP. Block copolymers of constant hydrophilic PVP block length ( $M_n \sim 10\,000$  g/mol) and varying hydrophobic block length were synthesized. In aqueous medium, the hydrophilic PVP segment forms the shell/corona region and hydrophobic PVAc segment forms

the bilayer membrane region where the hydrophobic molecules can be entrapped. In this dissertation the PVP-*b*-PVAc self-assembled system were formed via the dialysis method.

The self-assembly was confirmed by  $^1\text{H}$  NMR spectroscopy in  $\text{D}_2\text{O}$ . Both the morphology and the average size of the self-assembled PVP-*b*-PVAc were investigated by dynamic light scattering (DLS), transmission electron microscopy (TEM) and static light scattering (SLS). Results revealed the formation of spherical, vesicular-like particles of 180 – 200 nm in diameter. Considering their size, these particles are expected to be suitable for the delivery of drugs to tumors.<sup>1</sup> The self-assembly behaviour of the block copolymer in aqueous solution was further investigated by fluorescence spectroscopy. The critical micelle concentration (CMC) of the PVP-*b*-PVAc block copolymers was determined using pyrene as a fluorescent probe. Increasing the PVAc block length resulted in a lower CMC, which can be attributed to the increased hydrophobicity of the PVP-*b*-PVAc block copolymer. The CMC values were low ( $\sim 0.001$  mg/mL – 0.01 mg/mL), which is important in order for the self-assembled structures to remain intact after dilution upon intravenous administration. Furthermore, the stability of the block copolymers was also assessed under physiological conditions (PBS, pH 7.4, 37 °C) and were stable in the absence and presence of serum.

The feasibility of PVP-*b*-PVAc as a drug carrier for the solubilization and delivery of hydrophobic anti-cancer drugs was addressed in **Chapter 4**. To assess the potential of PVP-*b*-PVAc as a drug delivery vehicle, the loading of a model drug, clofazimine, and a commonly used anti-cancer drug, paclitaxel (PTX), into PVP-*b*-PVAc was investigated. A simple loading method, namely the dialysis method was used to entrap the drugs in the hydrophobic PVAc domain. It was found that PVP-*b*-PVAc was able to successfully solubilize the chemotherapeutic agents.  $^1\text{H}$  NMR spectroscopy confirmed the formation of phase-separated structures and the localization of the drug within the hydrophobic domain.

The method used allowed for reproducible formation of drug-loaded PVP-*b*-PVAc vesicles, in the size range of 180 – 200 nm. These particle sizes should be suitable for passive targeting via the enhanced permeation and retention (EPR) effect.

In order to find an optimal formulation for the drug-loaded PVP-*b*-PVAc, various factors that influence the loading capacity namely the length of the hydrophobic PVAc segment and the amount of feed drug were also investigated. Different ratios of drug and polymer were explored and it was found that the composition of 20 % (w/w) clofazimine: PVP<sub>90</sub>-*b*-PVAc<sub>290</sub> (w/w) and 10 % (w/w) for PTX: PVP<sub>90</sub>-*b*-PVAc<sub>290</sub> were the optimum formulations. Lower ratios led to lower efficiency, whereas at higher ratios the PVP-*b*-PVAc carrier exceeded its solubilization capacity resulting in drug precipitation. Generally, the different PVP-*b*-PVAc block copolymers of varying PVAc block length had different loading capacities, which indicated that the hydrophobic block length affects the ability to load hydrophobic drug within the bilayer membrane. Increasing the amount of feed drug also increased the drug loading capacity. DLS and TEM of the drug-loaded PVP-*b*-PVAc showed particle sizes of 200 nm which is suitable for passive targeting via the enhanced permeation and retention (EPR) effect. The effect of the drug loading on the particle size was also investigated and found to have no significance on the particle size of the PVP-*b*-PVAc carrier. The stability of the drug-loaded PVP-*b*-PVAc was investigated in physiological conditions (PBS, pH 7.4, 37 °C) in the presence and absence of serum. Drug-loaded PVP-*b*-PVAc was stable in the presence of serum indicating that the hydrophilic PVP corona was able to stabilize the vesicles.

Next, *in vitro* studies of PVP-*b*-PVAc were conducted and presented in **Chapter 5**. These studies are an essential first step to assess the drug carriers potential. Cytotoxicity assays confirmed the biocompatibility of the PVP-*b*-PVAc carrier. PVP-*b*-PVAc was shown to be non-toxic to healthy MCF12A breast cells and MDA-MB-231 multi-drug-resistant breast epithelial cancer cells. The MTT assays show that the PVP-*b*-PVAc carrier can deliver clofazimine and PTX and prohibit growth of cancer cells *in vitro*. In addition, the drug-loaded polymers showed increased cytotoxicity compared to free drug against breast cancer epithelial cells, indicating the enhanced therapeutic effect. To determine whether the PVP-*b*-PVAc carrier was taken up by the cells, fluorescently labeled PVP-*b*-PVAc was loaded with hydrophobic dye (perylene red) which mimicked the drug. In doing so, one is able to track whether the carrier is taken up by the cells and determine the fate of both the vesicles and the dye upon cellular internalization. Fluorescence indicated that the PVP-*b*-PVAc carrier was taken up by the cells within 3 hours

incubation and localized in the cytoplasm and perinuclear region, but not in the nucleus after 6 hours.

## 6.2 Perspectives

The results presented in the thesis indicate the potential of the amphiphilic PVP-*b*-PVAc block copolymer as a carrier for hydrophobic anti-cancer drugs. However, further optimization and development of the system need to be considered.

In terms of the PVP-*b*-PVAc drug carrier system developed so far in this study, the following aspects require further research:

- ***In vitro studies***

In **Chapter 5**, the cellular internalization and localization and the time taken for cellular uptake of the PVP-*b*-PVAc carrier was investigated. From the results, it was anticipated that the cellular uptake of the carrier is via endocytic pathways, which is suggested for most polymer carriers. However, the specific mechanism of endocytic uptake of the drug carrier, the intracellular trafficking pathway the carrier follows upon cell entry and the subcellular distribution still remains unknown. Understanding of the cellular uptake routes and trafficking is essential for the development of efficient drug delivery carriers. These questions can be answered by staining the organelles in the cell *e.g.* cell membrane or mitochondria by using, membrane- or organelle-selective dyes.<sup>2</sup> The answers to these essential questions could provide valuable information, which could further be used to improve the PVP-*b*-PVAc drug carrier system.

- ***In vivo studies***

In **Chapter 4** and **5**, data on the stability of the PVP-*b*-PVAc carrier in physiological conditions as well as data on the cytotoxic effect of the PVP-*b*-PVAc carrier and clofazimine and PTX-loaded PVP-*b*-PVAc on MDA-MB-231 multi-drug-resistant breast epithelial cancer cells are presented. For many polymer drug delivery systems, promising *in vitro* stability and efficacy data on culture cells has proven to be poorly representative of the performance or effectiveness of the drug carriers *in vivo*. To date we could only



evaluate and demonstrate the effectiveness of PVP-*b*-PVAc *in vitro*, however, *in vivo* evaluation needs to be considered. What remains to be achieved is to test whether drug-loaded PVP-*b*-PVAc can alter the pharmacokinetics of free drug *in vivo*.

In addition, the *in vivo* biodistribution and pharmacokinetic studies need to be performed to confirm the therapeutic efficacy of the drug-loaded PVP-*b*-PVAc carrier.

- ***Towards a more controlled drug delivery system***

The dissertation describes the first steps towards the development of a PVP-*b*-PVAc drug carrier. However, further development for a more effective drug release system should be considered. Firstly, an important requirement of a drug carrier is to maintain its integrity during circulation time upon intravenous administration. Because of the relatively high hydrophobic PVAc block length, the CMCs of the PVP-*b*-PVAc block copolymers developed and described in the thesis were low and the assemblies that were formed were correspondingly stable. This should maintain their integrity upon dilution. However, interaction with serum proteins can also destabilize the carrier. This results in premature release of the drug or alternatively accelerates the release of the drug from the carrier. One approach would be to covalently link the drug to the hydrophobic block via a hydrolytically sensitive linker (e.g. hydrazone linker). In this way, the drug remains stably linked to the polymer and only upon entering the acidic tumor environment or the acidic organelles is the drug released. To further improve the efficacy of the carrier, selective targeting groups can also be attached to the carrier. Alternatively, an amphiphilic copolypeptide drug carrier can also be considered whereby the hydrophobic drug is covalently linked to the carrier. Peptides exhibit high biological specificity which could further enhance the drug targeting property of the carrier.

- ***Combination therapy - Multiple drug delivery***

Over the past years, research has focused on single drug administration, while not much attention has been placed on combination administration. Recent cancer research is based on combination therapy – the use of synergistic anticancer drug “cocktails” whereby two different drugs are delivered to tumors simultaneously.

Synergistic drug combinations produce an even greater response rate than is possible with each drug used alone at its optimum dose.<sup>3</sup> Generally, anti-cancer drugs are typically administered at their individual maximum tolerated doses.<sup>4</sup> This is termed the “more-is-better” approach. However, this approach ignores the possibility of subtle concentration and ratio dependent dynamic interactions capable of causing a synergistic response.<sup>5</sup> Recently, a more rational approach for the combination of anticancer drugs has been proposed – the fixed ratio drug combinations (FRDC) approach – which holds the promise of capturing the maximum pharmacodynamic cytotoxic specificity for cancer cells.

Riminophenazines possess a potent anticancer multi-mechanism that is thought to be best utilised in combination with standard chemotherapeutics. Interestingly, these riminophenazines have been shown to inhibit P-glycoprotein (P-gp), the transmembrane efflux pump that is largely responsible for acquired resistance.<sup>6,7</sup> Recently, FRDC comprising clofazimine in combination with paclitaxel has demonstrated synergistic antiproliferative activity *in vitro* against a multi-drug resistant (MDR) cell line. Recently, the *in vitro* optimal synergistic fixed drug ratio combination of clofazimine-PTX has been determined (Combination Index Analysis (CI) < 1).<sup>8</sup> The work presented in this study has shown that PVP-*b*-PVAc may serve as a suitable carrier for single delivery of hydrophobic drugs namely clofazimine and PTX. Therefore, current work focuses on the encapsulation of the FRDC of clofazimine and paclitaxel into PVP-*b*-PVAc. Lastly, owing to the vesicular morphology of the self-assembled PVP-*b*-PVAc, its potential for the simultaneous delivery of a combination of hydrophobic (*e.g.* PTX) and hydrophilic drugs (*e.g.* doxorubicin) can also be explored.

**6.3 References**

- (1) Maeda, H.; Wua, J.; Sawa, T.; Matsumura, Y.; Horic, K. *J. Control. Rel.* **2000**, *65*, 271 - 284.
- (2) Savic, R.; Luo, L. B.; Eisenberg, A.; Maysinger, D. *Science* **2003**, *300*, 615 - 618.
- (3) Shin, H.; Alani, A. W. G.; Rao, D. A.; Rockich, N. C.; Kwon, G. S. *J. Control. Rel.* **2009**, *140*, 294 - 300.
- (4) Decker, S.; Sausville, E. A. *Ann. N.Y. Acad. Sci.* **2005**, *1059*, 61 - 69.
- (5) Mayer, L. D.; Harasym, T. O.; Tardi, P. G.; Harasym, N. L.; Shew, C. R. *Mol Cancer Ther* **2006**, *5*, 1854 - 1863.
- (6) Van Rensburg, C. E. J.; Van Staden, A. M.; Anderson, R. *Cancer Res.* **1993**, *53*, 318 - 323.
- (7) Van Rensburg, C. E. J.; Joone, G. K.; O'Sullivan, J. F. *Oncol. Rep.* **2000**, *7*, 193 - 195.
- (8) Koot, D.; *Strategic pre-clinical development of Riminophenazines as resistance circumventing anticancer agent* Univeristy of Pretoria, **2012**.

### **Acknowledgements**

First and foremost, I would like to acknowledge my promoter, Bert Klumperman for giving me the opportunity to study under his supervision. I consider it an honor to work within your research group. Thank you for your support, motivation and encouragement throughout my PhD study. Above of all, you have always shown continuous confidence in my capabilities and for that I am very grateful.

I would like to acknowledge Prof. R. Sanderson who my inspired me throughout my Honours, Masters and PhD years at the University of Stellenbosch. You were my mentor.

Some parts of the work presented in this dissertation could not have been accomplished without the contributions of my collaborators. Firstly, I would like to thank Dwayne Koot from the Department of Pharmacology (University of Pretoria) for answering my stream of endless “pharmaceutical” questions! All our discussions and your thoughtful suggestions were gratefully appreciated. Mark Thomas and Ben Loos from the Department of Physiology (University of Stellenbosch) - thank you for your guidance, your patience, your time and sharing of your knowledge. Mark, a very special thank you for your guidance and help in the cell culture laboratory. I have learnt mostly everything involving cell work from you and I am very grateful for your time and help. Mohammed Jaffer from the University of Cape Town – thank you for all your time and help with the TEM analyses.

I would like to thank Prof. W. Hennink and Prof B. Klumperman for giving me the opportunity to spend a few months at the Department of Pharmaceutics, Utrecht University, The Netherlands. A special thank you to Yang Shi for his assistance in the research labs during my visit.

Too many people to mention individually have assisted in so many ways during my work in the Department of Polymer Science. Om nooit te vergeten – Dr Eric van den Dungen - bedankt voor de raad, de leerzame besprekingen en bemoedigende woorden. Jouw kennis en toewijding op dit onderwerp is een inspiratie voor mij.

I would like to thank Dr Gwenaelle Pound for her guidance during the initial stages of my PhD. To all the research students in the Free Radical Lab - you all have my sincere gratitude. All our laughs and enjoyable moments in the lab kept me smiling during good times and difficult times. I also thank the support staff who aided me in so many aspects during my PhD – Erinda Cooper, Aneli Fourie, Margie Hurdell, Deon Koen, Calvin Maart and Jim Motshweni.

Of course no acknowledgments would be complete without giving thanks to my parents, to Chantal and to Claude. Thank you for your unconditional love, support, encouragement and believing in me. You have been my tower of strength.

*Nathalie*

*March 2012*